UNIVERSITY OF LIVERPOOL

Portable mass spectrometry for artificial sniffing

Thesis submitted in accordance with the requirements of the University of Liverpool for the degree of

Doctor in Philosophy

by

Stamatios Giannoukos

Department of Electrical Engineering and Electronics

The University of Liverpool

February 2015

Abstract

On-site chemical detection and monitoring of compounds related to homeland security applications, civil defence and forensics is difficult using conventional instrumentation. Target analytes include human chemical signatures (for detection of illegal immigration), drugs of abuse, explosives and chemical warfare agents (CWAs). A convenient solution is to complement existing techniques using portable membrane inlet mass spectrometry (MIMS).

This thesis deals with the mass spectrometric investigation of characteristic chemical odour signatures emitted by human exhaled breath and skin as chemical signs of human presence in a confined space. It also presents detection results of threat and threat related chemical compounds. Numerical modelling of ion injection and confinement in a non-scanning linear ion trap (LIT) mass analyser for achieving sensitivity enhancement was carried out. A novel portable artificial sniffer based on linear ion trap (LIT) technology has been designed and developed. Initial performance results are described. Preliminary field trials have led to positive outcomes which are currently being commercially exploited.

Acknowledgements

Seizing the opportunity given to me from this podium, I would like to acknowledge some people with whom I cooperated and interacted throughout the three years period of this project. First of all, I would like to express my great thanks and deepest appreciation to my academic supervisor Professor Stephen Taylor who trusted me and gave me the honour and the chance to work beside him. Professor Taylor was for me a mentor and a friend. He was always an active supporter and protector of my work, an extraordinary university educator and advisor, a unique provider of knowledge, of hope and of bright visions. I appreciate everything he did for me and I feel very lucky and proud for being a member of his research group. In this point, I would like to thank my thesis advisor Professor Jason Ralph for his support.

I would like to express my gratitude to Dr Boris Brkić who was my guide in this work and who transferred me his high scientific and moral values. Boris and I worked closely together in a unique and such a fruitful way that I will never forget. He was always next to me, offering wise advice, unlimited succour and the most precise solutions to issues which I was facing at times. Through our daily collaboration, a strong friendship was born. Special thanks are due to Dr Neil France from Q-Technologies Ltd., UK who was continuously providing me with his enthusiasm, his knowledge and technical assistance. Big thanks to Mr. Barry Smith from Q-Technologies Ltd., UK for his ethical support, his valuable comments on my work and his good fellowship.

I would also like to thank Dr. Tom Hogan from Pathway Systems Ltd., UK for supplying me with technical advice. His creative personality and broad range of experience were very helpful during our conversations and work plans. Particular acknowledgements are due to Mr. Collin Singer and Ms. Louise Wilson from Wagtail Ltd., UK for their contribution during the development and the progress of the experimental work in the field.

The research leading to this project has received funding from the European Community's Seventh Framework Programme managed by the Research Executive

Agency (FP7/2007-2013) under grant agreement no. 285045. I would like to thank all my project partners and more specifically Dr Carl Hauser and Dr Robert Murcott from TWI Ltd, Professor Yves Zerega and Dr Aurika Janulyte from the Aix-Marseille University, Dr Sjaak de Koning and Mr Edwin Beekwilder from Da Vinci Laboratory Solutions, Dr Fabrizio Siviero from SAES Getters Group, Envisiontec GbmH, Xaar and Wagtail UK Ltd.

In addition, very big thanks to Dr Kenneth Roberts and Dr Ray Smith for their friendship, their limitless support and the precious time we spent together. Last but not least, I would like to gratefully acknowledge all my family members individually, Nikos, Anna, Konstantinos, George and Evgenia as well as all my close friends in Greece, UK, Ireland and USA for their love, patience and the endless inspiration that they so generously offered me.

Contents

List of figures

List of tables

Acronyms

amu	Atomic mass unit
APCI	Atmospheric pressure chemical ionization
APPI	Atmospheric pressure photoionisation
ASAP	Atmospheric-pressure solids analysis probe
BEM	Boundary element method
CES	2-chloroethyl ethyl sulfide
CNC	Computer numerical control
CPO	Charged particle optics
CRDS	Cavity Ring-Down spectroscopy
C	Concentration
CWAs	Chemical warfare agents
D	Diffusion coefficient
Da	Dalton
d	Thickness of a sheet membrane
d_o	Outer diameter of a capillary membrane
d_i	Inner diameter of a capillary membrane
DAPCI	Desorption atmospheric pressure chemical ionization
DAPPI	Desorption atmospheric pressure photon ionization
DART	Direct analysis in real time
DESI	Desorption electrospray ionisation
DMMP	Dimethyl methylphosphonate
DNT	2,4-dinitrotoluene
DLP	Digital light processing
DMD	Digital micromirror device
e	Elementary charge of an electron
EASI	Easy ambient sonicspray ionisation
ECU	Electronic control unit
EI	Electron impact

EM	Electron multiplier
EN	Electronic nose
Ep	Activation energy for permeation
EPA	Environmental protection agency
ERM	Enhanced resolution mode
ESI	Electrospray ionisation
EU	European Union
FAIMS	Field asymmetric ion mobility spectrometry
FDM	Finite difference methods
FEM	Finite element methods
FID	Flame ionisation detector
FOC-GAP-RAIRS	Fibre optic coupled grazing angle probe reflection/adsorption IR spectrometry
GB	Sarin
GC	Gas chromatography
GC/FT-IR	Gas chromatography / Fourier transform infrared spectrometer
GD	Soman
GF	Cyclosarin
GUI	Graphical user interface
HCS	Human chemical signatures
HD	Distilled mustard gas
HDT	Heat deflection temperature
HSGC	High-speed gas chromatography
IMMS	Ion mobility mass spectrometry
IMS	Ion mobility spectrometry
ISLS	Ion source lens system
IR	Infrared spectroscopy
J (x, t)	Permeation rate
J_c	Permeation rate through a capillary membrane
J_s	Permeation rate through a sheet membrane
LC-MS	Liquid chromatography-mass spectrometry
LIBS	Laser-induced breakdown spectroscopy
LIDAR	Light detection and ranging

LIT-MS	Linear ion trap mass spectrometry
LOD	Limit of detection
LSI	Laser spray ionisation
LTP	Low temperature plasma
MCC-GC	Multi-capillary columns gas chromatography
MEMS	Micro-electromechanical systems
MIMS	Membrane inlet mass spectrometry
MI-QMS	Membrane inlet quadrupole mass spectrometry
MIP	Molecularly imprinted polymer
MOS	Metal oxide semiconductor
MS	Mass spectrometry
M.W.	Molecular weight
m/z	Mass to charge ratio
NIST	National institute of standards and technology
QA	Quality assurance
QC	Quality control
QMF	Quadrupole mass filter
PCP	Phencyclidine
PDMS	Polydimethylsiloxane
PES	Polyethersulfone
PMMA	Polymethylmethacrylate
PP	Polypropylene
PI	Photoionisation
ppm	Parts per million
ppb	Parts per billion
ppt	Parts per trillion
PSI	Paper spray ionisation
PTFE	Polytetrafluoroethylene
PTR-MS	Proton transfer reaction-mass spectrometry
r_a	Aperture radius
R^2	Coefficient of determination
SAR	Search and rescue
SAW	Surface acoustic wave

S/N	Signal to noise ratio
SVOC	Semi volatile organic compound
SERS	Surface enhanced Raman scattering
SESI	Secondary electrospray ionisation
SIMS	Secondary ion mass spectrometry
SIFT-MS	Selected ion flow tube-mass spectrometry
SORS	Spatially offset Raman spectroscopy
SPME	Solid phase microextraction
TATP	Triacetone triperoxide
TCD	Thermal conductivity detector
Th	Thompson
THC	Tetrahydrocannabinol
THz	Terahertz
TICs	Toxic industrial chemicals
TNT	2,4,6-trinitrotoluene
VOC	Volatile organic compound
VVOC	Very volatile organic compound
WHO	World Health Organization
$\partial C(x,t)/\partial x$	Membrane concentration gradient
U	Total DC bias applied to x- and/or y-electrodes
Ω	Angular frequency
ΔM	resolution

Chapter 1

Introduction

1.1. Rationale

The European Union (EU) is a political and economic partnership between 28 member states. As such, it requires the free and safe transportation of its citizens and their goods (Schengen Agreement, Luxembourg, 1985) and follows the same external borders protection code. One of the major EU priorities is the continuous provision of security and social welfare. With the rise of international terrorism and organised crime, homeland security, civil defence and military authorities deal with the problem of the early detection, monitoring and localization of threat substances. This includes the illicit carriage of drugs of abuse, explosive materials, bombs and chemical weapons. In addition, continued increase of illegal human trafficking exacerbates public safety conditions [1].

Europe faces a potential lack of protection tools and mechanisms, to prevent and avoid uncomfortable and undesirable lawless and/or terrorist actions or situations. At EU border checkpoints there are protective measures consisting of sniffer dogs, metal detection devices and electronic noses which screen and attempt threat blockade. However, security related issues remain important, demanding the development and employment of more flexible, highly sensitive field deployable technological instrumentation (either hand-held or stand-off) [2].

The aim of this project is to complement existing analytical instrumentation for on-site chemical analysis and the work of sniffer dogs by deploying, evaluating and providing portable electronic gas sensing systems based on mass spectrometry (MS). Instruments are to be capable of detecting hidden humans and illegal or hazardous chemical compounds [3].

1.2. Objectives and motivation

Within the above described framework, the main objectives of this project include the following:

a. To study and explore artificial sniffing mechanisms in field chemical analysis and especially in security applications, as well as to collect and compare information regarding existing already developed scent sensing devices which are commercially available for threat detection and monitoring purposes.
b. To study the volatile organic compounds (VOCs) which are associated with illegal, hazardous and terrorist events.
c. To investigate portable membrane inlet mass spectrometry (MIMS) for use in border control applications. This includes the investigation of: i) human detection and methodology optimization and ii) threat and threat associated compounds detection and monitoring. Development and testing of a high-throughput membrane sampling approach for achieving low limits of detection (LOD) and fast response times including MIMS evaluation during field experiments.
d. To build, optimise and test a novel portable artificial sniffer based on linear ion trap mass spectrometry (LIT-MS), through simulation and experimental development.

The motivation behind this thesis is to provide to the EU nations effective portable tools (with non-intrusive and high-resolution characteristics), based on portable mass spectrometry, for their protection from potential threats.

1.3. Outline of the thesis

The structure of this thesis is as follows. Following this introduction, there is a survey of the published literature in chapter 2. The work presented then divides into two parts. In part I (chapter 3, 4) experimental work using a membrane inlet quadrupole mass spectrometer (MI-QMS) is described. In part II (chapter 5, 6) theoretical and experimental studies of a LIT-MS are described. The transition from a QMS to a LIT-MS was the obvious evolution of the described below methodology. In part I, a triple filter QMS with mass range *m/z* 0 - 200 was employed due to the enhanced sensitivity and the enhanced long-term stability that if offers compared to a single filter QMS. In part II, the QMS was replaced by a built-in-house non-scanning LIT-MS system with a

higher mass range up to m/z 500. LIT devices compared to QMS systems, provide a wider mass detection range, higher ion storage capacity, tandem mass spectrometry (MS/MS) ability offering additional confirmation levels of unknown sample compounds identification as well as manufacturing simplicity.

Chapter 2 investigates recent developments and challenging issues related to field chemical analysis. Artificial sniffing mechanisms are surveyed and existing technologies with odour sensing capabilities used in homeland security and defence operations are described. A comparison of commercially available devices for onsite threat detection is presented. The chapter concludes by examining the biological and chemical origins of human body scent and compares VOCs emitted by various human body areas. Threat substances such as illicit drugs, explosives and chemical warfare agents (CWAs) are also tabulated.

Chapter 3 begins with an explanation of MIMS theory. The use of a portable MI-QMS for the chemical detection of human odours is described. Emissions from human exhaled breath and skin are chemical signs of human life which occur in confined spaces such as shipping containers. During tests with volunteers of both genders, a plethora of VOCs was detected, including CO_2 emissions, acetone, isoprene and carboxylic acids. Results of identified human chemical signatures are presented. Different human condition experiments such as the simultaneous presence of urine, deodorant use and alcohol consumption were also examined.

Chapter 4 investigates the mass spectrometric detection and monitoring of characteristic chemical odour signatures emitted by threat compounds using the same portable MI-QMS system as in Chapter 3. During the experiments, simulant compounds to the real threat substances, breakdown products, compounds that have been found in the headspace area above the parent compounds and precursors were investigated. Standard gas mixtures were prepared in dilution bottles. Excellent MIMS linearity, low detection limits and fast response times were demonstrated. Field experiments with real samples of target compounds were also undertaken and preliminary results are presented. Optimization experiments using a heated membrane sampling probe were also done.

Chapter 5 includes novel simulation work done for enhancing the sensitivity of linear ion trap mass spectrometers used for sensing low sample concentrations in field applications. Charged particle optics (CPO) software was used to model an electron impact (EI) ion source coupled to a miniature ideal LIT in order to achieve optimal

sensitivity. Simulation work was done for cocaine mass fragments m/z 182 and 304. Chapter 5 also demonstrates and utilizes a novel 3D simulation software package (LIT2) developed-in-house, in order to numerically optimise ion trapping in a non-scanning LIT mass analyser. Examined ion masses were m/z 182 and 304 for cocaine and m/z 210 and 227 for trinitrotoluene (TNT).

Chapter 6 presents the development and testing of an optimised LIT mass analyser fabricated by a rapid manufacturing technique: digital light processing (DLP). The LIT mass analyser was manufactured to be part of a portable MS device. Chapter 6 demonstrates the non-scanning operation of the DLP LIT-MS fabricated during the SNIFFLES project [3]. Moreover, the pre-prototype version of the LIT based portable gas sensor, its technical characteristics, and representative obtained threat compound results are reported. The ultimate version of this artificial sniffer: the beta LIT-MS unit is also described.

Chapter 7 summarises the project work undertaken and suggests future research goals and visions.

1.4. Main contributions

Personal contributions in Part I (chapter 3 and 4) of this thesis include the conception of the work (human chemical signatures and threat compounds detection using MIMS), the experimental design, the development of the experimental methodology as well as the data acquisition and interpretation. It also includes the design and fabrication of two novel and high throughput membrane sampling probes/approaches that were used during experiments. I also performed preliminary field experiments to examine MIMS performance on-site.

My contributions in Part II (chapter 5 and 6) involve novel simulation and modelling work for enhancing sensitivity of a built-in-house LIT-MS system. CPO and LIT2 software were used to numerically optimise ion injection, trapping and ejection in a non-scanning LIT mass analyser. Personal contributions also comprise the design, development and integration of a portable artificial sniffer for security applications as well as its lab-testing with threat simulant compounds.

1.5. Theory of quadrupole devices

A quadrupole mass analyser is an assembly of four rods in a parallel array [4-7]. The rods are usually either of hyperbolic or of circular shape as presented in Figure 1.1. The field within the mass analyser is produced by coupling opposite pairs of rods together and applying positive and negative DC and RF potentials (Figure 1.2).

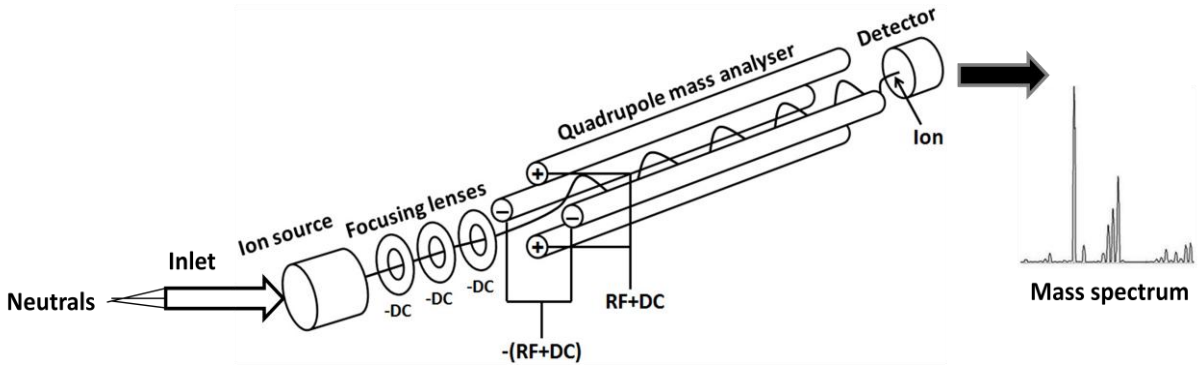

Figure 1.1: Schematic diagram for a Quadrupole Mass Spectrometer.

In a quadrupole device the field is described by its linear dependence on the co-ordinate position. The quadruple field is ideal and presents no space charge effects. The potential at any point (x,y,z) can be described by the equation [4]:

$$\phi = \frac{\phi_o}{r_o^2}(\lambda x^2 + \sigma y^2 + \gamma z^2) \tag{1.1}$$

where Φ_o is the applied field, λ, σ, γ are weighing constants for their coordinates and r_o is the inscribed radius of the electrodes. Φ_o is given by:

$$\phi_o = U - V\cos(\Omega t) \tag{1.2}$$

where U is the the amplitude of the DC voltage, V is the amplitude of RF voltage peak-to-peak and Ω (rad/s) is equal to 2πf (Hz).

It is important that the Laplace condition $\nabla^2\phi = 0$, be satisfied. That means that all quadrupole devices must comply with the below constraints: $\lambda + \sigma + \gamma = 0$ or $\Phi_o = 0$.

For a particular value of Φ_o the equipotentials (lines of constant potential) in the xy plane are four rectangular hyperbolas with asymptotes at 45° to the Cartesian axes.

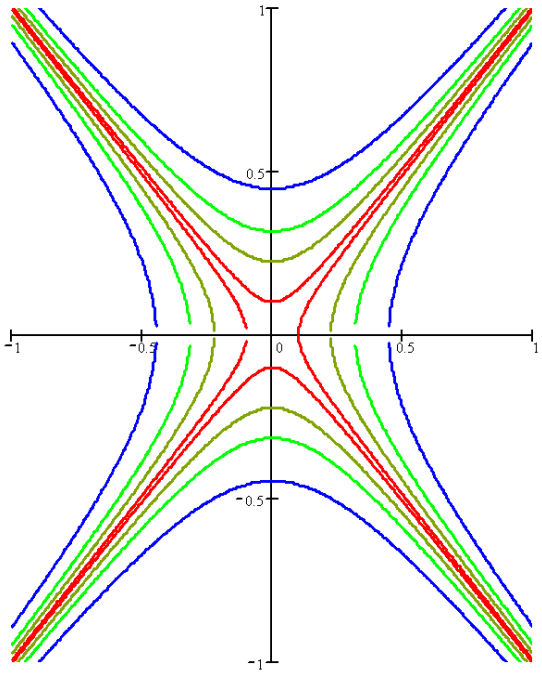

Figure 1.2: The equipotential lines for a quadrupole field.

If our interest is in the x,y coordinates of a quadrupole device $\gamma = 0$ and $\lambda = -\sigma$. If we set $\lambda = 1$ then:

$$\phi = \frac{\phi_o}{r_o^2}(x^2 - y^2) \tag{1.3}$$

The equations of ion motion for an ion with mass m and charge q are:

$$\frac{d^2x}{dt^2} + \left(\frac{e}{mr_0^2}\right)\Phi_\circ x = 0 \tag{1.4}$$

$$\frac{d^2y}{dt^2} + \left(\frac{e}{mr_0^2}\right)\Phi_\circ y = 0 \tag{1.5}$$

$$\frac{d^2z}{dt^2} = 0 \tag{1.6}$$

Substituting the equation 1.2 into the 1.4 and 1.5, the equation of motion for this ion becomes [4]:

$$\frac{d^2x}{dt^2} + \left(\frac{e}{mr_0^2}\right)(U - Vcos(\Omega t))\, x = 0 \tag{1.7}$$

$$\frac{d^2y}{dt^2} + \left(\frac{e}{mr_0^2}\right)(U - Vcos(\Omega t))y = 0 \tag{1.8}$$

Defining

$$a_u = a_x = -a_y = \frac{4eU}{mr_0^2\Omega^2} \tag{1.9}$$

$$q_u = q_x = -q_y = \frac{2eV}{mr_0^2\Omega^2} \tag{1.10}$$

and expressing time in terms of the parameter $\xi = {}^{\Omega t}/_{2} = 2\pi f t$, we obtain from 1.7 and 1.8, the following equation which is the canonical form of Mathieu equation:

$$\frac{d^2u}{d\xi^2} + (a_u - 2q_u cos2\xi)\, u = 0 \tag{1.11}$$

The solutions of Mathieu equation form the boundaries in (a, q) space between stable and unstable regions during the operation of a QMS system (Figure 1.3) [4].

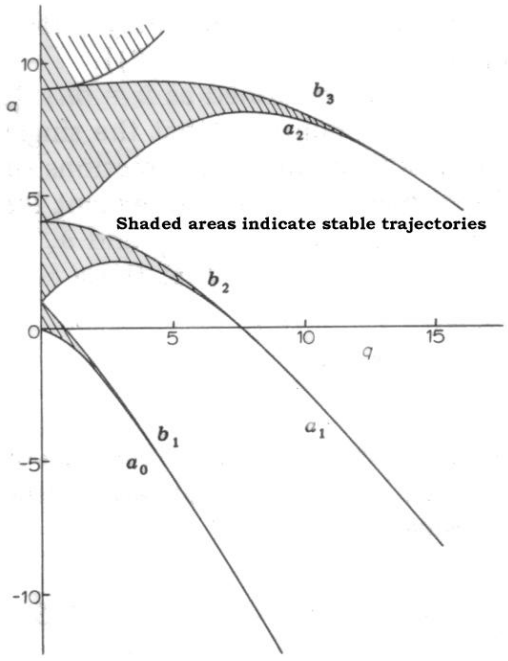

Figure 1.3: The Mathieu stability diagram (shaded areas indicate stable trajectories).

During mass analysis the produced by the ion source mass fragments travel through the mass analyser assembly. The applied potentials on the rods affect ion trajectories leading to ion separation according to their mass to charge ratio. That means that the lightest ions will be ejected and hit the detector firstly, whereas the heaviest ions will follow. Only the ions with stable ion trajectories are successfully transmitted to the detector and recorded. The ion fragments with unstable ion trajectories collide with the mass analyser electrodes and are not being ejected and finally detected. A mass spectrum is obtained by monitoring the ions passing through the quadrupole mass analyser and hitting the detector as the applied voltages on the electrodes change.

The mass range and the resolution [4, 5, 6] are two important operating characteristics of a quadrupole and they are both connected to the fundamental parameters of the quadrupole device. As such the mass range of a quadrupole mass analyser is closely connected to the diameter of the electrodes, the maximum available RF voltage and the frequency of the RF supply, whereas the resolution is mainly dependent on the length of the rods, the frequency of the RF supply and the ion injection energy.

The maximum mass of a quadrupole device is given by the following equation:

$$M_m = \frac{7\times10^6 V_m}{f^2 r_0^2} \tag{1.12}$$

where V_m is the rf voltage applied between adjacent rods, r_0 (m) is the inscribed radius of the electrodes and M_m is the maximum mass measured in amu.

The resolution (ΔM) of a quadrupole mass analyser is defined as the reciprocal of the ratio of the width of the transmitted mass spectrum peak at a defined level of transmission at a particular mass *M*. A representation of the relationship between mass and resolution is given by the equation below:

$$\frac{M}{\Delta M} = \frac{1}{K} N^n \tag{1.13}$$

Where ΔM is the width of a peak at mass M and M is the mass of the peak. N is the number of cycles of the RF field and K depends upon the method used to define ΔM and on the radius of the rods r_0.

1.6. References

[1] European Union, http://europa.eu/index_en.htm.

[2] J. Yinon, *Detection of Explosives by Electronic Noses,* Anal. Chem. **75,** 98-105 (2003).

[3] SNIFFLES, http://www.sniffles.eu/.

[4] P. H. Dawson, *Quadrupole Mass Spectrometry and its Application,* Elsevier, Amsterdam (1976).

[5] E. D. Hoffmann, V. Stroobant, *Mass spectrometry principles and applications*. Wiley (2007).

[6] A. E. Holme, W. J. Thatcher, J. H. Leck, *An investigation of the factors determining maximum resolution in a quadrupole mass spectrometer*, J. of Physics E: Scientific Instruments. ***5,*** 429-433 (1972).

[7] G. L. Glish, R. W. Vachet, *The basics of mass spectrometry in the twenty-first century*, Nature **2,** 140-150 (2003).

Chapter 2
Artificial sniffing for security applications

2.1. Introduction to artificial sniffing

Worldwide border policing for homeland security faces major challenges due to threats from national or international terrorism and well organised crime [1, 2]. Continued increase of illegal immigration and human trafficking (especially of children and women) is of particular concern as well as problems associated with illegal transportation of narcotics, explosives, chemical weapons and other restricted goods. Existing mainstream technology for bulk or trace detection of threat compounds (natural or chemical) and of human trafficking has limitations and is still investigated for improvements.

Olfaction arises from the stimulation of the olfactory system by odorous compounds and has always been and remains one of the most important biological procedures to discern certain information about the surrounding environment and more specifically for maintaining welfare conditions regarding defence against potential threats and/or safety conservation related issues. Both in microsmatic (human) and macrosmatic species (sniffer dogs) the sniffing process is approximately the same, whereas differences in the olfactory epithelium structure and in the olfactory acuity are massive. This sniffing process consists of inhaling air samples firstly in tiny quantities to detect odorants that carry certain information in low concentration levels. Depending on the morphological parameters of the olfactory system (nasal cavity, epithelium, bulb, lobe, receptor cells and neurons, etc.) and on genomic factors, brain signal interpretation and species physiology, this analytical process changes [3-6]. Briefly, the sniffing procedure can be described by the following steps:

a) pulsed sampling (inhalation) of air molecules during a certain period of time (data acquisition),
b) entrapment of specific odorant substances (VOCs) by the receptors covering the olfactory epithelium,
c) detection and odour discrimination according to the olfactory receptor neurons' function,
d) data processing and signals interpretation,
e) odour recognition.

Artificial sniffing may be described as the sum of those techniques and processes that attempt to reproduce the functionality of the sense of smell originating either from human beings or from animals (e.g. canines, sniffer dogs, mosquitoes, etc.). Artificial sniffing is a multidisciplinary field which employs, combines and integrates different areas of science, technology and engineering to explore (through a mimetic and metaphoric approach) and to replicate olfaction by developing smart systems or arrays which can exhibit trace odour sensing capabilities. Artificial sniffers or simpler artificial noses have been successfully used in a wide range of applications [6] such as: homeland security, search and rescue, forensics, environmental, health, medicinal products industry, food industry, doping screening, quality assurance (QA) and quality control (QC). These applications can be deployed both in controlled conditions (laboratory) and in harsh (*in-situ*) environments.

2.2. Field chemical analysis

Demands for real time or near real time accurate chemical analysis, increasingly require techniques that operate ‘‘in the field’’. Field chemical analysis eliminates sample transportation/storage costs and minimises sample contamination risks during shipment from a distant site back to the laboratory [7]. In addition to time and cost reduction, field analysis allows rapid problem-solving, decision-making and operational simplicity. Field chemical analysis is therefore a rapidly evolving and promising research area focusing on bringing the required (for each case) analytical equipment to the sampling area, instead of the traditional procedure; transportation of the sample to the laboratory.

This inversion of methodology has raised new functional and operational issues which need to be addressed. These are related to a) analytical instrumentation specifications, b) analytical performance and c) sample collection, preparation and sample introduction requirements [8]. New analytical criteria have been established to evaluate instrument performance and to accommodate or fulfil essential field requirements, such as portability (this includes: apparatus size-overall dimensions, total weight, hand carry or backpack carry option), field-applicability, robustness (absorption of vibrations, waterproof protection, heavy duty protection), reliability (analytical stability and reproducible results), power consumption (the lower, the better), user-friendliness (minimal training requirements and simple operation via graphical user interface), low maintenance costs, fast analysis (within seconds), high sensitivity (low detection limits) and accuracy [9-11].

During the last few years, the number of requests (from different research and industrial areas) for on-site chemical analysis increased vertically. However, quite often, the desire for field measurements hides potential health risks or hazards for the operating personnel. To prevent and to address possible health, safety and operational issues, analytical instrumentation for *in-situ* chemical analysis (or field technology) was further improved and is still under improvement and now instrument development teams can provide a range of handheld devices or stand-off distance or remote sensing devices. Concepts for field chemical analysis during security applications include: a) detection of targeted substances in solid, liquid and gas phase, b) on-line chemical monitoring, c) chemical characterisation, d) profiling, e) mapping, and f) fingerprinting.

Major existing challenging issues during field operations are: a) the complexity of the background chemical environment, b) potential instrumentation drawbacks/limitations and c) the complexity of the nature of targeted sample compounds. More specifically in this chapter in which artificial sniffing in border security and forensic applications is investigated, the following problems may arise on-site:

a) complex odorous chemical backgrounds interfering with targeted threat compounds and causing false-positive or false-negative alarms or even sometimes camouflaging potential threat events,
b) extremely low threat signals-concentration levels (e.g. very low chemical odorous signals are emitted from human body and are diluted in complex backgrounds with various interferences for the cases investigating illegal human trafficking, inventive

terrorism and crime scenarios for concealing illegal and hazardous substances for threat transportation cases, etc.),

c) complex mass transport phenomena of threat odour plumes are usually difficult to model and to simulate,
d) lack of fully integrated threat reference substances libraries,
e) threat samples nature (homemade, standard), quantity (trace or bulk) and properties (e.g. very low vapour pressure values make detection difficult or sometimes unfeasible),
f) geographic, environmental and weather conditions such as altitude, density of air, humidity, temperature, wind velocity and direction etc.,
g) lack of sufficient number of threat detection devices (able to detect, monitor and locate potential dangers) with fast response times and specially trained operating personnel (here the case of sniffer dogs-handlers is also included, as the current number of canines and their handlers is not sufficient to monitor all the security checkpoints),
h) high purchase and maintenance costs of threat detection devices.

2.3. Sniffer animals

A wide range of domestic, semi-domestic or other animals have been specially trained and successfully used for *in-situ* border control, security and forensic applications [12]. Most of them give good field performance (fast response times, trace threats detection and early localization), but usually are associated with high training time issues and cost drawbacks. For instance, sniffer dogs which can easily (within seconds) detect drugs, explosives, weapons, mines, live human bodies (illegal immigrants), tobacco, cash and cadavers in the field, usually require several months (approximately 4-6) of costly training (current estimate £10,000) before they obtain employment. The initial selection of a sniffer dog is usually done by a series of tests performed by specialist teams. Not all dog breeds are suitable for providing working dogs. The most popular breeds for security purposes use are the German, Dutch and Belgian shepherds, Labradors as well as the cocker spaniels. The canines effectiveness depends on their training, age, experience, searching protocols, their personality, and the developed collaboration/obedience level with their handler as well as with the environmental/weather conditions of the field (e.g. canines can detect targeted

substances with ease when the wind/air direction is towards them). Moreover, there are no sniffer dogs capable of versatile (i.e. universal) threat detection. Some canines are trained and able to detect explosives, others can detect narcotics, whereas others can detect live or dead human bodies etc. The dogs' training is based on stimulus-reward techniques and that usually employs simulant compounds to the original energetic compounds, precursors, breakdown products or taggants. Quite often, during action, canines require breaks (for every 40 minutes of work, they require 1 hour break before they can carry on working) and sometimes retraining or conservation of their attention with additional search-reward games. The dogs' task usually requires a dog-handler to be present and this increases highly the maintenance costs per year. In addition, canines' transportation costs during overseas operational searches in the field are usually high. Large volume facilities such as airports or cargo services require a number of handler-sniffer dog teams to maintain constantly secure. The above described limitations of sniffer dogs are disadvantages emanating from the financial and management point of view. However, from a scientific perspective, sniffer dogs have been proven to be unique in threat detection operations in the field due to their extremely delicate olfactory system and acute scent recognition-interpretation ability [12-17].

Some researchers have worked closely with insects and more specifically with honey bees. Honey bees' behaviour has been studied and they have been trained using Pavlovian conditioning techniques to detect explosive materials (TNT, C4, TATP) emitted by solid or liquid bombs at very low concentrations (ppt levels). Sniffer bees' training/conditioning can be completed rapidly within some days using relatively simple processes. Due to their speed, low-cost training and to their abundant populations, bees can be employed to fly over a certain area and scan it for potential threats within a short time. Their physiology and acute olfaction gives them the ability to sample all states of matter (liquids, gases, solids). However, honeybees are still not suitable for threat detection and localization applications in airports or confined spaces, due to practical issues, such as their interaction with humans. Moreover, it is essential to report here that honeybees are highly affected by the weather conditions and the presence or absence of light. For example honeybees cannot work during night or in a cold and rainy or high humidity environment. Further investigation of honeybees sniffing abilities in various experimental conditions is needed [12, 18, 19].

African giant pouched rats have also been used in the lab and on-site to search and alarm on vapours from explosives, landmines, bombs and drugs (e.g. cocaine) [20-22].

An advantage for sniffer rats' use is that their training, maintenance and transportation costs are relatively low compared to sniffer dogs. Moreover rats, due to their size and weight are very flexible during operations. Recently, pigs [23] have been reported for their sniffing abilities to detect landmines.

Eelworms such as the nematodes *Caenorhabditis elegans* have a very well developed chemosensory receptors system that allows them to provide olfactory detection of volatile compounds associated with explosive or precursors from different chemical classes at various concentration levels. In a recent study, *C. Elegans* response to 17 explosive-related compounds was examined, providing positive detection results [24]. However, they presented limited response to the original explosive materials. Finally, hard-wired moths [25] have been trained, using a novel prototype system that uses electromyography, to react to specific chemical odour signatures emitted from explosives or landmines.

2.4. Existing technologies for artificial sniffing

Chemical detection of target compounds related to border security applications, such as human body odour, drugs of abuse, explosives and chemical warfare agents (CWAs), as mentioned above is still limited with existing instruments available on the market. The following subsections present an overview of the existing available technologies reported in the scientific literature for threat screening, and offer brief descriptions about their functional principles. Emphasis will be given to technologies that have been developed for in-field security operations, but laboratory-developed and tested techniques will also be summarised.

2.4.1. Electronic noses

Electronic noses (EN) or e-noses are intelligent chemical sensor array systems, typically consisting of two major components: (a) a single chemical gas sensor or an array of chemical sensing systems and (b) a pattern recognition system [4-6, 26-28]. Most frequent sensors are the metal oxides semiconductors (MOS) and conducting polymer sensors. MOS are manufactured in a large scale, and are insensitive to humidity and have long self-life (5 years). Nevertheless, MOS sensors limitations

include the binding with substances like sulphur compounds and weak acids and the high working temperatures. Polymer sensors are cheap and operate at ambient temperatures. However, their relatively slow response times (20-40 sec) and drift over times are their main drawbacks, resulting to no repeatable results over long periods of time [26, 27].

EN functional principles are relatively simple [6]. During operation, every single chemical odorous component presented to the e-nose sensor system produces a response (e.g. an electric signal) which can be considered as the characteristic odour signature for the examined scent. The interaction of various different gas vapours with the embedded sensor transducer can yield to the production of a library-database with characteristic odour signatures. The chemical detection and identification of an odorant compound in the framework of a certain application can be done by comparing e-nose output signals with a standard reference signal. Sensor array systems generally are better performing compared to the single sensor systems, due to the fact that they offer enhanced selectivity and multi-component identification.

Traditionally, electronic noses were based on chemical gas sensors (chemiresistors or gravimetric sensors). However, demands on target threat (explosives, landmines, etc.) compounds selective detection, increased sensitivity and quantification issues, raised the need for employment of new technologies. Recent advances in other scientific areas or approaches combined with characteristics such as miniaturization and hand portability, led to the development of a wide range of sensing e-nose systems based on different technologies. Therefore, electronic noses have been benefited from developments in optics (e.g. fiber optics based detectors [29]), in piezoelectrics (surface acoustic waves detectors [30]), in fluorescent polymers [31], in nanotechnology (gold nanoparticle based chemiresistors [26]), and in micro-electromechanical systems (MEMS) [32, 33]. From a wider perspective, as electronic noses can also be considered analytical instruments with machine olfaction capabilities (gas detection, chemical determination and quantification); such as mass spectrometry (MS) based devices, ion mobility spectrometers (IMS), and gas chromatographers (GC) [26, 33, 34]. These technologies are described in detail below.

EN even their advantageous characteristics (small size, inexpensive, portable) and potential for reliable threat and illicit substances field detection, they still require further testing and improvements to cover (e.g. instability and specificity issues).

2.4.2. Mass Spectrometry

Mass spectrometry (MS) is a powerful established analytical technique widely considered to be the gold standard for chemical analysis [35, 36]. It works by creating ions from neutral atoms and molecules and separating them according to their mass-to-charge ratios. Mass spectrometers can be applied for both in-laboratory measurements and on-site operations, either as standalone devices or combined with other analytical instruments. MS offers high sensitivity, low detection limits (LODs), high selectivity, fast response times and board applicability (analysis of almost all the types of molecules; from small volatile compounds to big biomolecules and biological species). Moreover, targeted compounds for analysis can belong to all states of matter (gaseous, liquid, solid). Mass spectrometric output data carry qualitative and quantitative information that can be used for chemical detection, identification and characterization as well as for the investigation-prediction of molecular chemical structures. The main components of a mass spectrometer include:

1. Sample inlet (gas inlet, atmospheric pressure inlet, etc.)
2. Ion source (electron impact, electrospray, atmospheric, etc.)
3. Mass analyser (quadrupole mass filter, ion trap, time-of-flight, magnetic sector, etc.)
4. Detector (Faraday, electron multiplier, photomultiplier, etc.)
5. Vacuum system (usually turbomolecular pump backed by diaphragm or rotary pump)

Some decades ago, mass spectrometers were large analytical devices for only laboratory use. However, late developments in size and weight miniaturization (e.g. miniaturisation of mass analysers, detectors, vacuum system, etc.), as well as in power consumption reduction converted them into portable devices ideal for in-field operations worldwide [11]. Portable mass spectrometers were specially deployed to address specific applications. This gave them, in many ways, operational flexibility and advanced analytical capabilities. A very important stage for field (and not only) trace chemical analyses was the introduction of sample molecules into the MS vacuum system (e.g. direct leak, membrane inlet, pulsed sampling system etc.). To address the trace detection issue, sample pre-concentration [e.g. with solid phase microextraction (SPME) fibres, cartridges adsorption-desorption, etc.] and collection methods (tedlar

bags, wipes, etc.) were established prior analysis. Advanced methodologies which required no sample preparation and provided fast analysis times were developed [34].

Novel ambient environment ionisation techniques were also proposed, investigated, tested and evaluated to ionize substances with a range of sizes and structures as well as those with very low or extremely low vapour pressure values such as the common explosives and narcotics from complex matrices. Atmospheric pressure chemical ionization (APCI) [26, 37] integrates both sample and carrier gas (e.g. acetonitrile, etc.) ionization using a corona discharge. This technique has been used to detect explosive materials such as 2,4,6-trinitrotoluene (TNT) or 2,4-dinitrotoluene (DNT) in low concentration levels from human hands' surface using sample collection swabs.

Desorption electrospray ionisation (DESI) [38-44] combines the basic principles of desorption and electrospray ionisation and is one of the most well-known universal ionisation techniques *in situ*. In DESI a stream of charged droplets splash the surface under examination and this collision produces ions for MS analysis. Threat compounds (e.g. RDX, TNT, PETN, C-4, Semtex, TATP, etc.) were analysed and identified using this technique from various surface materials including glass, paper, clothing, metal surfaces, etc., in the low nanogram range. Direct analysis in real time (DART) [45] was also used to ionize threat components directly from surfaces (e.g. clothing, banknotes, etc.) without prior sample preparation. DART as a technique is akin to DESI. In DART an electric charged carrier gas is bombarding the under examination surface area and transfer sample ions into the MS for analysis.

Additional to the above described ambient environment ionisation techniques for threat detection, the following techniques were also developed to enhance sample introduction into the vacuum system: low temperature plasma (LTP) [10, 46], desorption atmospheric pressure photon ionization (DAPPI) [47], desorption atmospheric pressure chemical ionization (DAPCI) [48, 49], secondary electrospray ionisation (SESI) [50-53], secondary ion mass spectrometry (SIMS) [54], paper spray ionisation (PSI) [55, 56], easy ambient sonicspray ionisation (EASI) [57, 58]. In general terms, they presented positive detection results (low LODs and fast responses).

Commercial portable MS systems available in the market are presented in Table 2.1 (classification from the heavier system to the lighter). Information regarding their mass analyser and summarised specifications are given. Griffin^{TM} 824 from FLIR Systems Inc. (Wilsonville, USA) [59] uses a surface wipe sample introduction technique to inject sample molecules into the vacuum system. Sample molecules are ionised by a non-

radioactive positive ionisation source before they enter to the cylindrical ion trap mass analyser for separation. TRIDION™-9 GC-MS and GUARDION™-7 GC-MS from Torion Technologies, (UT, USA) [60] are man-portable GC-MS. Sample introduction is done by an SPME fibre or a needle trap. The field-portable GUARDION™-7 GC-MS has been successfully examined in the analysis and in the detection of CWAs such as sarin (GB), soman (GD), cyclosarin (GF), VX and distilled mustard gas (HD). Mini 10 and Mini 11 from Purdue University [61] have been tested with different inlet types (e.g. direct leak, MIMS, etc.) and ambient ionisation modes (e.g. DESI, DART, DAPPI, DAPCI, LTP, PSI, etc.). MMS-100™ from 1st Detect (Austin, TX, USA) uses a heated membrane inlet with a preconcentrator for enhanced sensitivity. The palm portable MS from the Samyang Chemical Corp was presented in the 6th Harsh Environment MS (HEMS) Workshop in 2010 and uses a pulsed gas valve for direct sample injection [63].

Table 2.1: Ion trap MS systems available in the market specially developed for threat detection.

Supplier	Model	Mass analyser	Mass range (m/z)	Power (W)	Weight (kg)
FLIR Systems Inc.	Griffin™ 824	Cylindrical ion trap	N/A	N/A	22.7
Torion Technologies	TRIDION™-9 GC-MS	Toroidal ion trap	45-500	80	14.5
Torion Technologies	GUARDION™-7 GC-MS	Toroidal ion trap	50-500	75	13
Purdue University	Mini 10	Rectilinear ion trap	N/A-550	70	10
1st Detect	MMS-100™	Cylindrical ion trap	15-625	N/A	8
Purdue University	Mini 11	Rectilinear ion trap	N/A-2000	30	4
Samyang Chemical Corp	Palm portable (without pump)	Quadrupole ion trap	N/A-300	5	1.5

2.4.3. Ion Mobility Spectrometry

Ion mobility spectrometry (IMS) is one of the most popular routine analytical technologies used *in-situ* for detection and monitoring of illegal drugs, explosives, chemical weapons and toxic industrial chemicals (TICs) [7, 64-72]. It works by analysing ions in the gas phase at ambient pressures. IMS offers rapid analysis, usually

within some seconds. Security and military authorities use widely handheld IMS based devices during in-field and real-time applications due to their advantageous characteristics such as: portability, robustness, operational simplicity, user-friendliness, selectivity and trace levels sensitivity. The IMS operational principle is based on the separation of ionized molecules according to their mobility through a drift tube with an applied electric field and a carrier buffer gas opposing ion motion. Ion motion depends on ion mass, shape, size and charge.

Sample collection and sample introduction techniques during border security screening can be done by various ways. Usually sample collection is performed in a non-intrusive manner. Most common sampling methods are: a) direct sampling of gaseous phase or vapour molecules, and b) sampling using a swab filter or a membrane with certain adsorption characteristics over a suspect surface (e.g. luggage, passenger hands, coat, colognes bottles, banknotes etc.) followed by thermal extraction of the molecules of interest in the IMS using desorption heating techniques or through a gas chromatography injection system. Desorption heating techniques are mainly applied and focus in the detection of non-volatile compounds or compounds with very low vapour pressure values (e.g. the majority of explosives and illegal drugs).

The next stage during IMS operation, after sample introduction, is the ionisation of sample analytes. IMS devices employ soft ionisation techniques at atmospheric pressure to create reactant ion clusters which will be mixed and interact with sample vapour phase analytes and will finally form target sample ions. The ionisation source traditionally is based on the following materials ^{63}Ni, ^{3}H or ^{241}Am. These materials are radioactive but retain the ionisation sources very stable and resistant during measurements. The radioactive nature of these sources raises safety concerns as well as often transportation issues. However, recent advances in IMS development brought up the use of nonradioactive ionisation sources [33, 68, 73] based on photoionisation (PI) [e.g. atmospheric pressure photoionisation (APPI) [74, 75]], corona discharge ionisation [76], electrospray ionisation (ESI) [77] or matrix-assisted laser desorption ionisation [78]. Ambient ionisation techniques such as desorption electrospray ionisation (DESI) [79], secondary electrospray ionisation (SESI) [80], laser spray ionisation (LSI) [81], atmospheric-pressure solids analysis probe (ASAP) [82], low temperature plasma (LTP) [83], direct analysis in real time (DART) [84], initially developed for the direct analysis of sample surfaces during MS operation, have also been successfully used with IMS.

When ions are created, they travel directly to the drift region of the IMS, passing firstly through an ion-gate. The presence of the ion-gate between the ionisation source region and the drift tube region offers electronic control of ion injection as discrete packets. In the drift tube region an electric field is applied. There are different types of IMS instruments available in the market such as systems working with low electric fields (e.g. 200-300 V/cm) and systems working with high electric fields (e.g. 10.000-30.000V/cm). Also different IMS analyzers [68, 69] work either in ambient pressure (e.g. drift-time, aspiration, differential, field asymmetric ion mobility spectrometers [85-87]) or in reduced pressures (e.g. drift-time, traveling-wage ion mobility spectrometers). The final part of an IMS device is the detector. Usually a Faraday plate is used to detect ion signals. However IMS can be coupled with and act as a pre-separation technique-stage to other analytical devices such as mass spectrometers, to offer enhanced analytical results. Ion mobility mass spectrometry (IMMS) [88] combines the principles and advantages of both IMS and MS. IMS devices fit properly with MS systems and offer clearer mass spectra (elimination of background noise) and fast separation-discrimination of molecules from complex mixtures (including separation of isomers, isobars and identification of conformers due to the vantage of ion mobility separation before the mass analysis step).

Gas chromatography (GC) can also interface with IMS devices [89]. This combination offers a gas chromatographic pre-separation stage of sample molecules prior to their entrance to the IMS ionisation chamber and the drift tube region. GC-IMS provides better ionisation as it reduces the number of interferences or interactions of sample molecules in the ionisation chamber. Moreover, it produces more reliable results with enhanced sensitivity as every single ionised compound (if we make the assumption of no overlapping peaks phenomena) enters individually in the drift tube. A GC-IMS device enables two-dimensional sample separation providing 3-D sets of data (x-y-z axis: IMS drift time - IMS intensity - GC run time). Additionally to a single column GC, multi-capillary columns (MCC) GC [90, 91] can be also used to increase further detection time and to reduce false alarms making them a good tool for field operations.

An SPME-IMS system [92] was recently reported to offer pre-concentration and low LODs in explosives (nitrocellulose, RDX, PETN), in volatile constituents of explosives (2,4-dinitrotoluene, 2,6-dinitrotoluene) and in taggants (2-nitrotoluene,4-nitrotoluene, 2,3-dimethyl-2,3-dinitrobutane) detection.

The main advantages of IMS devices are their instrumental simplicity and high sensitivity (ppt detection limits). Moreover, ion mobility spectrometers offer real time monitoring capabilities with fast response times and low power consumption. IMS are light weight portable instruments (with range from 800gr to 15kg) with small dimensions (W x D x H: 230 x 101 x 57 mm – 449 x 375 x 177 mm) and easy to operate (user-friendliness). They are also very robust with low maintenance costs. The above described characteristics justify why IMS devices have great potentiality for in-field applications and are used widely in airport security checkpoints.

However, IMS sensors themselves present some limitations (which can potentially be addressed and resolved, when IMS couples with other instruments) and these are mainly related to their limited selectivity and to potential false-positive alarms usually produced by environmental or complex sample interferences. Both moisture and temperature affect adversely IMS performance. Furthermore, highly contaminated chemical environments may be a serious analytical problem for IMS. Especially when high background concentrations are present, IMS can suffer from memory effects.

Commercial field-portable IMS instruments available in the market for trace threat detection purposes can be found in the Table 2.2. Overall device dimensions, weights and sample analysis time are also given. As can be seen, analysis time is within the range of some seconds. The presented instruments offer capabilities of both trace vapour sampling collection (e.g. SABRE 5000, MMTD, Itemiser® 3 Enhanced, Hardened MobileTrace®, MobileTrace®, RAID-M 100, μRAID, ChemPro®100i, ChemRAE, GDA-FR, Lonestar, QS-H150, IMS Mini-200, Easytec-XP, MO-2M, PKI-7315) and surface wipe sampling collection (e.g. IONSCAN 500DT, ITEMISER® 4DX, Itemiser® 3 Enhanced, DE-tector, EGIS™ Defender, QS-B220, GA2100, PKI-7315).

Table 2.2: Commercially available IMS based devices for security applications.

Supplier	Model	Technology	Weight (kg)	Dimensions (mm)	Analysis time (s)	Target analytes
Smiths Detection [93]	SABRE 5000	IMS	3.2	363 x 110 x 130	20	Explosives, Drugs, CWAs, TICs
Smiths Detection [93]	IONSCAN 500DT	IMS	19	400 x 310 x 400	5-8	Explosive, Narcotics

Smiths Detection [93]	MMTD	IMS	5	483 x 216 x 203	10	Explosives, Drugs, CWAs, TICs
SAFRAN Morpho [94]	ITEMISER® 4DX	Ion Trap Mobility Spectrometry	12	180 x 480 x 460	8	Drugs, Explosives
SAFRAN Morpho [94]	Itemiser® 3 Enhanced	Ion Trap Mobility Spectrometry	12	180 x 480 x 460	8	Drugs, Explosives
SAFRAN Morpho [94]	Hardened MobileTrace®	Ion Trap Mobility Spectrometry	5.44	438 x 159 x 324	12	Explosives, Drugs, CWAs, TICs
SAFRAN Morpho [94]	MobileTrace®	Ion Trap Mobility Spectrometry	4.3	409 x 152 x 315	8	Drugs, Explosives
Bruker Daltonics [95]	RAID-M 100	IMS	3.5	400 x 115 x 165	NA	CWAs, TICs
Bruker Daltonics [95]	DE-tector	IMS	19	520 x 435 x 400	10	Drugs, Explosives
Bruker Daltonics [95]	µRAID	IMS	1.2	130 x 64 x 223	NA	CWAs, TICs
Environics [96]	ChemPro®100i	Aspirated IMS	0.88	230 x 101 x 57	2.5	CWAs, TICs
RAE SYSTEMS [97]	ChemRAE	Open Loop IMS	0.8	228 x 102 x 50	NA	CWAs, TICs
AIRSENSE Analytics [98]	GDA-FR	IMS, PID, MOS, EC	4.2	395 x 112 x 210	> 60	CWAs, TICs, explosives
OWLSTONE [99]	Lonestar	FAIMS	7.8	383 x 262 x 195	1	TICs
Thermo SCIENTIFIC [100]	EGIS™ Defender	HSGC-DMS	27	560 x 560 x 250	10-18	Drugs, Explosives
Implant Sciences Corporation [101]	QS-H150	IMS	5.1	493 x 127 x 188	5-30	Explosives
Implant Sciences Corporation [101]	QS-B220	IMS	14.6	396 x 366 x 412	NA	Drugs, Explosives
IUT Berlin [102]	IMS Mini-200	IMS	6.5	280 x 100 x 280	NA	CWAs, TICs
Ion Applications, Inc. [103]	Easytec-XP	IMS	1.8	NA	NA	Explosives, Drugs, CWAs
Excellims [104]	GA2100	HPIMS	NA	NA	NA	Explosives
Sibel [105]	MO-2M	Non linear IMS	1.4	305 x 120 x 86	2	Drugs, Explosives
PKI-electronic[106]	PKI-7315	IMS	4	430 x 113 x 205	5-10	Explosives

2.4.4. Instruments based on other technologies

2.4.4.1. Gas chromatography

Gas chromatography (GC) is a technique that separates complex mixtures that travel through a mobile phase (gas) over a stationary phase (liquid or solid) [107]. The partition of each single substance and subsequently the order of elution; depends on the physical and chemical properties of the each individual compound (boiling point, polarity, etc.) as well as on their interaction with the stationary phase. The most common detectors used during GC analysis are the flame ionisation detectors (FID) and the thermal conductivity detectors (TCD). Usually GC is combined with other analytical techniques such as MS or IMS to offer improved chemical detection and accurate compounds identification. However, a typical GC analysis time can vary from a few minutes to more than an hour.

High-speed gas chromatography (HSGC) has been used combined with micro differential IMS and has produced a commercial drugs and explosives (e.g TATP, HMTD, plastic explosives, etc.) portable fast detection system (EGIS^{TM} Defender) [100] provided by Thermo Fisher Scientific Inc. (Table 2.2). DLP-E4500 portable explosives detector from DPL-Surveillance-Equipment.com [108] is a lightweight (5 kg) GC-chemiluminencence system, capable of detecting nitro based and peroxide explosives within some seconds. Chemical weapons and associated with them compounds were also detected using a GC system coupled to a Fourier transform infrared spectrometer (GC/FT-IR) [109]. GRIFFIN 400 from FLIR Systems Inc. [59] is a GC/MS system that can be used for narcotics, explosives, TICs and CWAs detection and can be integrated in mobile lab units or in security checkpoints.

2.4.4.2. Infrared spectroscopy

Infrared spectroscopy (IR) usage has also been demonstrated in explosives detection. IR principle is based on the measurement of an infra-red beam that is absorbed from a target sample. This infra-red beam gives a characteristic fingerprint spectrum of the under examination chemical compound and provides information regarding its chemical bonds, characteristic chemical groups and its structure [110]. In combination with other analytical techniques (MS, NMR, UV), it can be used for the identification of unknown chemical compounds and their structure. The traditional IR techniques present slow

response times. Fourier-transform IR (FTIR) firstly developed in the seventies, offers faster measurement times (simultaneous scan of all target wavelengths), high sensitivity (at least one order of magnitude compared to the conventional IR systems) and internal automated calibration. FTIR devices provide reliable and repeatable results that can be used for both qualitative and quantitative chemical analysis [111].

A fibre optic coupled grazing angle probe reflection/adsorption IR spectrometry (FOC-GAP-RAIRS) method has been developed and tested successfully to detect and quantify high explosive trace materials on metallic surfaces [112]. Detection limits of 160 ng/cm^2 for TNT, 220 ng/cm^2 for PETN and 400 ng/cm^2 for HMX were achieved. This combined technique allows on-site measurements of nitroexplosives whereas further exploration on other threat compounds detection, identification and quantification on different surfaces (glass, plastic, etc.) is required. Commercially available IR device is the MIRAN SapphIRe portable ambient multi-gas analyser from Thermo Fisher Scientific Inc. which permits non-destructive substance identification and monitoring in the sub-ppm area [100]. Thermo Scientific TruDefender FT and TruDefender FTi are lightweight (1.3 kg and 1.5 respectively) handheld ergonomic FTIR spectroscopy systems for unknown chemicals and explosives identification within some seconds [100].

2.4.4.3. Cavity Ring-Down spectroscopy

Cavity Ring-Down spectroscopy (CRDS) is based on reflactometry. A pulse of laser light is injected into a cavity with highly reflective mirrors containing a sample material. Once the laser light is turned off, the laser exponential degradation is measured in correlation to time and then compared with the laser exponential decay in the case when the cavity is empty. The obtained spectrum and the decay rate are characteristic of the under examination sample compound. CRDS offer real-time measurements and presents a very high sensitivity but a lack of selectivity in the near infra-red region [113]. Picarro CRDS analyser, developed by Picarro Inc. (California, USA), has been tested to detect vapour traces (low ppb) of common explosives (TNT, TATP, RDX, PETN and Tetryl) [114].

2.4.4.4. Laser-induced breakdown spectroscopy

Laser-induced breakdown spectroscopy (LIBS) utilise a high intensity laser pulse to vaporise sample and produce a plasma plume. The emitted light from the plasma plume has a characteristic frequency and can be used for the identification and characterisation of the sample material. Portable LIBS is ideal for *in-situ* operations as it offers direct sensitive and non-destructive real time chemical analysis with no sample preparation requirements. LIBS offers also stand-off threat detection capabilities for prevention of terrorist events at distances up to 100 m. Double pulse LIBS provides an enriched produced plasma plume, allowing by this way an improved discrimination among sample molecules and atmospheric components and eliminating potential false positive alarms [115, 116].

A representative commercial LIBS based device is the mPulse from Oxford Instruments plc. [117]. Applied Photonics Ltd [118] has also developed a LIBS system, the ST-LIBS^{TM}, for remote chemical, biological, radiological, nuclear and explosive materials (CBRNE) detection with range capability in excess of 100 metres. U.S. Army Research Laboratory in collaboration with Ocean Optics Inc. developed a man-portable LIBS sensor for hazardous compounds (explosive, CWAs, biological agents, landmine) detection [119].

2.4.4.5. Raman spectroscopy

When a sample undergoes laser light excitation, the scattered photons transit up or down in the energy-level diagram. Raman spectroscopy relies on the inelastic scattering of photons and measures their vibrational transitions. By this way identification of unknown chemicals can be done. Raman spectroscopy has the ability to penetrate various surfaces such as polymer or glass containers and identify potential threat or hazardous compounds. This can be explained by the fact that, when a weakly focused incident laser beam pass through varying qualities, colours and thicknesses of glass and polymers leads to relatively weak Raman scattering and different weak Raman spectra from the containers. This allows samples analysis with no significant spectral contribution from their container. Raman spectroscopy is a well established technique with fully integrated threat libraries, implemented in security checkpoints for public safety [120, 121].

Field-portable Raman spectrometers for threat detection include the compact and lightweight (2.7 kg) RespondeR RCI and the ACE-ID (0.45 kg) provided by Smiths Detection Inc. [93]. The ACE-ID instrument can be operated with just one hand and is especially designed for harsh environments applications. The FirstDefender RM (0.8 kg), FirstDefender RMX (0.92 kg) and AhuraFD (1.8 kg) are also hand portable instruments developed and provided by Thermo Fisher Scientific Inc. [100] for the same explosive and threat components identification and detection purpose. The portable i-Raman®EX from B&W Tek Inc. (Newark, DE, USA), uses Raman spectroscopy to deliver explosives, CWAs and forensic related analytes detection. SAFRAN Morpho S.A. (France) [94] has developed StreetLab® Mobile (3 kg); an ergonomic, ruggedized, handheld Raman technology based device for TICs, explosives, narcotics and chemical weapons detection in the field. Cobalt Light Systems Ltd. (Oxfordshire, UK) [122] used spatially offset Raman spectroscopy (SORS) to develop a fast bench top (but not handheld) liquid explosive detection system, the Insight100. SORS offers precise chemical screening of liquids concealed in non-metallic bottles or containers with various outer characteristics. Insight100 has already been deployed in many airports, offering stand-alone services or complementing other security screening systems.

2.4.4.6. Terahertz spectroscopy

Terahertz spectroscopy (THz) employs electromagnetic fields with frequencies in the terahertz region (0.1×10^{-12} Hz to 10×10^{-12} Hz) to penetrate objects, surfaces, materials (especially non metallic such as textiles, etc.) and through the absorbed radiation to detect concealed explosives or weapons. Threat substances give characteristic THz spectral signatures (THz fingerprints), allowing their detection through THz spectroscopy based sensors. THz radiation is not ionizing radiation (compared to X-radiation) so it is safe for screening humans at security checkpoints [123-125].

TPS Spectra 300 from TeraView Ltd (Cambridge, UK) [126] is a flexible transportable THz based explosive system. It has been successfully evaluated with Semtex, PE-4, RDX, PETN, HMX and TNT hidden beneath clothes (made from different fibre materials e.g. cotton, nylon, wool, leather, polyester, silk, etc.) and in the soles of shoes.

2.4.4.7. Fluorescence spectroscopy

Fluorescence spectroscopy comprises the manipulation of a beam of light to excite electrons in molecules and cause them to emit light. Fluorescence sensors have been deployed to detect explosive vapours at ultra low levels [127].

Fido® X3 and Fido® NXT from FLIR Systems Inc. (OR, USA) [59] are lightweight (1.36 kg each of them) hand portable fluorescence polymer sensors for the rapid and non-invasive explosive threats detection fielded in many U.S. airports. They are capable of detecting both solid and liquid explosives, including ammonium nitrate, plastic explosives, hydrogen peroxide and nitromethane.

2.4.4.8. Optical sensor based systems

Optical sensors for security or military purposes are classic detection systems, utilising optics technology to locate threat components. A robust, remotely operated robot for military field use is the TALON® from QinetiQ (Farnborough, UK), which integrates optical, infrared, thermal, night vision and fisheye cameras to locate and disarm explosive devices [128].

2.4.4.9. Chemical sensors

Chemical sensing systems are based on a selective chemical reaction when they interact with a threat component that yields to a characteristic distinct outcome (e.g. colour variation, etc.).

EXPRAY from Plexus Scientific Inc. (VA, USA) is a commercially available portable kit for explosives and explosive residues detection. It offers nanogram detection limits within 60 sec with high reliability and easy operation. The DropEx Plus kit from the same company has the same principles and can be applied in a wide range of explosives including: nitroaromatics, nitrate esters and nitramines, inorganic nitrated based, chlorates and bromates as well as peroxide-based explosives [130].

2.4.4.10. Electrochemical sensor based systems

Electrochemical sensors have been developed for the fast trace detection of explosives and CWAs. They are based on the output electrical signal (voltage, current,

conductivity) of a chemical reaction of a target compound of interest with the surface of a sensing electrode. For example, when a vapour sample enters into an electrochemical sensor, it passes firstly through a gas permeable membrane barrier that ensures certain sample importation and then it meets a sensing electrode with which is reacts with oxidation, with a reduction mechanism etc. and produces an electrical signal [130].

AreaRAE Steel multi gas system (6.3 kg) provided by RAE Systems Inc. (CA, USA) is commercially available and incorporates electrochemical, photoionisation and catalytic combustion sensors to monitor toxic gases and other potential threats [97].

2.4.4.11. Surface acoustic waves based sensors

Surface acoustic wave (SAW) sensors utilise acoustic waves to sense and monitor chemical signatures emitted by hazardous compounds, explosives, landmines and CWAs. HAZMATCAD Plus from Microsensor Systems Inc. (Kentucky, USA) uses a hybrid technology of SAW and electrochemical sensors to detect TICs and CWAs. Electronic Sensor Technology Inc. (California, USA) have manufactured zNose® 4600 which is a portable GC-SAW system that offers speed (5-60 sec) field detection of narcotics (e.g. heroin, cocaine, marijuana, LSD, methamphetamines, etc.), bombs, chemical agents (e.g. GB, GD, HD, etc.) and explosives (e.g. RDX, PETN, TNT, ammonium nitrate, black powder, etc.). It works by separating sample molecules passing through the GC and then chemical detection on the SAW detector. The zNose® 4200 instrument developed by the same company is also based in the same operating principle of GC-SAW detection. Furthermore, the Joint Chemical Agent Detector (JCAD) is a lightweight device (0.9 kg) provided from BAE Systems Plc. (London, UK) that uses SAW technology to detect vapours arising from a broad variety of CWAs (VX, GA, GB, HD, L, AC, CK, etc.).

2.4.4.12. Colorimetric sensors

Colorimetric analysis has been extensively used in narcotics and explosives field detection. It uses visible light interactions with chromophore molecules which are able to absorb certain wavelengths of light and can reflect a colour. TraceX explosive detection kit from Morphix Technologies Inc. (VA, USA) is designed to address common explosive and bomb detection issues at trace levels within few minutes [131].

KeDetect XD4 from KeTech (Nottingham, UK) [132] is a portable swab kit for ammonium nitrate based explosives detection, whereas KeDetect XD6 was developed for high explosive detection such as PETN, RDX and TNT. KeDetect XD8 belongs in the same colorimetric test kit series and was specifically generated to detect peroxide or chlorate based explosives in less than a minute. Ex-Detect^{TM} Mini XD-2 from Spectrex Corporation (California, USA) [133] is also a compact and tested explosive and gun propellants detection kit with detection limits in the nanogram area. The Seeker XDU^{TM} supplied by DetectaChem (TX, USA) [134] is a handheld system able to detect explosives (e.g. nitroaromatics, nitrate esters, nitramines, inorganic nitrates, chlorates, peroxides, perchlorates, etc.) in both bulk and trace amounts. It utilise a swipe-card sample collection method, which is the key element for this field chemical analysis. Swipe sampling can be applied on surfaces varying from constructive materials to textiles, body parts, etc.

2.4.4.13. Immunochemical sensors

Immunochemical sensors employ molecular antibody-antigen interactions to specifically detect explosive compounds. These types of sensors are still under development, so there are not yet commercial available for in-field security and military operations. In the lab investigations though, have been done with various explosives such as TNT, PETN and DNT [135].

2.4.4.14. Nanotechnology sensor based systems

Nanotechnology use as a potential detection tool has become very popular, nowadays. Recent developments in carbon nanotubes technology, in molecularly imprinted polymers (MIPs) and in nanoparticles render enhanced sensitivity and selectivity threat detection and monitoring capabilities [136-138]. Nanotechnology is still under development and requires continuous improvements before it will reach the open market. Characteristically, Vaporsens device from Vaporsens Inc. (UT, USA), [139] is based on a nano-fibre sensor able to detect trace drugs, TICS and explosives. Moreover, Tracense Systems (Hertzelia, Israel) [140] has developed a miniaturised nano-wire based device for detecting chemical hazards and threats.

2.4.4.15. Flame spectrophotometry sensors

Flame photometry belongs in the atomic emission spectroscopy that is used to determine specific atoms (in the case of CWAs, sulphur and phosphorus atoms measurement). Commercial instrumentation includes the AP2C and the AP4C, both developed by Proengin Inc. (Florida, USA) [141]. These hand-held detectors are capable of detecting sulphur containing components (e.g. sulphur mustard) as well as phosphorus containing compounds such as all G (e.g. tabun, sarin, soman, cyclosarin, isopropyl ester) and V (e.g. Vx-agent, Ve-agent, amiton) warfare agents. AP4C is also able to detect all the precursors of the above chemicals. Detection can be done within 2 seconds, in sample agents emanating from all states of matter.

2.4.4.16. Comparison of the existing technologies for artificial sniffing

At this point, it is essential to provide a comparative presentation of the main advantages and drawbacks that the existing available technologies for artificial sniffing exhibit (Table 2.3).

Table 2.3: Advantages and limitations of the existing technologies for artificial sniffing.

Technique	**Advantages**	**Limitations**
EN	1. Simplicity 2. Fast response times 3. Portability 4. Inexpensive	1. Unstable results 2. Specificity issues
MS	1. High sensitivity (low LODs) 2. High specificity 3. High mass range 4. High resolution 5. Real time measurements 6. Measurements' stability 7. Accuracy 8. Portability 9. Fast analysis times (s)	1. size and weight 2. power consumption 3. high costs (purchase and maintenance)

	10. Qualitative and quantitative analysis 11. No sample preparation	
IMS	1. Instrumental simplicity 2. Small size 3. Light weight 4. Robustness 5. Low-power consumption 6. Fast response times 7. High sensitivity	1. False positive alarms 2. Potential compounds' adsorption onto IMS surfaces 3. Limited selectivity 4. Lack of performance in highly contaminated environments 5. Humidity, temperature, and composition of the sample may affect detector's response 6. Bureaucracy due to the integrated radioactive sources
GC	1. Accuracy 2. Couples with other analytical techniques	1. Slow analysis time
IR	1. Reliable and repeatable results 2. Qualitative analysis 3. Quantitative analysis 4. Non-invasive technique	1. Lack of flexibility 2. Indoor use
CRDS	1. Real-time measurements 2. High sensitivity	1. Lack of selectivity in the near infra-red region
LIBS	1. Direct analysis 2. Sensitivity 3. Non-destructive real time analysis No sample preparation	1. False positive alarms 2. Plasma conditions vary with the environmental conditions
Raman	1. No sample preparation	1. Cannot be used for

	2. Sensitive to homo-nuclear molecular bonds 3. Fully integrated threat libraries 4. Portability 5. Non-destructive 6. Fast response times 7. Analysis through glass and polymer packaging	metals or alloys 2. Fluorescence of the sample background may lead to false negative alarms
THz spectroscopy	1. Penetrate though materials 2. Non-destructive 3. Many non-metallic or non-polar materials are transparent to Thz	1. Limited penetration in high-water content or metal objects 2. Distance limitations
Fluorescence	1. Excellent signal-to-noise ratio	1. Limit of linear intensity
Instruments based on various sensors (e.g. chemical, optical, colorimetric, etc.)	1. Portability 2. Sensitivity 3. Reliability 4. Easy operation 5. Low LODs 6. Fast response times	1. Lack of stand-off detection
Flame photometry	1. Sensitivity	2. Small number of excited atoms 3. Sample interferences 4. Reproducibility

2.5. VOCs associated with security operations

2.5.1. VOCs theory

Volatile organic compounds (VOCs) are an important chemical class localised almost everywhere in our daily lives. VOCs can be found in both indoor and outdoor environments; they participate in many natural, manmade or industrial activities and can affect human health status. VOCs are also of concern as environmental pollutants and play a significant role in photochemical smog and in global warming. Besides the

interest on the VOCs effects upon the environment, there is a broad research focus on VOCs emanations or applications originating from the medical, security, defence, search and rescue (SAR), agricultural, pharmaceutical and R&D field. VOCs carry pivotal information, which when are decoded are of great significance. Several international organizations have tried to give a clear definition of what the volatile organic compounds are:

- ✓ VOCs include all organic compounds (with key elements carbon and hydrogen), with boiling points in the range between 50°C - 260°C, excluding pesticides (WHO, World Health Organization) [142].
- ✓ VOCs are any compounds of carbon, excluding carbon monoxide, carbon dioxide, carbonic acid, metallic carbides or carbonates carbides and ammonium carbonate, which participate in atmospheric photochemical reactions (EPA, U.S. Environmental Agency, 1992) [143].
- ✓ VOC means any organic compound having an initial boiling point less than or equal to 250°C measured at a standard pressure of 101.3 kPa (EU, Directive 2004/42/CE of the European Parliament and the Council, 2004) [144].

Additional definition of VOCs comes in relation to the vapour pressure property (P^S):

- ✓ Organic compounds which have vapour pressure P^S over than 0.1 Torr at 25°C and 760 mmHg are considered as VOCs (EPA, US, TO-15).

The above definitions given by the WHO, the EPA and the EU indicate the importance of the boiling point and vapour pressure in the VOCs characterisation. A more comprehensive definition for the VOCs could be the following: VOCs are defined the organic compounds that: a) have a vapour pressure P^S over 0.1 Torr at 25°C and 760 mmHg and b) have boiling point below 260°C. Generally and in simple terms, the VOCs can be defined as the organic compounds whose formation allows them to evaporate or transit in the gaseous phase under normal atmospheric temperature and pressure conditions. Every VOC (according to its physical and chemical properties and especially its vapour pressure) is usually accompanied by the release of a specific scent.

VOCs can be produced by both indoor and outdoor sources. Indoor found VOCs are all the organic compounds that can volatilise under room temperature and pressure. For example, indoor VOCs can be released from paints, furniture, carpets, cleaning equipment, etc. Outdoor met VOCs are those chemical compounds that affect ambient

environment conditions (e.g. photochemical oxidation) and usually are produced by industrial processes, fires, solvent use, cars, etc.

VOCs can be classified according to their origin in anthropogenic and biogenic. Anthropogenic VOCs derive mainly from manmade activities such as industrial processes whereas biogenic VOCs derive from activities such as greenhouse plants and microorganism. An additional VOCs discrimination is based on their ease for volatilisation. VOCs boiling point plays a major role in this categorisation. Chemical compounds with boiling point between 1°C and 50-100°C are described as very volatile organic compounds (VVOCs). Organic compounds with boiling points in the range of 50-100°C to 240-260°C are characterised as volatile whereas compounds with boiling points 240-260°C to 380-400°C are named as semi volatile (SVOCs). A third classification puts at the centre the man and discriminates VOCs in endogenous and exogenous (especially important information for health research e.g. in breathe analysis for biomarkers discovery and for diagnostic purposes). Endogenous compounds are those that are produced from various metabolic processes in the human body and exogenous compounds are those which originate from the surrounding environment and usually enter human body by the inhalation process [143].

In order to understand the chemical behaviour of a VOC of interest is critical to investigate its physical and chemical properties such as the molecular weight, the chemical structure, the vapour pressure, the boiling point, the polarity, the solubility, the Henry constant, the Octanol-Water partition coefficient etc. The chemical properties of known VOCs in a simple or complex mixture are the selection criteria of an appropriate-required methodology or pathway for their chemical analysis.

2.5.2. Human chemical signatures

2.5.2.1. The complexity of human scent

Chemical signs of human life are a novel and challenging research field seeking exploration. Research is being carried out to specify and establish characteristic volatile chemical compounds emitted from exhaled human breath, sweat, skin, urine and other biological excretes. Human odour as a total is a complex mixture of thousands of evolved chemical compounds which depend on personal characteristics (e.g. age, gender, diet, health condition, exercise, etc.) and still has not been fully identified. Furthermore, human body odour belongs in the trace chemical analysis area, as most of

the VOCs have concentration levels from low ppt to some hundreds of ppb. Complex constant or dynamic odorous chemical backgrounds (e.g. those found at cargo services, airports, security checkpoints, etc.) with various environmental conditions (e.g. temperature, humidity, etc.) make the human chemical signatures' detection issue, difficult for investigation. It is noteworthy that there is a lack of ''odourprint'' databases storing human body odours compared to existing integrated human fingerprints, DNA or retinal scans databases. Creation of such ''odourprint'' libraries could be of great assistance for law enforcement personnel and civil security services.

2.5.2.2. Biological and chemical origin of human body odour

Human skin comprises approximately 12-15% of body weight and is colonised by a vast number of both aerobic and anaerobic bacterial microflora. Main hosted bacteria include Gram-positive cocci of *Staphylococcus* and *Micrococcus* as well as a variety of Gram-positive rods, mainly *Corynebacterium*. Other known skin hosted bacteria involve *Corynebacterium*, *Streptococcus*, *Pseudomonas*, *Bacillus*, *Acinetobacter*, propionibacteria etc. Some of them are potentially pathogenic, especially if the epidermis is injured and they can find a way to have access under skin. Some others are "friendly" to individuals and simply symbiotic. Their number changes with age, gender and origin [145, 146].

Human skin also contains three different types of glands (eccrine, sebaceous glands, apocrine), distributed in different body regions, which produce sweat. Sweat, in its primary form, is a sterile and mostly odourless biological fluid. When this fluid is metabolised by the microbiota hosted on the human skin, it is converted to an odorous liquid with hundreds of VOCs that transmit to the body's surrounding area through a complex heat transfer mechanism.

Human body odour depends on two different kinds of factors: a) the stable factors over time and b) those that vary with environmental or other conditions. It is very difficult to distinguish the genetic influences from those coming from other sources such as different lifestyles, socioeconomic status, etc. Stable factors over time are the genetic factors, such as those that are responsible for human gender, colour, and ethnic background. The characteristic odour originating from genetic factors is called "***primary odour***". The term "***secondary odour***" describes constituents that are present because of diet and environmental factors. Finally, the term "***tertiary odour***" involves compounds

that are present due to the influence of outdoor factors like perfumes, soaps, lotions etc [145].

Human axillae area is mainly responsible for personal odour. Due to the upright stance and position in human body is responsible for chemical communication [147]. The axillary area is the most complex microbial habitat, with sebaceous, apocrine and eccrine glands. The principal source of normal axillary smell is the conversion of water-soluble precursor compounds into volatile aliphatic acids by the activity of *Corynebacterium* species.

Axillary glands are more active in men than in women and give the characteristic "sweaty armpit odour". The 3-methyl-2-hexanoic acid and 3-hydroxy-3-methylhexanoic acid are typical emanations of the axiliary area. Other contributors to the axiliary malodour are: produced sulphur compounds and odorous steroids. The 3-methyl-3-sulfanylhexanol is also a major component found in the axiliary odour. Characteristic identified odorous steroids are the 16-androsterenes, the 5α-androsterol and the 5α-androsterone [148]. Table 2.4 gives an overview of the volatile odorous emissions involving in human scent and originating from different human body regions.

2.5.2.3. Differentiation between genders

Humans can easily be distinguished among each other through their body smell. Several studies have found male odours unpleasant, whereas female odours have been described as pleasant. The basic body odour differences between the two genders are firstly the distinct levels of sex steroid hormones (androstenes) and secondly the fact that females generally have smaller body areas than males. The second difference means that the amount of sweat produced by a woman is on average less compared to that of a man. Furthermore, women's body odour changes during the different phases of their lives (menstrual cycle, fertile phase, etc.) [147].

Table 2.4: Volatile compounds produced from various human body areas.

Compounds identified in Human Body Scent																
	Odour Source:	**Axilla (underarms)**								**Non axillary skin**						
	Skin Emanation:	**Axillary area**								**Hands / Arm**			**Feet**	**Back**	**Forearm**	**Upper Back & Forearm**
	Author:	**Brooksbank et al., 1974 [149]**	**Zeng et al., 1991 [150]**	**Zeng et al., 1992 [151]**	**Zeng et al., 1996 [152]**	**Munk et al., 2000 [153]**	**Curran et al, 2005 [154]**	**Curran et al, 2005 [155]**	**Penn et al., 2007 [147]**	**Bernier et al., 2000 [156]**	**Bernier et al., 2002 [157]**	**Zhang et al., 2005 [158]**	**Kanda et al., 1990 [159]**	**Haze et al., 2001 [160]**	**Ostrovskaya et al., 2001 [161]**	**Gallagher et al., 2008 [162]**
	No of candidates:		**6**	**28**	**6**	**14**	**2**	**8**	**197**	**4**	**2**	**15**	**10**	**22**	**50**	**25**
Chemical Class	**Compounds**															
Alkenes	Alpha-pinene											X				
	Caryophylene											X				
	D-Limonene											X				
	Pentadecene											X				
Alkanes	Eicosane											X				
	Hexadecane											X				
	Pentadecane											X				

	Tetradecane											X				
	Tridecane											X				
	Dodecane											X				
	4-phenyltridecane								X							
	3-methyloctadecane								X							
	3-methylnonadecane								X							
Alcohols & Phenols	Cedrol											X				X
	2-ethyl hexanol											X				
	5-methyl-2-isopropyl cyclohexanol											X				
	Benyl alcohol											X				
	Hexadecanol		X		X									X		
	Phenol		X		X		X	X								X
	2-phenylethanol								X	X		X				
	1-tridecanol								X	X						
	tetradecanol		X													
	Geraniol								X							
	2-hexanol															X
	3-hexanol															X
	Butanol															X
	Eugenol								X							
Aldehydes	Benzaldehyde											X				X
	Decanal											X		X	X	X
	Nonanal						X				X	X		X	X	X
	2-Nonenal					X	X	X						X		X

	Hexanal					X	X	X						X		
	Heptanal						X	X			X			X		
	Octanal					X								X	X	X
	Undecanal							X	X							
	Dodecanal															X
	Geranial								X							
	Tridecanal								X							
	Lilial								X			X				
Esters	Methyl salicylate											X				
	Isobornyl propionate											X				
	Hexadecanoic acid-methyl ester															
	Hexadecanoic acid-dimethyl ester															
	Nonanoic acid-methyl ester															
	Tridecanoic acid-methyl ester															
Acids	7-Octenoic acid		X	X	X					X	X		X			
	Propanoic acid															X
	Butanoic acid															X
	Hexanoic acid		X	X	X	X							X			X
	Heptanoic acid		X		X	X							X			
	Octanoic acid		X	X	X								X			X
	Nonanoic acid			X	X			X					X			
	Decanoic acid		X	X	X											
	undecanoic acid		X	X	X											
	Dodecanoic acid						X	X		X	X					X

	3-methyl-2-hexenoic acid		X	X	X											
	3-methyl-2-hexanoic acid															
	3-hydroxy-3-methylhexanoic acid															
	2-methylhexanoic		X													
	2-methylheptanoic		X													
	2-methyloctanoic		X													
	2-ethylhexanoic		X													
	4-ethyldecanoic		X													
	Acetic acid															X
	Lactic acid															X
Aliphatic/aromatic	naphthalene					X										
	Nonane						X	X			X					
	Toluene						X	X			X					
Ketones	6-Methyl-5-hepten-2-one						X	X			X				X	
	2-propanone (or acetone)															X
Steroids	Cholesterol		X													
	Squalene		X													
	5a-androst-16-en-3a-ol		X													
	5a-androst-16-en-3b-ol		X													
	5a-androst-16-en-3-one	X	X													
Misxellaneous	Diphenyl ether								X			X				
	tetramethyl thiourea											X				
	Acetophenone											X				

2.5.3. Overview of threat substances

Threat substances incorporate chemical components that present hazardous and/or toxic effects on human beings and other living organisms (animals or plants). They can potentially cause undesirable catastrophes in urban or rural environments and hamper human activities causing socioeconomic issues and concerns. They include illegal drugs, explosives, bombs, landmines and CWAs as well as their precursors or breakdown products [163-171].

Illegal drugs are controlled by the government and their use and trafficking is not permitted in any circumstances. Illicit drugs affect human senses, responses and body reactions. They are mainly categorised in three major families: a) stimulants, b) hallucinogens and c) central depressants. Representatively, cocaine, GHB (at low doses) and amphetamine are stimulants for the central nervous system causing psychological euphoria. LSD is a hallucinogen drug, whereas cannabis and GHB at high doses belong in the depressants drugs.

Explosive material can be described a reactive, usually unstable compound or mixture of compounds; which comprise a huge amount of energy (chemical, nuclear, etc.) that can be released after a sudden deflagration or other type of reaction. According to their rate of decomposition, explosive materials can be characterised as low or high explosives. Low explosives deflagrate rapidly without causing a shock wave, whereas high explosives are produced by detonation and cause a large shock wave. High explosives can be classified in primary, secondary and tertiary explosives according to their sensitivity and to the shock wave that they can produce.

CWAs or chemical weapons employ toxic properties of some chemical agents to spread immediate or delayed terror, pain and death. Chemical agents, according to their effects, can be distinguished in the following main categories: a) blister agents (e.g. mustard gas, ED, lewisite), b) nerve agents (e.g. sarin, soman, tabun), c) precursors and degradation products (e.g. dimethyl phosphate), d) tear gases (e.g. agent CS, CN, PS), e) psychogenic agents (e.g. agent BZ) and f) arsenical irritants (e.g. agent DA). Representative common threat substances are listed in Table 2.5.

Most of the above described threats have vapour pressure values in extremely low levels. The technologies discussed in section 2.4 were developed to address this issue and render on site threat compounds detection possible. The following chapters are also

an attempt to enrich this field detection mechanism utilising two portable membrane inlet mass spectrometers (a QMS and a built-in-house LIT-MS).

Table 2.5: Most common homeland security, civil defence and military related substances, classified according to their threat family [172].

	Common threat compounds		
	Compound	**CAS Number**	**Molecular Weight**
Drug	Cocaine	50-36-2	303.35
	Heroin; (Diacetylmorphine)	561-27-3	369.41
	Amphetamine	300-62-9	135.20
	Ecstasy; (N-Methyl-3,4-methylenedioxyamphetamine)	42542-10-9	193.25
	LSD; (D-Lysergic acid N,N-diethylamide)	50-37-3	323.43
	MDA; (tenamfetamine)	4764-17-4	179.22
	Cannabis; (THC)	1972 08 03	314.45
	PCP; (phencyclidine)	77-10-1	243.38
	GHB; (γ-Hydroxybutyric acid)	591-81-1	104.1
Explosive	RDX	121-82-4	222.12
	PETN	78-11-5	316.14
	TNT	118-96-7	227.13
	Nitroglycerin	55-63-0	227.08
	DMNB	3964-18-9	176.17
	Picric Acid	88-89-1	229.11
	Benzyl alcohol	100-51-6	108.14
CWA	Mustard Gas (H)	505-60-2	159.08
	Ethyldichloroarsine (ED)	598-14-1	174.89
	Lewisite	541-25-3	207.31
	Sarin (GB)	107-44-8	140.11
	Soman (GD)	96-64-0	182.19
	Tabun (GA)	77-81-6	162.13
	VX	50782-69-9	267.37
	Cyclohexyl sarin (GF)	329-99-7	180.16
	Dimethyl phosphate	868-85-9	110.05
	Agent CS	2698-41-1	188.62
	Agent CN	532-27-4	154.6
	Agent PS	76-06-2	164.37
	Agent BZ	6581-06-2	337.42
	Agent DA	712-48-1	264.59

2.6. References

[1] U.S. Department of Homeland Security, www.dhs.gov.

[2] European Defence Agency, http://www.eda.europa.eu/.

[3] T. C. Pearce, S. S. Schiffman, H. T. Nagle, J. W. Gardner, *Handbook of Machine Olfaction: Electronic Nose Technology,* Wiley-VCH Verlag GmbH & Co. Weinheim, Germany (2002).

[4] H. V. Shurmer, J. W. Gardner, *Odour discrimination with an electronic nose,* Sensors and Actuators B **8,** 1-11 (1992).

[5] J. W. Gardner, P. N. Bartlett, *A brief history of electronic noses,* Sensors and Actuators B **18-19,** 211-220 (1994).

[6] F. Rock, N. Barsan, U. Weimar, *Electronic Nose: Current Status and Future Trends,* Chem. Rev. **108,** 705-725 (2008).

[7] V. Lopez-Avila, H. H. Hill, *Field Analytical Chemistry,* Anal. Chem. **69,** 289R-305R (1997).

[8] D. S. Moore, *Recent Advances in Trace Explosives Detection Instrumentation,* Sens. Imaging **8,** 9-38 (2007).

[9] M. Trojanowicz, *Challenges of Modern Analytical Chemistry,* Mod. Chem. Appl. **1,** e113 (2013).

[10] P. I. Hendricks, J. K. Dalgleish, J. T. Shelley, M. A. Kirleis, M. T. McNicholas, L. Li, T. C. Chen, C. H. Chen, J. S. Duncan, F. Boudreau, R. J. Noll, J. P. Denton, T. A. Roach, Z. Ouyang, R. G. Cooks, *Autonomous in situ analysis and real-time chemical detection using a backpack miniature mass spectrometer: concept, instrumentation development, and performance.* Anal. Chem. **86,** 2900-2908 (2014).

[11] B. Brkic, S. Giannoukos, N. France, R. Murcott, F. Siviero, S. Taylor, *Optimized DLP linear ion trap for a portable non-scanning mass spectrometer,* Int. J. Mass Spectrom.**369,** 30-35 (2014).

[12] M. K. Habib, *Controlled biological and biomimetic systems for landmine detection,* Biosensors and Bioelectronics **27,** 1-18 (2007).

[13] G. A. A. Schoon, J. C. De Bruin, *The ability of dogs to recognize and cross-match human odours,* Forensic Sci. Int. **69,** 111-118 (1994).

[14] G. A. Schoon, *A first assessment of the reliability of an improved scent identification line-up,* J. Forensic Sci. **43,** 70-75 (1998).

[15] D. Komar, *The use of cadaver dogs in locating scattered, scavenged human remains: preliminary field test results,* J. Forensic Sci. **44,** 405-408 (1999).

[16] N. Lorenzo, T. Wan, R. J. Harper, Y. L. Hsu, M. Chow, S. Rose, K. G. Furton, *Laboratory and field experiments used to identify Canis lupus var. familiaris active odor signature chemicals from drugs, explosives, and humans,* Anal. Bioanal. Chem. **376,** 1212-1224 (2003).

[17] A. Concha, D. S. Mills, A. Feugier, H. Zulch, C. Guest, R. Harris, T. W. Pike, *Using Sniffing Behavior to Differentiate True Negative from False Negative Responses in Trained Scent-Detection Dogs,* Chem. Senses **39,** 749-754 (2014).

[18] J. A. Shaw, N. L. Seldomridge, D. L. Dunkle, P. W. Nugent, L. H. Spangler, J. J. Bromenshenk, C. B. Henderson, J. H. Churnside, J. J. Wilson, *Polarization lidar measurements of honey bees in flight for locating land mines,* Opt. Express **13,** 5853-5863 (2005).

[19] P. J. Rodacy, S. F. A. Bender, J. J. Bromenshenk, C. B. Henderson, G. Bender, *The Training and the Deployment of Honeybees to Detect Explosives and other Agents of Harm,* SPIE, Detection and Remediation Technologies for Mines and Minelike Targets VII, **4742,** 474-481 (2002)

[20] A. Poling, B. Weetjens, C. Cox, N. W. Beyene, A. Sully, *Using giant African pouched rats (Cricetomys gambianus) to detect landmines,* The Psychological Record, **60,** 715-728 (2010).

[21] A. Poling, B. Weetjens, C. Cox, N. W. Beyene, H. Bach, A. Sully, *Using trained pouched rats to detect land mines: another victory for operant conditioning,* Journal of Applied Behavior Analysis **44,** 351-355 (2011).

[22] J. Otto, M. F. Brown, W. Long, *Training rats to search and alert on contraband odors,* Appl. Anim. Behav. Sci. **77,** 217–232 (2002).

[23] A. Corcelli, S. Lobasso, P. Lopalco, M. Dibattista, R. Araneda, Z. Peterlin, S. Firestein, *Detection of explosives by olfactory sensory neurons,* J. Hazard. Mater. **175,** 1096-1100, (2010).

[24] C. Liao, A. Gock, M. Michie, B. Morton, A. Anderson, S. Trowell, *Behavioural and Genetic Evidence for C. Elegans' Ability to Detect Volatile Chemicals Associated with Explosives,* PLOS ONE **5,** 1-9 (2010).

[25] T. L. King, F. M. Horine, K. C. Daly, B. H. Smith, *Explosives Detection With Hard-Wired Moths,* IEEE Transactions on Instrumentation and Measurement **53,** 1113-1118 (2004).

[26] J. Yinon, *Detection of Explosives by Electronic Noses,* Anal. Chem. **75,** 98-105 (2003).

[27] S. Sankaran, L. R. Khot, S. Panigrahi, *Biology and applications of olfactory sensing system: A review,* Sensor Actuat. B: Chem. **171-172,** 1-17 (2012).

[28] A. D. Wilson, M. Baietto, *Applications and advances in Electronic-Nose Technologies,* Sensors **9,** 5099-5148, (2009).

[29] J. Ma, W. J. Bock, *Fiber-Optic Sensors for Explosives Detection,* The Open Optics Journal **7,** 141-158, (2013).

[30] O. K. Kannan, R. Bhalla, J. C. Kapoor, A. T. Nimal, U. Mittal, R. D. S. Yadava, *Detection of Landmine Signature using SAW-based Polymer-coated Chemical Sensor,* Defence Science Journal **54,** 309-315, (2004).

[31] F. Chu, G. Tsiminis, N. A. Spooner, T. M. Monro, *Explosives detection by fluorescence quenching of conjugated polymers in suspended core optical fibers,* Sens Actuat. B: Chem **199,** 22-26, (2014).

[32] D. Kong, Y. Qi, L. Zhou, B. Lin, Z. Li, R. Zhu, C. Chen, *MEMS based sensors for explosive detection: Development and discussion,* 3rd IEEE International Conference on Nano/Micro Engineered and Molecular Systems, 265-269, (2008).

[33] D. S. Moore, *Instrumentation for trace detection of high explosives,* Rev. Sci. Instrum. **75,** 2499-2512, (2004).

[34] D. S. Moore, *Recent Advances in Trace Explosives Detection Instrumentation,* Sens. Imaging **8,** 9-38 (2007).

[35] Z. Ouyang, R. J. Noll, R. G. Cooks, *Handheld miniature ion trap mass spectrometers,* Anal. Chem. **81,** 2421-2425 (2009).

[36] J. A. Contreras, J. A. Murray, S. E. Tolley, J. L. Oliphant, H. D. Tolley, S. A. Lammert, E. D. Lee, D. W. Later, M. L. Lee, *Hand-portable gas chromatograph-toroidal ion trap mass spectrometer (GC-TMS) for detection of hazardous compounds,* J. Am. Soc. Mass Spectrom. **19,** 1425–1434 (2008).

[37] Y. Takada, H. Nagano, M. Suga, Y. Hashimoto, M. Yamada, M. Sakairi, K. Kusumoto, T. Ota, J. Nakamura, *Detection of Military Explosives by Atmospheric*

Pressure Chemical Ionization Mass Spectrometry with Counter-Flow Introduction, Propell. Explos. Pyrotech. **27,** 224-228 (2002).

[38] I. Cotte-Rodriguez, H. Hernandez-Soto, H. Chen, R. G. Cooks, *In Situ Trace Detection of Peroxide Explosives by Desorption Electrospray Ionization and Desorption Atmospheric Pressure Chemical Ionization,* Anal. Chem. **80,** 1512–1519 (2008).

[39] I. Cotte-Rodriguez, Z. Takats, N. Talaty, H. W. Chen, R. G. Cooks, *Desorption Electrospray Ionization of Explosives on Surfaces: Sensitivity and Selectivity Enhancement by Reactive Desorption Electrospray Ionization,* Anal. Chem. **77,** 6755–6764 (2005).

[40] D. R. Justes, N. Talaty, I. Cotte-Rodriguez, R. G. Cooks, *Detection of explosives on skin using ambient ionization mass spectrometry,* Chem. Commun. **21,** 2142–2144 (2007).

[41] J. T. Kauppila, N. Talaty, T. Kuuranne, T. Kotiaho, R. Kostiainen, R. G. Cooks, *Rapid analysis of metabolites and drugs of abuse from urine samples by desorption electrospray ionization-mass spectrometry,* Analyst **132,** 868–875 (2007).

[42] R. G. Cooks, Z. Ouyang, Z. Takats, J. M. Wiseman, *Ambient Mass Spectrometry, Science* **311,** 1566–1570 (2006).

[43] Z. Takats, J. M. Wiseman, B. Gologan, R. G. Cooks, *Mass Spectrometry Sampling Under Ambient Conditions with Desorption Electrospray Ionization, Science* **306,** 471–473 (2004).

[44] I. Cotte-Rodriguez, R. G. Cooks, *Non-proximate detection of explosives and chemical warfare agent simulants by desorption electrospray ionization mass spectrometry,* Chem. Comm. **28,** 2968–2970 (2006).

[45] R. B. Cody, J. A. Laramee, H. D. Durst, *Versatile New Ion Source for the Analysis of Materials in Open Air under Ambient Conditions,* Anal. Chem. **77,** 2297-2302 (2005).

[46] Y. Zhang, X. Ma, S. Zhang, C. Yang, Z. Ouyang, X. Zhang, *Direct detection of explosives on solid surfaces by low temperature plasma desorption mass spectrometry,* Analyst **134,** 176-181 (2009).

[47] M. Haapala, J. Pol, V. Saarela, V. Arvola, T. Kotiaho, R. A. Ketola, S. Franssila, T. J. Kauppila, R. Kostiainen, *Desorption atmospheric pressure photoionization,* Anal. Chem. **79,** 7867-7872, (2007).

[48] Y. Song, R. G.Cooks, *Atmospheric pressure ion/molecule reactions for the selective detection of nitroaromatic explosives using acetonitrile and air as reagents,* Rapid Commun. Mass. Spectrom. **20,** 3130-3138 (2006).

[49] J. P. Williams, V. J. Patel, R. Holland, J. H. Scrivens, *The use of recently described ionisation techniques for the rapid analysis of some common drugs and samples of biological origin,* Rapid Commun. Mass Spectrom. **20,** 1447-1456 (2006).

[50] C. Wu, W. F. Siems, H. H. Hill, *Secondary electrospray ionization ion mobility spectrometry/mass spectrometry of illicit drugs,* Anal. Chem. **72,** 396-403, (2000).

[51] W. E. Steiner, B. H. Clowers, P. E. Haigh, H. H. Hill, *Secondary ionization of chemical warfare agent simulants: atmospheric pressure ion mobility time-of-flight mass spectrometry,* Anal. Chem. **75,** 6068-6076 (2003).

[52] M. Tam, H. H. Hill, *Secondary electrospray ionization-ion mobility spectrometry for explosive vapor detection,* Anal. Chem. **76,** 2741-2747 (2004).

[53] P. Martínez-Lozano, J. Rus, G. F. de la Mora, M. Hernández, J. F. de la Mora, *Secondary electrospray ionization (SESI) of ambient vapors for explosive detection at concentrations below parts per trillion,* J. Am. Soc. Mass Spectrom. **20,** 287-294 (2009).

[54] E.Hoffmann, V.Stroobant, Mass spectrometry: principles and applications, 3rd edition. Wiley, London, (2007).

[55] J. Liu, H. Wang, N. E. Manicke, J. M. Lin, R. G. Cooks, Z. Ouyang, *Development, Characterization, and Application of Paper Spray Ionization,* Anal. Chem. **82,** 2463-2471 (2010).

[56] H. Wang, J. Liu, R. G. Cooks, Z. Ouyang, *Paper spray for direct analysis of complex mixture using mass spectrometry,* Angew. Chem. Int. Ed. **49,** 877-880 (2010).

[57] A. Hirabayashi, M. Sakairi, H. Koizumi, *Sonic spray mass spectrometry,* Anal. Chem. **67,** 2878-2882 (1995).

[58] R. Haddad, R. Sparrapan, M. N. Eberlin, *Desorption sonic spray ionization for (high) voltage-free ambient mass spectrometry,* Rapid Commun. Mass Spectrom. **20,** 2901-2905 (2006).

[59] FLIR Systems Inc., http://www.flir.com/GB/.

[60] Torion Technologies, http://torion.com/home.html.

[61] Aston Labs, Purdue University, http://aston.chem.purdue.edu/.

[62] 1st Detect, http://www.1stdetect.com/.

[63] Harsh-Environment Mass Spectrometry (HEMS) Workshop, http://www.hems-workshop.org/index.html.

[64] R. G. Ewing, D. A. Atkinson, G. A. Eiceman, G. J. Ewing, *A critical review of ion mobility spectrometry for the detection of explosives and explosive related compounds,* Talanta **54,** 515-529 (2001).

[65] B. H. Clowers, W. F. Siems, H. H. Hill, S. M. Massick, *Hadamard Transform Ion Mobility Spectrometry,* Anal. Chem. **78,** 44–51 (2006).

[66] G. A. Buttigieg, A. K. Knight, S. Denson, C. Pommier, M. B. Denton, *Characterization of the explosive triacetone triperoxide and detection by ion mobility spectrometry,* Forensic Sci. Int. **135,** 53–59 (2003).

[67] I. Marquez-Sillero, E. Aguilera-Herrador, S. Cardenas, M. Valcarcel, *Ion-mobility spectrometry for environmental analysis,* Trends Anal. Chem. **30,** 677-690 (2011).

[68] S. Armenta, M. Alcala, M. Blanco, *A review of recent, unconventional applications of ion mobility spectrometry (IMS),* Anal. Chim. Acta **703,** 114-123 (2011).

[69] Z. Karpas, *Ion mobility spectrometry: A tool in the war against terror,* B. of the Israel Chem. Soc. **24,** 26-30 (2009).

[70] T. L. Buxton, P. B. Harrington, *Rapid multivariate curve resolution applied to identification of explosives by ion mobility spectrometry,* Anal. Chim. Acta **434,** 269-282 (2001).

[71] M. A. Mäkinen, O. A. Anttalainen, M. E. T. Sillanpää, *Ion Mobility Spectrometry and Its Applications in Detection of Chemical Warfare Agents,* Anal. Chem. **82,** 9594–960 (2010).

[72] W. E. Steiner, S. J. Klopsch, W. A. English, B. H. Clowers, H. H. Hill, *Detection of a Chemical Agent Simulant in various Aerosol Matrixes by Ion Mobility Time-of-Flight Mass Spectrometry,* Anal. Chem. **77,** 4792-4799 (2005).

[73] J. S. Caygill, F. Davis, S. P. J. Higson, *Current trends in explosive detection techniques,* Talanta, **88,** 14-29 (2012).

[74] M. Tubaro, E. Marotta, R. Seraglia, P. Traldi, *Atmospheric pressure photoionization mechanisms. 2. The case of benzene and toluene,* Rapid Commun. Mass Sp. **17,** 2423-2429 (2003).

[75] J. Laakia, A. Adamov, M. Jussila, C. S. Pedersen, A. A. Sysoev, T. Kotiaho, *Separation of different ion structures in atmospheric pressure photoionizationion*

mobility spectrometry-mass spectrometry (APPI-IMS-MS), J. Am. Soc. Mass Spectr. **21,** 1565-1572 (2010).

[76] K. Liu, F. Tang, X. H. Wang, L. Zhang, X.Y. Wei, *Negative Corona Discharge Ion Source Under Ambient Conditions with Mini Line-cylinder Electrodes,* Chin. J. Chem. Phys. **22,** 107-112 (2009).

[77] C. Krueger, C. Hilton, M. Osgood, J. Wu, C. Wu, *High resolution electrospray ionization ion mobility spectrometry,* Int. J. Ion. Mobility Spectrom. **12,** 33-37 (2009).

[78] S. Sundarapandian, J. C. May, J. A. McLean, *Dual source ion mobility-mass spectrometer for direct comparison of electrospray ionization and MALDI collision cross section measurements,* Anal. Chem. **82,** 3247-3254 (2010).

[79] P. A. D'Agostino, C. L. Chenier, *Desorption electrospray ionization mass spectrometric analysis of organophosphorus chemical warfare agents using ion mobility and tandem mass spectrometry,* Rapid Commun. Mass Sp. **24,** 1617-1624 (2010).

[80] M. Tam, H. H. Hill, *Secondary electrospray ionization-ion mobility spectrometry for explosive vapor detection,* Anal. Chem. **76,** 2741-2747 (2004).

[81] E. Inutan, S. Trimpin, *Laserspray ionization (LSI) ion mobility spectrometry (IMS) mass spectrometry.* J. Am. Soc. Mass Spectr. **21,** 1260-1264 (2010).

[82] A. Ahmed, Y. J. Cho, M. H. No, J. Koh, N. Tomczyk, K. Giles, J. S. Yoo, S. Kim, *Application of the Mason-Schamp Equation and Ion Mobility Mass Spectrometry To Identify Structurally Related Compounds in Crude Oil.* Anal. Chem. **83,** 77-83 (2011).

[83] M. T. Jafari, *Low-temperature plasma ionization ion mobility spectrometry,* Anal. Chem. **83,** 797-803, (2011).

[84] G. A. Harris, M. Kwasnik, F. M. Fernandez, *Direct Analysis in Real Time Coupled to Multiplexed Drift Tube Ion Mobility Spectrometry for Detecting Toxic Chemicals,* Anal. Chem. **83,** 1908-1915, (2011).

[85] G. A. Eiceman, E. V. Krylov, N. S. Krylova, E. G. Nazarov, R. A. Miller, *Separation of Ions from Explosives in Differential Mobility Spectrometry by Vapor-Modified Drift Gas,* Anal. Chem. **76,** 4937-4944 (2004).

[86] B. M. Kolakowski, Z. Mester, *Review of applications of high-field asymmetric waveform ion mobility spectrometry (FAIMS) and differential mobility spectrometry (DMS),* Analyst **132,** 842-864 (2007).

[87] M. J. Pollard, C. K. Hilton, H. Li, K. Kaplan, R. A. Yost, H. H. Hill Jr, *Ion mobility spectrometer-field asymmetric ion mobility spectrometer-mass spectrometry*, Int. J. Ion Mobil. Spectrom. **14,** 15-22 (2011).

[88] A. J. Marr, D. M. Groves, *Ion mobility spectrometry of peroxide explosives TATP and HMTD,* Int. Soc. Ion Mob. Spectrom. **6,** 59-61 (2003).

[89] C. Kwan, A. P. Snyder, R. P. Erickson, P. A. Smith, W. M. Maswadeh, B. Ayhan, J. L. Jensen, J. O. Jensen, A. Tripathi, *Chemical Agent Detection Using GCIMS: A Comparative Study*, IEEE Sensors Journal, **10,** 451-460 (2010).

[90] B. Bödeker, W. Vautz, J. Baumbach, *Peak finding and referencing in MCC/IMS-data,* Int. J. Ion. Mobility Spectrom. **11,** 83-87 (2008).

[91] G. A. Eiceman, Y. Feng, *Limits of separation of a multi-capillary column with mixtures of volatile organic compounds for a flame ionization detector and a differential mobility detector,* J. Chrom. A **1216,** 985-993 (2009).

[92] J. M. Perr, K. G. Furton, J. R. Almirall, *Solid phase microextraction ion mobility spectrometer interface for explosive and taggant detection,* J. Separ. Sci. **28,** 177-183 (2005).

[93] Smiths Detection, http://www.smithsdetection.com/.

[94] SAFRAN Morpho, http://www.morpho.com/.

[95] Bruker Daltonics, http://www.bruker.com/.

[96] Environics, http://www.environics.fi/.

[97] RAE SYSTEMS, http://www.raesystems.com/.

[98] AIRSENSE Analytics, http://www.airsense.com/.

[99] OWLSTONE, http://www.owlstonenanotech.com/.

[100] Thermo Fisher Scientific, http://www.thermoscientific.com/en/home.html.

[101] Implant Sciences Corporation, http://www.implantsciences.com/.

[102] IUT Berlin, http://www.iut-berlin.info/176.0.html?&L=1.

[103] Ion Applications, Inc., http://spinoff.nasa.gov/Spinoff2010/ps_7.html

[104] Excellims, http://www.excellims.com/.

[105] Sibel, http://www.sibel.info/en/.

[106] PKI-electronic, http://www.pki-electronic.com/.

[107] A. Sambouli, A. El Bouri, T. Bouayoun, M. A. Bellimam, *Headspace-GC/MS detection of TATP traces in post-explosion debris,* Forensic Sci. Int. **146,** 191–194 (2004).

[108] DPL Surveillance Equipment.com, http://www.dpl-surveillance-equipment.com/

[109] M.T. Soderstrom, R.A. Ketola, *Identification of nerve agents and their homologues and dialkyl methylphosphonates by gas chromatography/fourier transform infared spectroscopy (GC-FTIR)* Fresenius J. Anal. Chem. **350,** 162-167 (1994).

[110] J. Oxley, J. Smith, J. Brady, F. Dubnikova, R. Kosloff, L. Zeiri, Y. Zeiri, *Raman and infrared fingerprint spectroscopy of peroxide-based explosives,* Appl Spectrosc. **62,** 906-915 (2008).

[111] O. M. Primera-Pedrozo, Y. M. Soto-Feliciano, L. C. Pacheco-Londoño, S. P. Hernández-Rivera, *Detection of High Explosives Using Reflection Absorption Infrared Spectroscopy with Fiber Coupled Grazing Angle Probe/FTIR,* Sens Imaging **10,** 1-13 (2009).

[112] O. M. Primera-Pedrozo, Y. M. Soto-Feliciano, L. C. Pacheco-Londono, S. P. Hernandez-Rivera, *Using reflection absorption infrared spectroscopy with fiber coupled grazing angle probe / FTIR,* Sens Imaging **10,** 1-13 (2009).

[113] B. A. Paldus, A. A. Kachanov, *An historical overview of cavity-enhanced methods,* Can. J. Phys. **83,** 975-999 (2005).

[114] Picarro Inc., http://www.picarro.com/.

[115] J. L. Gottfried, F. C. De Lucia Jr., C. A. Munson, A. W. Miziolek, *Laser-induced breakdown spectroscopy for detection of explosives residues: A review of recent advances, challenges, and future prospects,* Anal. Bioanal. Chem. **395,** 283-300 (2009).

[116] Y. Dikmelik, C. McEnnis, J. B. Spicer, *Femtosecond and nanosecond laser-induced breakdown spectroscopy of trinitrotoluene,* Opt. Express. **16,** 5332-5337 (2008).

[117] Oxford Instruments plc, http://www.oxford-instruments.com/.

[118] Applied Photonics Ltd, http://www.appliedphotonics.co.uk/

[119] Ocean Optics Inc., http://oceanoptics.com/

[120] J. C. Carter, S. M. Angel, M. Lawrence-Snyder, J. Scaffidi, R. E. Whipple, J. G. Reynolds, *Standoff detection of high explosive materials at 50 meters in ambient light conditions using a small Raman instrument,* Appl. Spectrosc. **59,** 769-775 (2005).

[121] D. A. Stuart, K. B. Biggs, R. P. Van Duyne, *Surface-enhanced Raman spectroscopy of half-mustard agent,* Analyst **131,** 568–572 (2006).

[122] Cobalt Light Systems Ltd, http://www.cobaltlight.com/.

[123] Y. C. Shen, T. Lo, P. F. Taday, B. E. Cole, W. R. Tribe, M. C. Kemp, *Detection and identification of explosives using terahertz pulsed spectroscopic imaging,* Appl. Phys. Lett. **86,** 241116 (2005).

[124] F. Huang, B. Schulkin, H. Altan, J. F. Federici, D. Gary, R. Barat, D. Zimdars, M. H. Chen, D. B. Tanner, *Terahertz study of 1,3,5-trinitro-s-triazine by time domain and Fourier transform infrared spectroscopy,* Appl. Phys. Lett. **85,** 5535–5537 (2004).

[125] H. B. Liu, Y. Chen, G. J. Bastiaans, X. C. Zhang, *Detection and identification of explosive RDX by Thz diffuse reflection spectroscopy,* Opt. Express **14,** 415-423 (2006).

[126] TeraView Ltd, http://www.teraview.com/.

[127] D. Gao, Z. Wang, B. Liu, L. Ni, M. Wu, Z. Zhang, *Resonance energy transfer-amplifying fluorescence quenching at the surface of silica nanoparticles toward ultrasensitive detection of TNT,* Anal. Chem. **80,** 8545-8553 (2008).

[128] QinetiQ, https://www.qinetiq.com/Pages/default.aspx.

[129] Plexus Scientific Inc., http://www.plexsci.com/.

[130] P. Rabenecker, K. Pinkwart, *A look behind electrochemical detection of explosives,* Propellants Explos Pyrotech. **34,** 274-279 (2009).

[131] Morphix Technologies Inc., http://www.morphtec.com/.

[132] KeTech, http://www.ketech.com/.

[133] Spectrex Corporation, http://www.spectrex.com/html_files2/index.php.

[134] DetectaChem, http://www.detectachem.com/home.

[135] P. Singh, T. Onodera, Y. Mizuta, K. Matsumoto, N. Miura, K. Toko, *Dendrimer modified biochip for detection of 2,4,6 trinitrotoluene on SPR immunosensor: Fabrication and advantages,* Sens Actuators B: Chem. **137,** 403-409 (2009).

[136] J. Wang, S.B. Hocevar, B. Ogorevc, *Carbon nanotube-modified glassy carbon electrode for adsorptive stripping voltammetric detection of ultratrace levels of 2,4,6- trinitrotoluene,* Electrochemistry Communications **6,** 176-179 (2004).

[137] X. Liu, L. Zhao, H. Shen, H. Xu, L. Lu, *Ordered gold nanoparticle arrays as surfaceenhanced Raman spectroscopy substrates for label-free detection of nitroexplosives,* Talanta **83,** 1023-1029 (2011).

[138] S. Chang, H. Ko, S. Singamaneni, R. Gunawidjaja, V.V. Tsukruk, *Nanoporous membranes with mixed nanoclusters for Raman-based label-free monitoring of peroxide compounds,* Anal. Chem. **81,** 5740-5748 (2009).

[139] Vaporsens Inc., http://www.vaporsens.com/.

[140] Tracense Systems, http://www.tracense.com/.

[141] Proengin Inc., http://www.proengin.com/.

[142] World Health Organization, http://www.who.int/en/.

[143] US Environmental Protection Agency, http://www.epa.gov/.

[144] European Parliament, http://www.europarl.europa.eu/portal/en.

[145] A. P. Wood, D. P. Kelly, Skin Microbiology, Body Odor, and Methylotropic Bacteria, Handbook of Hydrocarbon and Lipid Microbiology, 3204-3213, (2010).

[146] C. D. Natale, A. Macagnano, R. Paolesse, E. Tarizzo, A. Mantini, A. D'Amico, *Human skin odor analysis by means of an electronic nose,* Sens. and Actuat. B **65,** 216-219, (2000).

[147] D. J. Penn, E. Oberzaucher, K. Grammer, G. Fischer, H. A. Soini, D. Wiesler, M. V. Novotny, S. J. Dixon, Y. Xu, R. G. Brereton, *Individual and gender fingerprints in human body odour,* J. R. Soc. Interface **4,** 331-340, (2007).

[148] C. Austin, J. Ellis, *Microbial pathways leading to steroidal malodour in the axilla,* J. Steroid. Biochem. Mol. Biol. **87,** 105-110, (2003).

[149] B. W. L. Brooksbank, R. Brown, J. A. Gustafsson. *The detection of 5α-androst-16-en-3α-ol in human male axillary sweat,* Experientia **30,** 864-865 (1974).

[150] X. Zeng, J. J. Leyden, H. J. Lawley, K. Sawano, I. Nohara, G. Preti, *Analysis of Characteristic Odors From Human Male Axillae,* Journal of Chemical Ecology **17**, 1469-1492, (1991).

[151] X. Zeng, J. J. Leyden, J. G. Brand, A. I. Spielman, K. J. McGinley, G. Preti, *An Investigation of Human Apocrine Gland Secretion for Axillary Odor Precursors,* Journal of Chemical Ecology **18**, 1039-55, (1992).

[152] X. Zeng, J. J. Leyden, A. I. Spielman, G. Preti, *Analysis of Charactercistic Human Female Axillary Odors: Qualitative Comparison to Males,* Journal of Chemical Ecology **22**, 237-257, (1996).

[153] S. Munk, P. Munch, L. Stahnke, J. Adler-Nissen, P. Schieberle, *Primary Odorants of Laundry Soiled with Sweat/Sebum: Influence of Lipase on the Odor Profile,* Journal of Surfactants and Detergents **3**, 505-515, (2000).

[154] A. M. Curran, S. I. Rabin, K. G. Furton, *Analysis of the Uniqueness and Persistence of Human Scent,* Forensic Science Communications **7**, 2, (2005).

[155] A. M. Curran, S. I. Rabin, P. A. Prada, K. G. Furton, *Comparison of the Volatile Organic Compounds Present in Human Odor Using SPME-GC/MS,* J Chem Ecol. **31**, 1607-1619, (2005).

[156] U. R. Bernier, D. L. Kline, D. R. Barnard, C. E. Schreck, R. A. Yost, *Analysis of Human Skin Emanations by Gas Chromatography/Mass Spectrometry,* Anal. Chem. **72**, 747-56, (2000).

[157] U. R. Bernier, D. L. Kline, C. E. Schreck, R. A. Yost, D. R. Barnard, *Chemical Analysis of Human Skin Emanations: Comparison of Volatiles from Humans That Differ in Attraction of Aedes aegypti (Diptera: Culicidae),* J Am Mosq Control Assoc. **18**, 186-195, (2002).

[158] Z. M. Zhang, J. J. Cai, G. H. Ruan, G. K. Li, *The study of fingerprint characteristics of the emanations from human arm skin using original sampling system by SPME-GC/MS,* J. Chromatogr. B **822,** 244-252 (2005).

[159] F. E. Kanda, M. Yagi, K. Fukuda, T. Nakajima, O. Nakata, *Elucidation of Chemical Compounds Responsible for Foot Malodour,* Br. J. Dermatol. **122**, 771-776, (1990).

[160] S. Haze, Y. Gozu, S. Nakamura, Y. Kohno, K. Sawano, H. Ohta, K. Yamazaki, *2-Nonenal Newly Found in Human Body Odor Tends to Increase With Aging,* J. Invest. Dermatol. **116**, 520-524, (2001).

[161] A. Ostrovskaya, P. A. Landa, M. Sokolinsky, A. D. Rosalia, D. Maes, *Study And Identification of Volatile Compounds From Human Skin,* Journal of Cosmetic Science **53**, 147-148, (2001).

[162] M. Gallanher, C. J. Wysocki, J. J. Leyden, A. I. Spielman, X. Sun , G. Preti, *Analyses of volatile organic compounds from human skin,* Br. J. Dermatol. **159,** 780-791 (2008).

[163] E. B. Russo, *Taming THC: potential cannabis synergy and phytocannabinoid-terpenoid entourage effects,* Br. J. Pharmacol. **163,** 1344-1364 (2011).

[164] J. Yinon, *Field detection and monitoring of explosives,* Trends in Anal. Chem. **21,** 292-300 (2002).

[165] H. Lai, A. Leung, M. Magee, J. R. Almirall, *Identification of volatile chemical signatures from plastic explosives by SPME-GC/MS and detection by ion mobility spectrometry,* Anal. Bioanal. Chem. **396,** 2997-3007 (2010).

[166] P. Guerra, H. Lai, J. R. Almirall. Analysis of the volatile chemical markers of explosives using novel solid phase microextraction coupled to ion mobility spectrometry. *J. Sep. Sci.* **2008,** *31*, 2891-2898.

[167] J. E. Riviere, C. E. Smith, K. Budsaba, J. D. Brooks, E. J. Olajos, H. Salem, N. A. Monteiro-Riviere, *Use of methyl salicylate as a simulant to predict the percutaneous absorption of sulphur mustard*, J. Appl. Toxicol. **21,** 91–99 (2001).

[168] D. H. Ellison, Handbook of Chemical and Biological Warfare Agents, Second Edition, CRC Press, (2007).

[169] J. Paxman, R. Harris, *A Higher Form of Killing : The Secret Story of Chemical and Biological Warfare*, Hill and Wang, New York, **187-189,** pp. 206-210, (1982).

[170] J. A. F. Compton, *Military Chemical and Biological Agents: Chemical and Toxicological Properties*, Telford Press: Caldwell, NJ, 194-204. (1988).

[171] H. Kurata, *Lessons learned from the destruction of the chemical weapons of the Japanese Imperial Forces,* in *Chemical Weapons: Destruction and Conversion*, Stockholm International Peace Research Institute, Taylor and Francis: London, 77-93, (1980).

[172] National Institute of Standards and Technology, Chemistry Web Book, http://webbook.nist.gov/chemistry/.

Part I

Chapter 3

Human scent monitoring using membrane inlet mass spectrometry

3.1. Introduction

Worldwide border and homeland security is facing tremendous challenges due to threats from terrorism and/or national/transnational criminal organizations. During the last few decades, a continuous increase of transportation of illicit substances (drugs, explosives) and weapons as well as illegal human trafficking has been observed and is of particular concern [1]. A plethora of different possible scenarios of illegal human transportation are reported daily in media, such as the cases of hidden people in vans, big boxes, coffins and shipping containers. Most of these situations are investigated by specially trained sniffer dogs using their extremely sensitive and delicate olfactory system [2−5]. Human chemical signatures (HCS), which basically refer to the characteristic human body odour signals, are an innovative and upcoming research field. Both human expired air compounds with human skin and sweat scent compose and declare an individual's characteristic odour or, in other words a person's unique and distinctive chemical "odourprint" that is analogous to a fingerprint [6, 7].

Volatile organic compound (VOC) emissions from human exhaled breath, sweat, skin, and other biological excretes have been used for a wide range of applications including diagnostic purposes in medicine, search and rescue operations, forensic and toxicological analysis [8-12]. Human exhaled air is a complex mixture of both inorganic gases and traces of VOCs [13] and its composition depends on several factors, which are found in the daily life habits (diet, smoking (or not), exercise, medication, etc.), ethnic background, gender, age, living and working environments, etc. [14-16]. Most of the VOCs in breath have typical concentration ranges at ppb or ppt concentration levels

and are responsible for human breath odour. It has been reported qualitatively and quantitatively that the most abundant compounds present in human breath are ammonia, acetone, isoprene, methanol, ethanol, propanol, isopropanol, butanone, 1-pentene, 1-butene, and acetaldehyde [17-32]. Previous research proposed a "core" of volatile compounds identified in the exhaled breath of 15 volunteers that could potentially be used for early localization of human victims in the debris of collapsed buildings after natural disasters in urban areas [8]. In the trapped human experiment, monitoring of human breath, skin volatile metabolites and inorganic gas emissions were demonstrated in a collapsed building simulator [33].

Human skin is the largest human organ [34]. It has a complex structure comprising glands that produce sweat and other metabolites. These glands can be grouped in three major categories: eccrine (mainly contain water, salt, amino acids, sugars, lactic acid and glycoproteins), sebaceous (mostly include lipids) and apocrine glands (consist of water, proteins and lipids), and are situated in different regions of the human body surface [35]. This complicated gland allocation system delivers different compositions of secretions among different body regions with different chemical profiles and dissimilar density levels. For example, axillary area presents a high density of sebaceous glands, soles have a high density of eccrine glands, whereas arms and legs appear to have a low density of eccrine and sebaceous glands.

As mentioned in the section 2.5.2.2, human sweat when secreted, in its primary form, is an odourless biological fluid produced from the above glands. Skin is colonized by a very rich microbiota that consumes and metabolizes this biological fluid through complex biochemical processes, concluding in the transformation of this odourless fluid to an odorous liquid [35-38]. In total, VOCs found in human body scent can be classified in the following chemical families: short-chain and long-chain carboxylic acids, ketones, aldehydes, alcohols and phenols, esters, hydrocarbons (alkanes, alkenes), aliphatic/aromatic compounds, amines, and steroids [39-47].

Existing mainstream technology for laboratory analysis of expired breath and human sweat utilize mass spectrometry (MS) based techniques such as the proton transfer reaction-mass spectrometry (PTR-MS) [48] and selected ion flow tube-mass spectrometry (SIFT-MS) [49], ion mobility spectrometry techniques (IMS) [50, 51], as well as the use of electronic noses [52] and laser spectroscopy [53, 54]. Gas

chromatography/mass spectrometry (GC/MS) is considered to be the gold standard for VOC analysis and can be used to analyze sweat as well as to distinguish genders [15, 55]. Thermal desorption combined with GC/MS techniques has been used to identify and quantify volatile compounds in exhaled breath, sweat, urine, and other biological excretes. For volatile emissions from human body, solid-phase microextraction (SPME)-GC/MS [39] has also been used widely. Curran et al. [39] by using SPME-GC/MS concluded uniqueness in human scent through both qualitative and quantitative measurements and analysis from different humans sweat samples. Gas chromatography coupled to Fourier transform-infrared spectrometry (GC/FT-IR) [56] has been also used for underarm sweat analysis. However, in field operations (security, forensic, search and rescue), human presence detection with portable analytical instrumentation through breath and skin VOC emissions is still limited.

To overcome limitations and certain portability issues of the existing analytical technology for field chemical analysis, membrane inlet mass spectrometry (MIMS) [57, 58] coupled to a portable mass spectrometer can be used for air and aqueous analysis and monitoring. MIMS offers high sensitivity (low ppt) and fast and accurate analysis with no sample preparation requirements and can be used for both simple and multicomponent mixtures simultaneously [59-64]. Also compared to other MS techniques (e.g., PTR-MS and SIFT-MS), MIMS offers lower size, weight, and cost. This study was developed to investigate the possibility of illegal human detection in border checkpoints (airports, sea ports, and land borders). This chapter reports, for the first time, the use of a portable MIMS instrument (23 kg) for monitoring human chemical signatures in a container simulator.

3.2. Membrane inlet mass spectrometry

Membrane inlet mass spectrometry (MIMS) is a powerful analytical technique widely characterised for its simplicity in use, high sensitivity (ppt detection limits), accuracy and fast chemical analysis (within seconds). It can be used qualitatively and quantitatively for both gas and liquid samples analysis with limited or no sample preparation requirements. MIMS operational principle is based on a three phase process called pervaporation [57, 58]. As it can be seen from Figure 3.1, sample analytes pass through three main steps during the pervaporation process:

a) adsorption of sample molecules onto the membrane surface,

b) diffusion of sample through the membrane material (permeation),

c) desorption of the sample into the vacuum system of the MS.

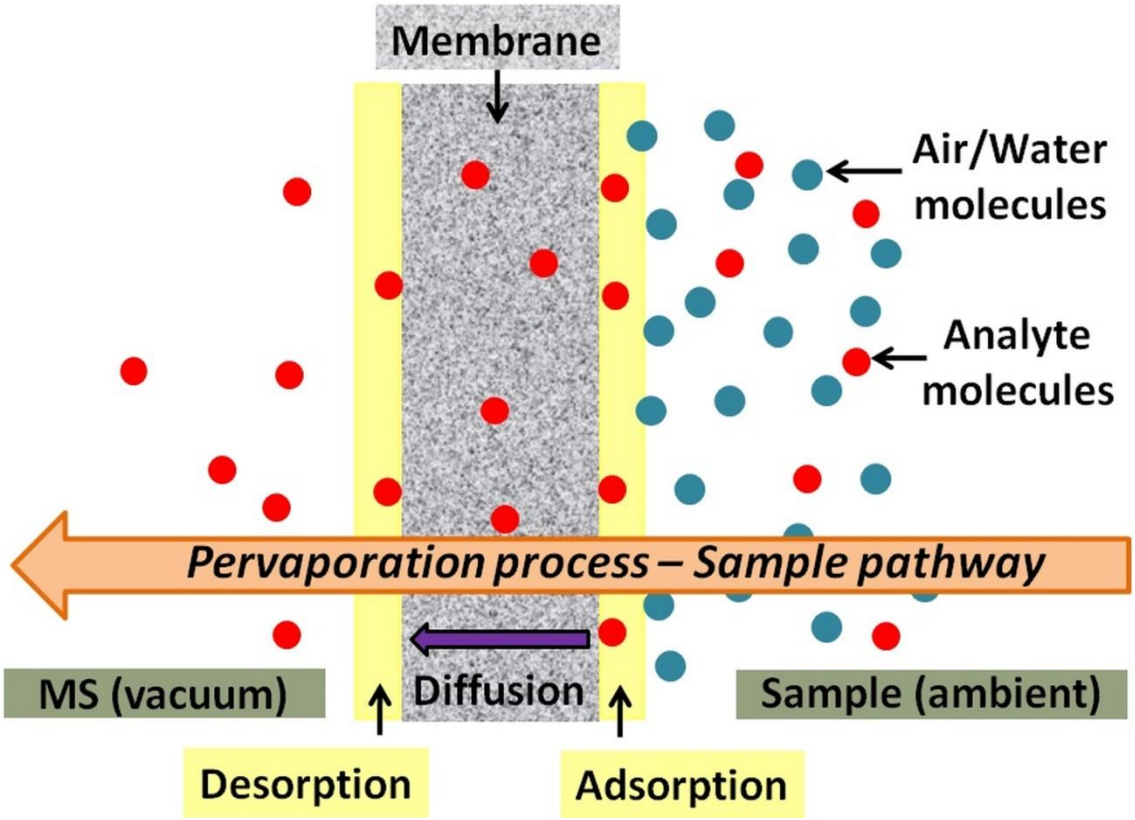

Figure 3.1: Schematic diagram of the pervaporation process that takes place on a sheet-type membrane during MIMS analysis. Sample molecules (in liquid or in gas phase) follow a three stage process (adsorption-diffusion-desorption) to pass through the membrane into the MS vacuum system as vapour molecules before ionization and chemical analysis.

Permeation stage through a membrane [58, 65, 66] is linked with diffusivity property. Diffusion (under steady-state conditions) is described by Fick's first law given by the following equation:

$$J(x,t) = -AD\left(\frac{\partial C(x,t)}{\partial x}\right) \quad (3.1)$$

where J (mol/sec) is the permeation rate, A (cm^2) is the surface area of the membrane and D (cm^2/s) is the diffusion coefficient or diffusivity of the target sample analyte in the membrane. Diffusivity D depends on the membrane concentration gradient ($\partial C(x,t)/\partial x$) and is correlated to sample molecules properties and on membrane material properties. The negative sign in Fick's first law can be explained by the fact that the analyte molecules move from a high to a low concentration area.

A membrane acts as a barrier between the sampling area (which is in ambient pressure) and the MS vacuum system (approximately in the range of 10^{-6}-10^{-5} Torr during operation) offering selective permeation of targeted compounds (usually volatile or semi-volatile organic compounds). Depending on membrane material, structure, thickness, porosity and hydrophilicity/hydrophobicity, molecules with various sizes, properties and from different chemical families can penetrate into the MS system for analysis. The most common membrane material involved in MIMS operations is polydimethylsiloxane (PDMS). PDMS can have a flat formulation (sheet membrane) or can be of tubing shape (capillary membrane). PDMS or silicone membranes belong to the hydrophobic membranes family and are ideal for analysing small molecular weight non-polar molecules. Heavier molecules or slightly polar molecules may mass through the membrane into the MS system, but with more difficulties and slower response times. Applied heating and/or applied suction flow rates (internal or external) on the membrane material have shown to enhance samples permeation (and thus their detection limits) and accelerate analysis time [58-61].

The permeation rate (J_s) through a sheet membrane can be approximated by converting equation (3.1) into the following equation [65, 66]:

$$J_s = ADK\frac{C_{S1}-C_{S2}}{d} \tag{3.2}$$

where A is the surface area of the used membrane, D is the diffusion coefficient of the sample analyte in the membrane, C_{S1} is the sample concentration on the membrane adsorption area and C_{S2} is the sample concentration on the membrane desorption area. K is the partition coefficient for a given sample analyte and d is the thickness of the sheet membrane.

Additionally, (3.1) can give the following equation to describe permeation rate (J_c) through a capillary membrane [65]:

$$J_c = \frac{2\pi LDK(C_{S1}-C_{S2})}{\ln(d_o/d_i)} \quad (3.3)$$

where L is the length of the capillary membrane, D is the diffusion coefficient of the sample analyte in the membrane, C_{S1} is the sample concentration on the membrane adsorption area, C_{S2} is the sample concentration on the membrane desorption area and d_o and d_i are the outer and inner diameters of the capillary membrane respectively.

Membrane response times (both rise and fall times) are crucial for the evaluation of a MIMS system performance. Response times for a specific membrane are usually experimentally measured by the obtained signal intensities for samples at known concentration levels. Usually 50% or 90% response times are reported. The 90% rise response time is the time required for the signal intensity to reach the 90% of its maximum value after the sample inlet valve has been opened and sampling process has started [64]. Fall response time can be defined as the time required for the membrane material to purge and peaks signals return to base/noise level.

Fick's second law which describes non-steady state permeation determines target analyte response time by the following equation [65, 66]:

$$\frac{\partial C}{\partial t} = -D\frac{\partial^2 C}{\partial x^2} \quad (3.4)$$

where *C* is the analyte concentration at location x in the membrane at time t. Non-steady permeation rate for an analyte is given by the following equation [66]:

$$J_t = J_{SS}\left\{1 + \left[2\sum_{n=1}^{\infty}(-1)^n e^{-(n\pi/d)^2 Dt}\right]\right\} \quad (3.5)$$

where J_t is the analyte permeation rate at a time t and J_{SS} is the steady-state flow rate. Using first-order approximation in (3.5) for $n = 1$ at $t_{50\%}$, the diffusion coefficient D is given by the following equation [66]:

$$D = 0.14\frac{d^2}{t_{50\%}} \quad (3.6)$$

where d is the membrane thickness and $t_{50\%}$ (sec) is the time required to achieve 50% steady-state permeation as described above.

Heating of the membrane material result in increased diffusivities and therefore in faster response times for the same analyte (V_p=const). Permeation is given by the equation:

$$P = P_0 \exp\left[-E_p\left({}^{1}/_{RT} - {}^{1}/_{RT_0}\right)\right] \quad (3.7)$$

where P_0 is the initial permeability at some initial temperature, T_0 and Ep is the activation energy for permeation.

3.3. Experimental section

3.3.1. Concept

The basic concept of this work was the chemical detection of human presence in an enclosed space such as a trailer or a container after several hours of confinement. This can correspond to the concealment of an illegal immigrant or other hidden personnel. A small room was used to simulate a shipping container like those used in cargo services at airports, ports, and land borders. During experiments, environmental weather conditions (temperature, humidity, wind velocity) and the temperature inside the container simulator were recorded on a daily basis. The tests ran for over a month and were done for volunteers of both genders, all healthy and under the age of 30. Participation was developed under a voluntary basis and individuals agreed to follow instructions regarding their personal food diet and hygiene before sampling and during the period of the experiments. This was done in order to investigate detection of human chemical signatures under different conditions. During sampling, the participants were asked to follow a 6 h protocol in which their body scent was filling the container simulator. VOCs emitted from human sweat, skin, breath, and other biological excretes were being monitored during time with a MIMS probe coupled to a quadrupole mass spectrometer (QMS). All the sampling experiments were repeated three times to ensure reproducibility and consistency of the results.

3.3.2. Human subjects and ethical issues

Four young, healthy volunteers (three male and one female) were recruited to participate in the experiments. Table 3.1 gives details regarding volunteers' phenotype. The diluted body scent of the participants in the container's air was monitored continuously throughout the scheduled experimental day in a systematic way. Spectra were recorded every 1 hour using the MIMS instrument described below. For safety reasons a member of the research group checked the participant's condition every 2

hours to ascertain any needs and well being and also to determine whether or not to carry on with the experimental procedure. In this case, the experiment could be paused or halted if any of the volunteers were dissatisfied for any reason. The experimental protocol was approved by the Ethics Sub-Committee of the University of Liverpool with reference number RETH000650.

Table 3.1: Summary of participants' phenotype.

Ref. No	Gender	Age (yr)	Mass (kg)	Height (m)	Ethnic background
1	Male	25	75	1.77	White European
2	Male	22	84	1.90	White European
3	Male	23	75	1.79	White European
4	Female	29	70	1.68	Asian

3.3.3. Test environment and experimental setup

The tests for monitoring human chemical signatures (HCSs) using a MIMS were developed and completed in a container simulator in the facilities of the University of Liverpool, U.K. The container simulator was a safe and isolated small room with dimensions of 3.37 m × 5.00 m × 2.50 m. The size of the container simulator was found to be similar to a standard container size.

Before the start of the experiments, the room was properly purified, ventilated, and sealed. All the exogenous sources of volatile emissions were eliminated and removed to other spaces in order to avoid background interferences during experiments. Mass spectra of the simulator's ambient air using the MIMS were taken systematically every 1 hour during the 3 days prior to the start date of the experiments as well as one measurement every morning during the experimental process to ensure the absence of exogenous analytes. The temperature of the simulator was stable at 25 °C. Figure 3.2 shows a schematic diagram for the MIMS experimental setup that was built specifically for the human detection tests. Figure 3.3 shows the experimental setup for the Liverpool MIMS HCS monitoring system. The monitoring results were recorded and analyzed on a laptop computer.

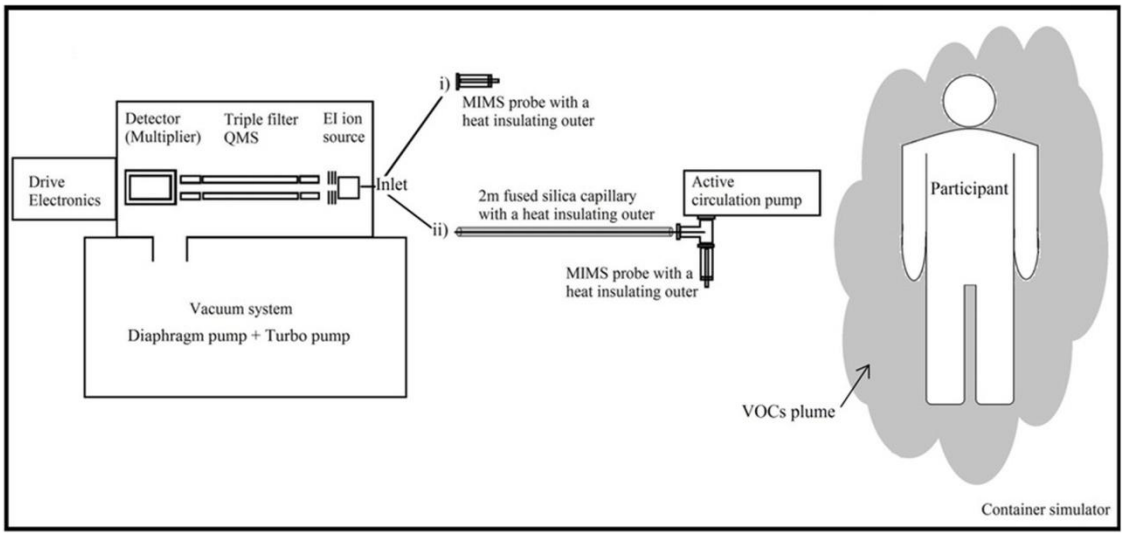

Figure 3.2: Schematic diagram for the MIMS system used for human VOCs monitoring. Two different sample introduction techniques were used for detecting odorous emissions from human body.

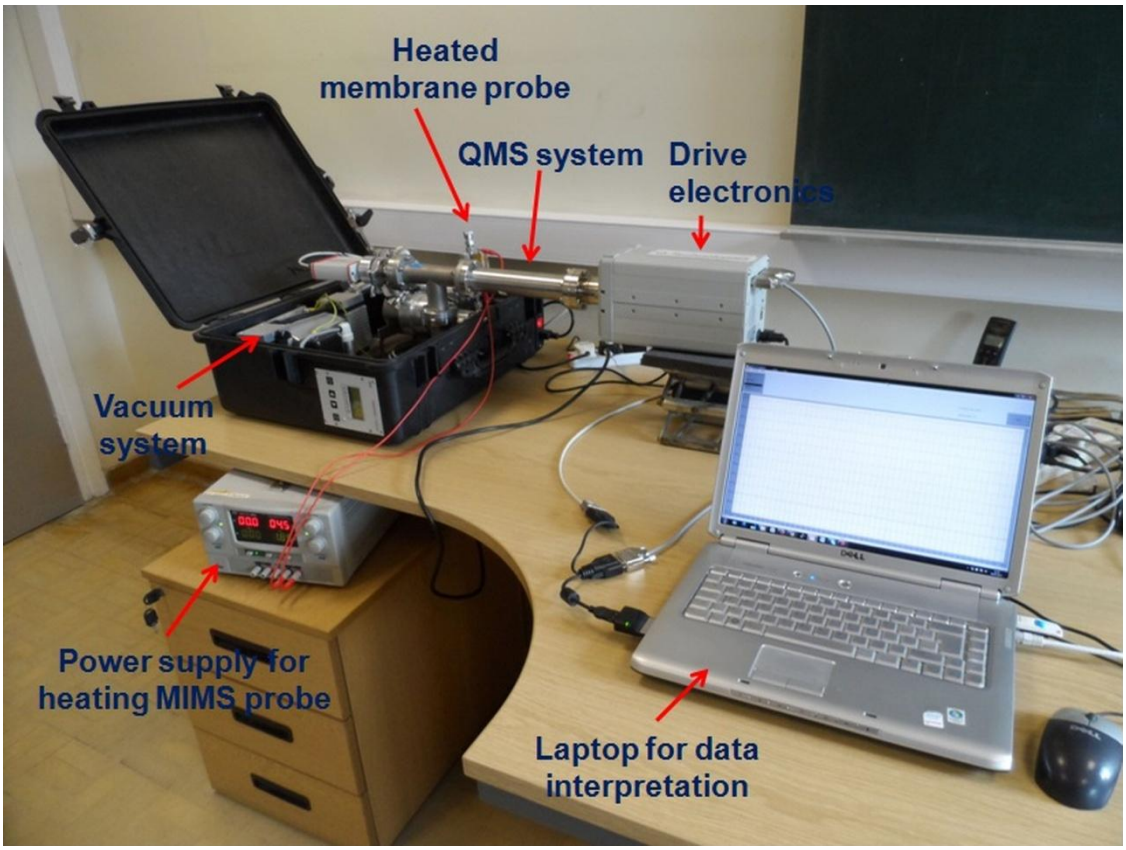

Figure 3.3: Liverpool portable MIMS setup in the container simulator.

3.3.4. Sample introduction

During tests, two different sample introduction techniques were used. The first technique was performed by a membrane probe manufactured by the University of Liverpool. The probe was connected directly to the vacuum valve, sampling the ambient air of the container simulator. It is schematically described in Figure 3.2, i). The probe and membrane were heated at 70 °C through heat transfer from a 100 W aluminum housed resistor provided by TE Connectivity, Berwyn, PA. The probe was heated to allow volatile compounds to pass through the membrane material, and it was found that 70 °C was safest maximum heating temperature for the membrane to gain maximum sensitivity. The membrane surface temperature was monitored using a glass laboratory thermometer.

The second technique, described in Figure 3.2, ii), used a fused silica capillary inlet connected with a membrane sampling probe. The capillary column used for transferring the gas samples into the QMS was a 2 m long fused silica, housed within a stainless steel and heat insulating outer cover, provided by European Spectrometry Systems Ltd., U.K. A heater unit for the capillary inlet was used to heat it to 110 °C. The front side end of the capillary inlet was connected directly with the QMS, whereas the back side end of the capillary was connected with a 6.35 mm Swagelok stainless steel tee ring coupling. A membrane probe heated at 70 °C was attached to the one side of the tee ring coupling for sampling of simulator air. From the other side of the tee ring coupling, an active circulation pump for gases (Rietschle Thomas Ltd., U.K., model SMG4 24 V DC) was providing an air flow rate of 0.1–1.1 L/min. Both heating and airflow were used to achieve an intensive suction of the molecules from the membrane material.

The membrane probe assembly contained two thin (i.d. 0.40 mm, o.d. 1.60 mm) stainless steel tubes mounted into a thicker (i.d. 4.00 mm, o.d. 6.35 mm) stainless steel tube with a loop of cross-linked membrane tubing made from polydimethylsiloxane (PDMS). The PDMS capillary membrane was provided by Helix Medical Inc., Carpinteria, CA. The total length of the stainless steel probe was 100 mm, whereas the PDMS membrane tubing was approximately 70 mm long with 0.55 mm wall thickness. Figure 3.4 presents in detail the above described membrane probe. A second, in-house developed membrane sampling probe was used additionally for the measurements, and

it consists of stainless steel tubing coupled with a membrane sheet supported in the one end side with a 6.35 mm Swagelok stainless steel vacuum fitting union (Figure 3.5). Table 3.2 shows all the membranes (both hydrophilic and hydrophobic) that were tested in order to examine and to achieve maximum VOCs detection with the two types of sampling probes coupled to our portable MIMS instrument. Eight different membrane materials with different porosities and various membrane wall thicknesses were tested.

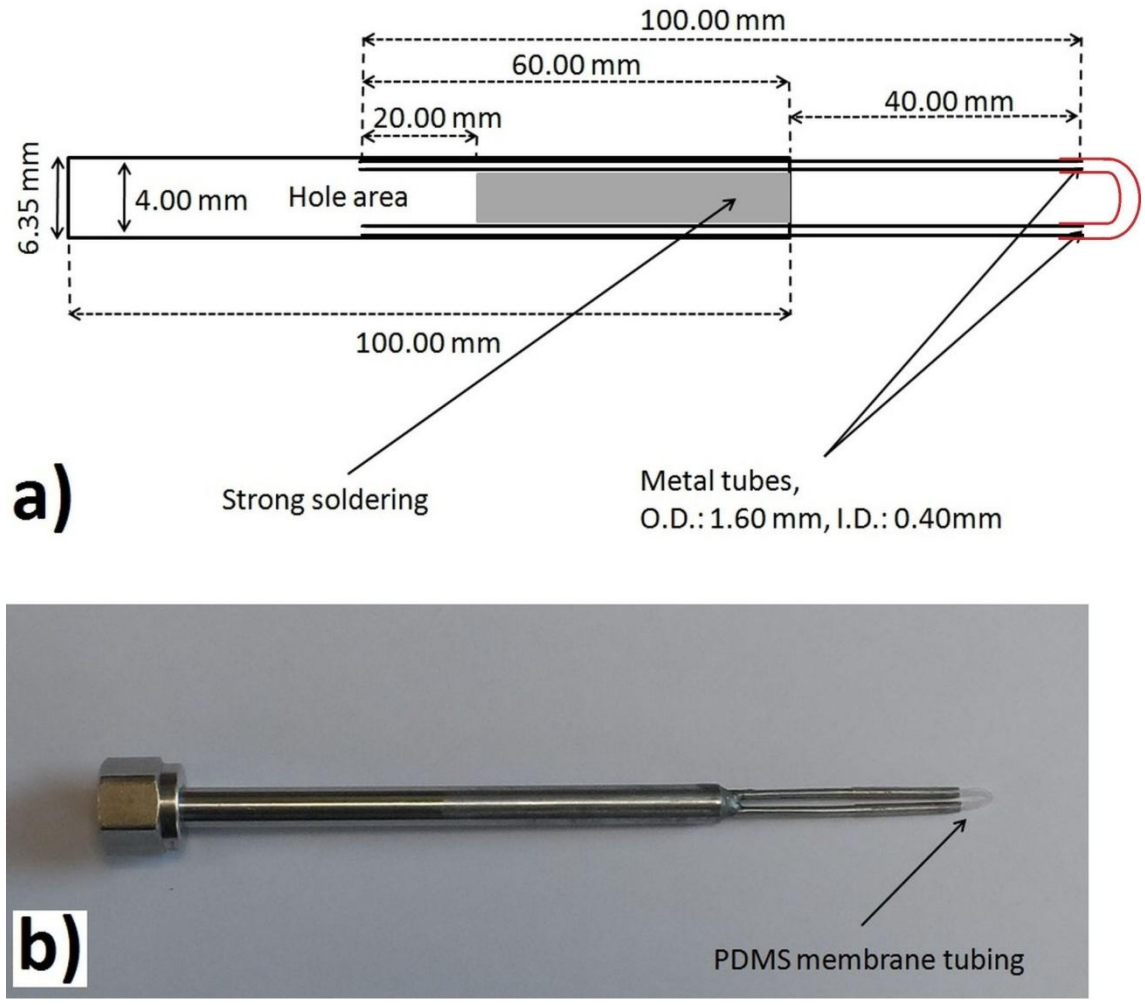

Figure 3.4: a) Design (plan view) of the main membrane sampling probe used in the human scent monitoring experiments, b) Liverpool membrane sampling probe coupled with a loop of cross-linked PDMS membrane tubing.

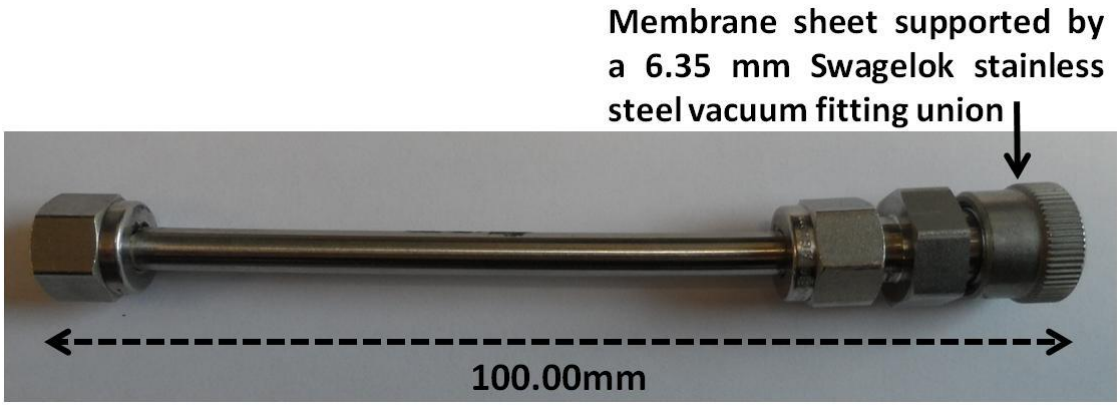

Figure 3.5: Liverpool sheet membrane sampling probe. Membrane sheet is supported in the one end side with a 6.35 mm Swagelok stainless steel vacuum fitting union.

Table 3.2: Membranes tested with MIMS instrument to evaluate their performance in human chemical signatures analysis and in human detection in a confined space.

No	Membrane name	Material	Form	Hydrophobicity/ Hydrophilicity	Pore size (µm)	Thickness (mm)
1	TF-200	PTFE	sheet	Hydrophobic	0.2	0.139
2	Supor®-100,	PES	sheet	Hydrophilic	0.1	0.102
3	High Consistency Silicone Rubber	Silicone	sheet	Hydrophobic	NA	0.300
4	Mitex Membrane	PTFE	sheet	Hydrophobic	10	0.130
5	Nylon Membrane	Nylon	sheet	Hydrophilic	0.45	NA
6	Porelle microporous,345	PU	sheet	Hydrophobic	< 1	0.045
7	SIL-TEC membrane sheeting	silicone	sheet	Hydrophobic	NA	0.120
8	Standard silicone tubing	silicone	tubing	Hydrophobic	NA	0.280

3.3.5. Mass spectral analysis

Mass spectral analysis of the ionized sample gas passing through different types of membranes was done using a triple filter quadrupole mass spectrometer (QMS) system supplied by Q-Technologies Ltd., U.K. The main components of the portable mass

spectrometer are the electron impact (EI) ion source, the mass filter, and the detector. The enclosed EI ion source has dual Thoria filaments assembly at about 1.68 mA electron emission current. The mass analyzer contains a prefilter (25mm length), a main filter (125mm length), and a post filter (25mm length) with rods of 6.3mm diameter. It has a mass range of *m*/*z* 1–200 with a unit resolution over the entire mass range. The sensitivity of the quadrupole analyzer is 1×10^{-4}A/mbar. The detector comprises a Faraday cup for detecting usual ion currents and a Channeltron type electron multiplier for detecting very low currents like those produced from low level concentration VOCs emitted from the human body. During data acquisition, 10 acquisition points were recorded per unit mass with an average number of 20 scans per measurement throughout the whole mass range. In order to eliminate possible false-positives with interferences, peaks with relative abundance >3% above baseline were examined.

3.3.6. Vacuum system

The QMS was housed in a stainless steel chamber pumped by a vacuum system consisting of an Oerlikon DIVAC 0.8 LT diaphragm pump and a Pfeiffer Balzers turbomolecular pump. The diaphragm pump provides pressure down to 1×10^{-2} Torr, while the turbomolecular pump gives a base pressure of 1×10^{-7} Torr. The system pressure was continuously being monitored by a highly accurate digital pressure gauge supplied by Pfeiffer (MRT 100, DN 25 ISO-KF) that uses a Pirani/Cold cathode method of measurement. Operating pressure for mass analysis with an attached membrane sampling probe or heated GC column was 5×10^{-6} Torr.

3.4. Results and discussion

3.4.1. Human chemical signature analysis

This experiment was done with a single volunteer to prove the principle of detection of human presence in a confined space such as a container similar to those used in cargo services. During the tests, VOC emissions from human breath, sweat, and skin were present in the container simulator. In each test, the human VOC plume in the ambient air of the simulator was continuously monitored every hour for 6 hours in total. Blank measurements of the container air were taken before the start date of the experiments as well as every experimental day to ensure the absence of exogenous compounds

contamination. All the data were recorded and further analyzed using the NIST Chemistry WebBook as reference for spectral peaks of each compound.

Figure 3.6 shows a representative mass spectrum indicating human presence in the container simulator after 6 hours of presence with the mass range *m*/*z* 40–115. The differences between no human presence and human presence in the confined space used for the experiments are clearly seen. Moreover, peak intensities after 1 and 6 hours of human enclosure in the container simulator increase by a factor of 5. Key mass fragments detected during tests are shown in Table 3.3. CO_2 responses are of particular concern indicating a characteristic inorganic gas of human detection in a confined space. During the 6 hours of the experiments, CO_2 levels slowly increased (approximately 1.3% for the single human experiment). The CO_2 signal level in the container simulator was between 20-30 times greater than the signals of the VOCs of interest. Other organic compounds of interest are acetone (*m*/*z* 43, 58) and isoprene (*m*/*z* 67, 68), which are characteristic for human breath and skin emissions. Carboxylic acids like propanoic acid (*m*/*z* 73, 74) and lactic acid (*m*/*z* 45, 90) present in human sweat emanations were also detected.

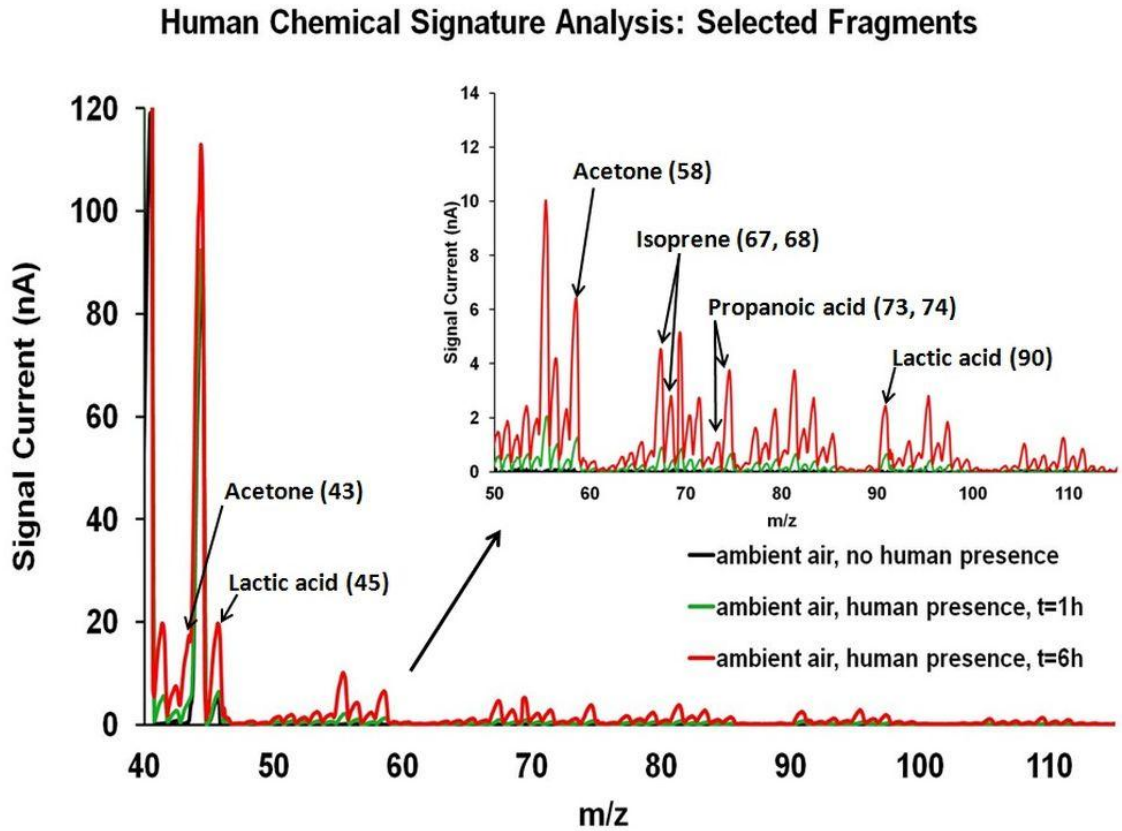

Figure 3.6: Mass spectra of the ambient air in the container simulator including no human presence and human presence for 1 and 6 hours.

Table 3.3: Potential VOCs emitted from human breath and body in the container simulator with their characteristic mass fragments and their signal intensity changes during time.

Potential human odor compounds detected			
No	**Compound Name**	**Characteristic Mass Fragments (*m/z*)**	**Intensity Change**
1.	H_2O	17, 18	increased
2.	NH_3	16, 17	increased
3.	CO_2	44	increased
4.	CO	28, 12	increased
5.	Methanol	29, 30, 31, 32	increased
6.	O_2	32, 16	decreased
7.	Acetaldehyde	29	increased
8.	Hexane	57, 86	increased
9.	Lactic acid	45, 90	increased
10.	Nonanal	57, 70, 98	increased
11.	Isoprene	53, 67, 68	increased
12.	Acetone	43, 58	increased
13.	Limonene	68, 93, 121, 136	increased
14.	Phenol	31, 45, 46, 94	increased
15.	Pentane	41, 42, 57, 72	increased
16.	Heptane	55, 56, 57, 70, 71, 85	increased
17.	1-pentene	55, 70	increased
18.	Hexanal	56, 57, 58, 82	increased
19.	Isopropanol	27, 45, 59	increased
20.	2-nonenal	55, 56, 57, 70, 83	increased
21.	Ethanol	27, 29, 30, 31, 45, 46	increased
22.	Propanoic acid	73, 74	increased

3.4.2. Optimization experiments

In order to achieve optimal sensitivity for human detection in a confined space, eight series of experimental measurements were carried out in total for a single volunteer. The first experimental set was performed to examine ambient air analysis of the container simulator directly from the vacuum valve (setup i). The second set was performed with a heated GC column connected to the vacuum valve (setup ii). The third set examined the use of a capillary PDMS sampling probe coupled to the vacuum valve (setup iii). The vacuum valve was fully open with the operational pressure at 5×10^{-6} Torr. The fourth set was developed with a heated capillary PDMS sampling probe again directly connected to the vacuum valve (setup iv), while the fifth set used a heated capillary PDMS sampling probe coupled with a GC column as a transfer line (setup v). The probe was heated as described above with a sampling flow rate of 1.1 L/min from a small differential pump. This was done to achieve an efficient suction of molecules from the membrane surface into the vacuum system and the MS. The sixth set involved ambient air analysis of the simulator with a sheet PDMS membrane probe connected to the MS vacuum valve (setup vi). The seventh set examined the use of a heated sheet PDMS membrane probe (setup vii). Finally, the eighth set investigated the use of a heated sheet PDMS sampling probe coupled with a GC column, heated and with a sampling flow of 1.1 L/min (setup viii).

During the tests, oxygen levels were decreased over time as expected but remained sufficiently high for safe human life during the measurements. On the other hand, CO_2 levels slowly increased as expected. Organic compounds such as acetone, isoprene, and carboxylic acids (propanoic acid and lactic acid) were also detected and showed an upward trend. It can be seen from Figure 3.7 that a heated sampling probe with capillary PDMS membrane (setup iv) has the best performance for sensitivity compared to the remaining seven experimental sets. It was also found that heating affects membrane response time and that high suction flow rates (L/min) applied on the membrane materials give better results than low suction flow rates (mL/min).

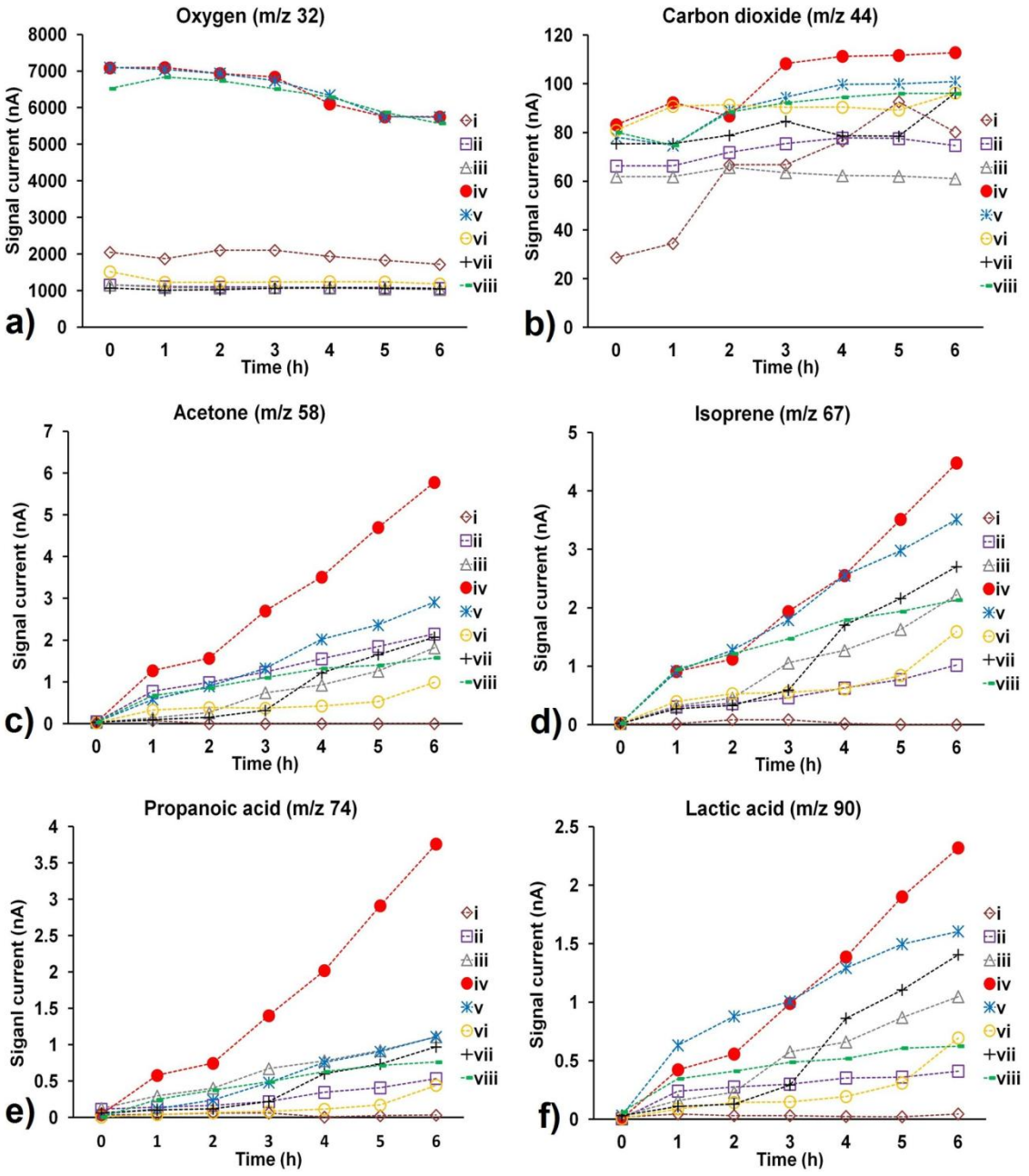

Figure 3.7: Signal intensity change for mass fragments of oxygen (*m/z* 32), carbon dioxide (*m/z* 44), acetone (*m/z* 58), isoprene (*m/z* 67), propanoic acid (*m/z* 74), and lactic acid (*m/z* 90) during six hours of human presence in a container simulator using 8 different experimental setups. Ambient air analysis using (i) vacuum valve, (ii) a GC column inlet, (iii) a capillary PDMS sampling probe, (iv) a heated capillary PDMS sampling probe, (v) a heated capillary PDMS sampling probe coupled to a heated GC column inlet, (vi) a sheet PDMS sampling probe, (vii) a heated sheet PDMS sampling probe, (viii) a heated sheet PDMS sampling probe coupled to a heated GC column inlet.

3.4.3. Membrane experiments

In order to choose the best membrane material for our experiments, a series of measurements with both hydrophilic and hydrophobic membranes were done. Membranes presented in Table 3.2 were tested. It has been observed that membrane nos. 7 and 8 of Table 3.4 have the best performance with high selectivity of volatile compounds and high sensitivity. They have fast response times in the detection of volatile compounds from the human body. Table 3.4 shows 90% response times for each membrane material. The 90% response time is the time required for the signal intensity to reach the 90% of its maximum value after the sample valve has been opened [64].

Table 3.4: Membranes response times and their selectivity in the detection of human chemical signatures.

No	Membrane name	90% response time (sec)	Acetone	Isoprene	Propanoic acid	Lactic acid
1	TF-200	190	X	X	X	X
2	Supor®-100	190	X	X	-	-
3	High consistency silicone rubber	120	X	X	X	X
4	Mitex membrane	90	X	X	X	X
5	Nylon membrane	170	X	X	-	-
6	Porelle microporous 345	120	X	X	X	X
7	SIL-TEC membrane sheeting	60	X	X	X	X
8	Standard silicone tubing	50	X	X	X	X

3.4.4. Human gender experiments

This section describes the difference in HCS profiles between different genders. Figure 3.8 presents simultaneously the differences in the chemical profiles between a male and a female volunteer in the container simulator after 6 hours of enclosure. In both cases the following targeted VOCs were detected: acetone, isoprene, propanoic

acid, and lactic acid. It is noticeable from the mass spectra in Figure 3.8 that the above compounds show greater levels of abundance for the male participant instead of the female. Characteristically the male volunteer appears to produce in the ambient air of the container simulator appreciable quantities of the above-described carboxylic acids than the female volunteer. This can be justified by the fact that men are more prone to sweating than women [67]. Moreover, skin surface plays an important role in sweat secretions. The selection of male volunteers for further study under different conditions was done because it has been found by Wagtail UK Ltd., a specialist sniffer dog company, that the percentage according to gender distribution of illegal immigrants who attempt to pass through the borders of European Union countries is approximately 94% male and 6% female [68].

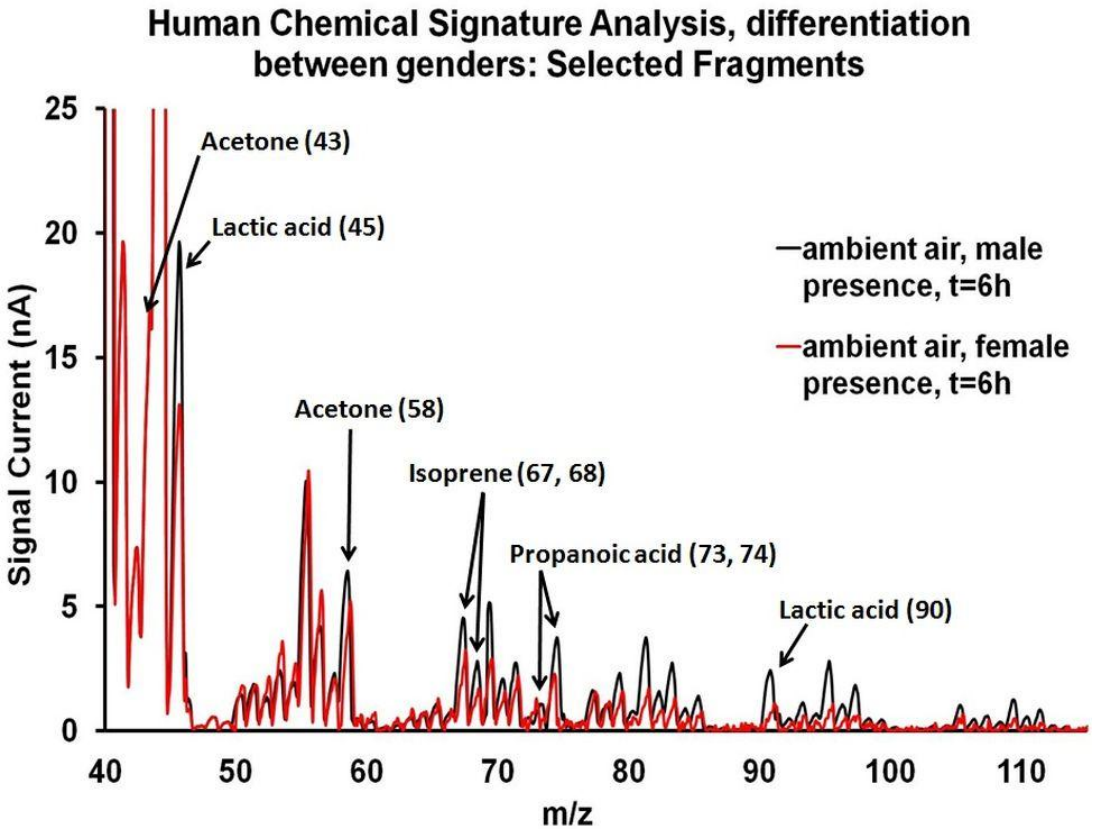

Figure 3.8: Representative mass spectra corresponding to the differences between male and female chemical signatures after 6 hours of presence in the container simulator.

3.4.5. Concentration experiments

In order to obtain an approximate estimation of the concentrations of acetone, isoprene, propanoic acid, and lactic acid in human odour in a small container, a series of

concentration measurements were performed. Substance samples used for generating calibration curves were in the liquid phase with their concentrations set using a micropipette. All the chemicals that were used were of high purity (>99%) and were obtained from Sigma Aldrich, St. Louis, MO.

Exact ppb concentrations in the range from 2 ppb to 20 ppb were prepared by mixing small quantities of target substances with deionized water in a flask. Deionized water was bought from ReAgent Chemical Services Ltd., Cheshire, U.K. A membrane probe was inserted into the liquid solution in the flask with the top cover of the flask isolated with a suitable tape to prevent evaporation. Flask was put on a hot plate that was used to set the temperature of a substance solution and membrane probe to 70 °C as used during air sampling experiments. This was used to approximate conditions during air sampling, where the temperature of sample molecules in air becomes close to 70 °C when they approach the membrane. The substance mixture was maintained constant by using a stirring rod inside the flask.

In order to achieve reliable concentration measurements, a suitable m/z with the highest linearity calibration curve was chosen for each targeted compound. For each individual substance concentration, 10 readings were taken. From these readings, the mean values were calculated for each concentration. Calibration curves of our MIMS instrument exhibited linearity with R^2 values in the range from 0.9546 to 0.9727 as shown in Table 3.5. From the calibration curves, the following approximate concentrations were estimated for the targeted volatile compounds for a male volunteer in the container simulator after 6 hours of enclosure: acetone at 18 ppb, isoprene at 11 ppb, and propanoic acid and lactic acids at around 6 ppb. For the case of a female volunteer, approximate concentrations for acetone, isoprene, propanoic acid, and lactic acid were, respectively, 14 ppb, 7 ppb, 2 ppb, and 2 ppb.

Table 3.5: Summary of the R^2 values obtained by the calibration curves for the targeted compounds using our MIMS system.

No	Compound	Characteristic peaks (*m/z*)	R^2 value
1	Acetone	43, 58	0.9611
2	Isoprene	67, 68	0.9727
3	Propanoic acid	73, 74	0.9546
4	Lactic acid	45, 90	0.9556

3.4.6. Multiple human experiments

This section describes the case of using MIMS instrument for detection of 3 humans in the same confined space. Three male volunteers were asked to follow the experimental protocol and remain in the container simulator for 6 hours. Volatile compounds emissions from their breath and sweat were filling the ambient air of the simulator while data were continuously recorded. Figure 3.9a shows a representative mass spectrum obtained after 6 hours of human presence in the container simulator whereas Figure 3.9b presents peak change for acetone (*m/z* 58), isoprene (*m/z* 67), propanoic acid (*m/z* 74) and lactic acid (*m/z* 90) as a function of time during multiple human experiments. As expected, the levels of acetone, isoprene, lactic acid and propanoic acid significantly increased compared to the case when one human was confined. Concentration levels were estimated for the targeted compounds. Acetone exhibits approximately a concentration much higher than 20 ppb, isoprene 19 ppb, propanoic acid 10 ppb and lactic acid 9 ppb.

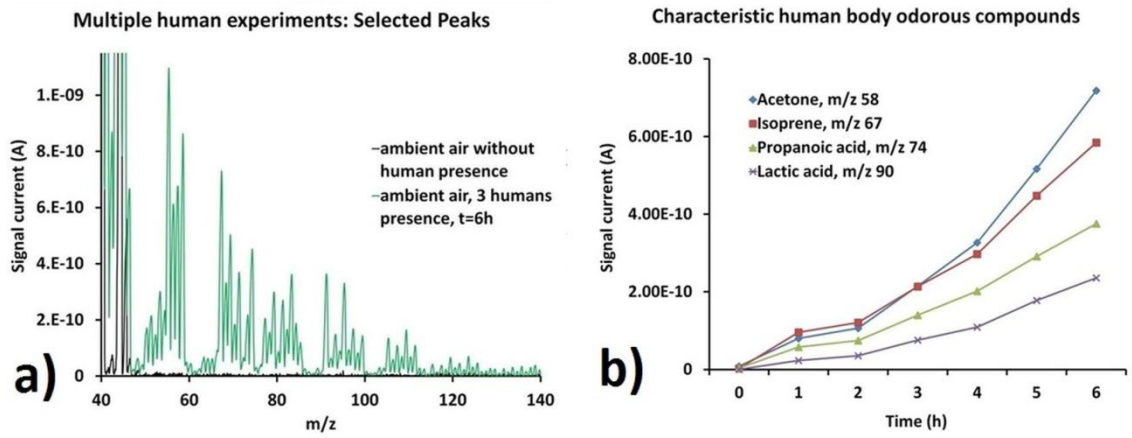

Figure 3.9: Comparative presentation of mass spectra obtained from the ambient air of the container simulator a) without and with multiple human presence after 6h, and b) peak change for acetone (*m/z* 58), isoprene (*m/z* 67), propanoic acid (*m/z* 74) and lactic acid (*m/z* 90) during multiple human experiments.

3.4.7. Human condition experiments

In a real case scenario, the testing environment could potentially be a dirty container or a confined space with various influences from human or animal remains (urine, feces, vomit, etc.), food items, luggage, etc. Moreover, the hidden human may have used a deodorant in the axillary area, a perfume, or may have consumed a quantity of alcohol and food. In order to simulate a real situation of hidden human presence under different experimental conditions, a series of experiments involving (1) use of deodorant spray, (2) simultaneous urine presence, and (3) alcohol consumption were done. During the different experimental conditions, the same volunteer was recruited. For the first series, the participant was asked to wear a generous quantity of a deodorant spray on the axillary area and over the body area prior the start of the measurements. Before the start time of the experiment, the participant was also asked not to follow any specific diet protocols or any special personal hygiene rules. During sampling, the participant's body odour and the used deodorant were filling the container simulator while data from the container simulator's ambient air were recorded every 1 hour of the 6 hours total duration of the experiment. Figure 3.10a shows an ideal mass spectrum of a human without interference of external conditions. Figure 3.10b shows a representative mass spectrum of a human using a deodorant, in the container simulator after 6 hours of enclosure, with the mass range *m*/*z* 40–115. VOCs such as acetone, isoprene, propanoic acid, and lactic acid were detected at the following approximate concentrations: 20 ppb, 20 ppb, 10 ppb, and 8 ppb, respectively. The small increase of the concentration levels of the detected compounds can be justified by the presence of the deodorant peaks which interfered with human body odorous emissions. Figure 3.10c examines the second series of experiments, in which a male volunteer was asked to remain in the container simulator with simultaneous urine present for 6 hours. After the 6 hours, the targeted analytes were again detectable, with approximate concentrations over 20 ppb for acetone, 18 ppb for isoprene, 10 ppb for propanoic acid, and 9 ppb for lactic acid. Again a minor increase of the selected peaks can be explained by the presence of 200 mL of a urine sample in the container simulator. Figure 3.10d shows the third series of experiments that explores how chemical signatures may differ or vary after alcohol consumption. In this case, the targeted analytes appear to have approximate concentrations over 20 ppb for acetone, 16 ppb for isoprene, 11 ppb for propanoic acid, and 12 ppb for lactic acid.

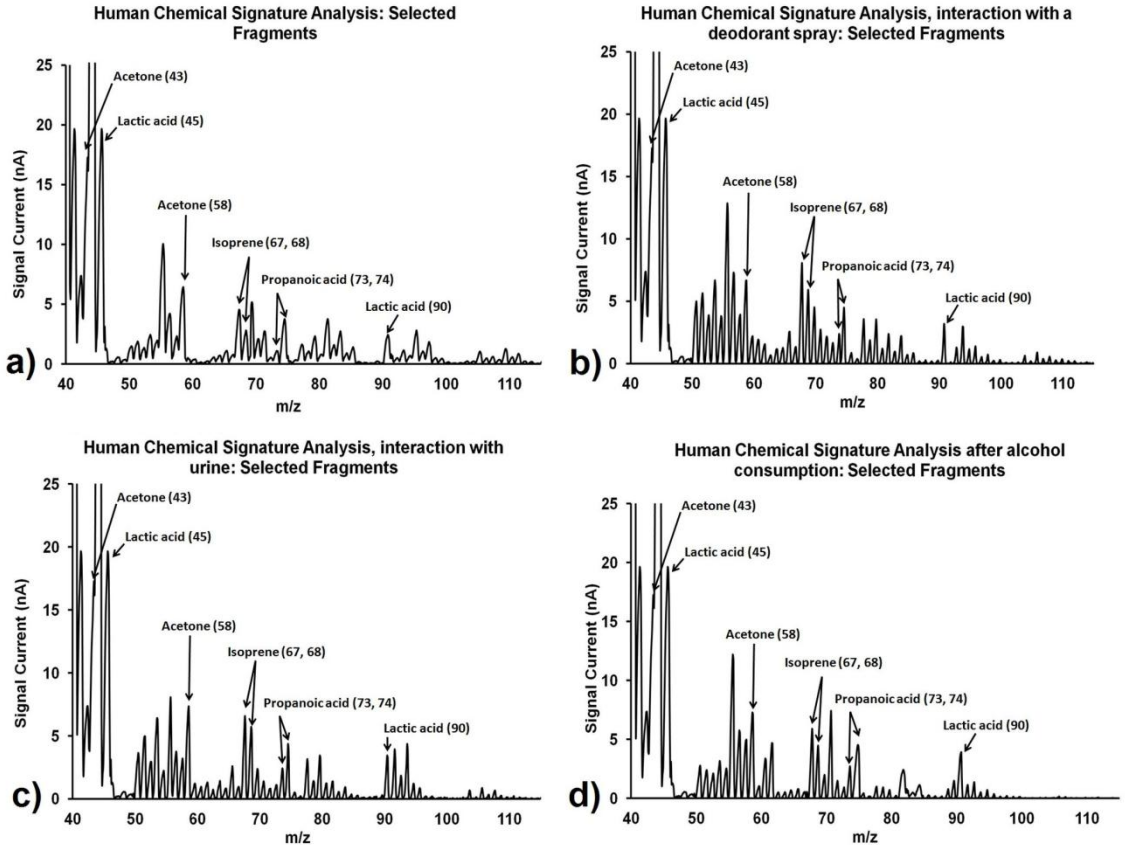

Figure 3.10: Mass spectra of the ambient air of the container simulator including human presence after 6 hours of enclosure under 4 different experimental conditions: a) ideal case for a single man-volunteer, who followed a personal hygiene and food protocol prior and during the tests without any external interferences, b) human volunteer after use of a commercial deodorant spray in axillary area of his body just before the start time of the experiment, c) presence of a human volunteer with urine sample, d) human volunteer after alcohol consumption.

3.5. Conclusions

The possibility of hidden human detection in a confined space such as a container has been demonstrated using a portable membrane inlet mass spectrometer. During monitoring of human chemical signatures, a series of different experimental scenarios were investigated. Experiments took place for both genders in a container simulator under different experimental conditions and interferences. Eight different membranes were examined to test their response times and for achieving maximum and optimum human VOC detection.

Membrane heating and different sample suction flow rates were used for improving selectivity and sensitivity of our technique. It was found that a small decrease in O_2 levels and increases of the abundances of CO_2, acetone, isoprene, propanoic acid, and lactic acid may be potential markers of human presence in a container after several hours of actual physical presence. Preliminary data were presented while a further study involving more human subjects with variant phenotype characteristics (race, background origin, age, gender, habits, etc.), and additional instrumentation is required for more detailed odour explanations on human body scent. An algorithm of the profile of the detectable human scent compounds will need to be developed and clarified. Apart from security applications, this work is also highly relevant for search and rescue operations.

3.6. References

[1] U.S. Department of Homeland Security, www.dhs.gov.

[2] G. A. Schoon, J. C. De Bruin, *The ability of dogs to recognize and cross-match human odours,* Forensic Sci. Int. **69,** 111-118 (1994).

[3] G. A. Schoon, *A first assessment of the reliability of an improved scent identification line-up,* J. Forensic Sci. **43,** 70-75 (1998).

[4] D. Komar, *The use of cadaver dogs in locating scattered, scavenged human remains: preliminary field test results,* J. Forensic Sci. **44,** 405-408 (1999).

[5] N. Lorenzo, T. Wan, R. J. Harper, Y. L. Hsu, M. Chow, S. Rose, K. G. Furton, *Laboratory and field experiments used to identify Canis lupus var. familiaris active odor signature chemicals from drugs, explosives, and humans,* Anal. Bioanal. Chem. **376,** 1212-1224 (2003).

[6] M. Callagher, C. J. Wysocki, J. J. Leyden, A. I. Spielman, X. Sun, G. Preti, *Analyses of volatile organic compounds from human skin,* Brit. J. Dermatol. **159,** 780-791 (2008).

[7] A. M. Curran, S. I. Rabin, K. G. Furton, *Analysis of the Uniqueness and Persistence of Human Scent,* Forensic Science Commun. **7,** (2) (2005).

[8] M. Statheropoulos, E. Sianos, A. Agapiou, A. Georgiadou, A. Pappa, N. Tzamtzis, H. Giotaki, C. Papageorgiou, D. Kolostoumbis, *Preliminary investigation of using*

volatile organic compounds from human expired air, blood and urine for locating entrapped people in earthquakes, J. Chromatogr B **822,** 112-117 (2005).

[9] W. Vautz, J. I. Baumbach, *Exemplar application of multi-capillary column ion mobility spectrometry for biological and medical purpose,* Int. J. Ion Mob. Spectrom. **11,** 35-41 (2008).

[10] W. Vautz, J. Nolte, R. Fobbe, J. I. Baumbach, *Breath analysis-performance and potential of ion mobility spectrometry,* J. Breath Res. **3,** 1-8 (2009).

[11] W. Vautz, J. Nolte, A. Bufe, J. I. Baumbach, M. Peters, *Analyses of mouse breath with ion mobility spectrometry: a feasibility study,* J. Appl. Physiol. **108,** 697-704 (2010).

[12] T. Perl, E. T. H. Carstens, A. Hirn, M. Quintel, W. Vautz, J. Nolte, M. Jünger, *Determination of serum propofol concentrations by breath analysis using ion mobility spectrometry,* Brit. J. Anaesth. **103,** 822-827 (2009).

[13] B. Buszewski, M. Kesy, T. Ligor, A. Amann, *Human exhaled air analytics: biomarkers of diseases,* Biomed. Chromatogr. **21,** 553-566 (2007).

[14] K. Ackerl, A. Atzumuller, K. Grammer, *The Scent of Fear,* Neuroendocrinol. Lett. **23,** 79-84 (2001).

[15] D. Penn, W. K. Potts, *Chemical signals and parasite-mediated sexual selection,* Trends Ecol. Evol. **13,** 391-396 (1998).

[16] D. Singh, P. M. Bronstad, *Female body odour is a potential cue to ovulation,* Proc. R. Soc. B **268,** 797-801 (2001).

[17] C. Turner, P. Spanel, D. Smith, *A longitudinal study of ammonia, acetone and propanol in the exhaled breath of 30 subjects using selected ion flow tube mass spectrometry, SIFT-MS,* Physiol. Meas. **27,** 321–337 (2006).

[18] C. Turner, P. Spanel, D. Smith, *A longitudinal study of breath isoprene in healthy volunteers using selected ion flow tube mass spectrometry (SIFT-MS),* Physiol. Meas. **27,** 13–22 (2006).

[19] C. Turner, P. Spanel, D. Smith, *A longitudinal study of ethanol and acetaldehyde in the exhaled breath of healthy volunteers using selected-ion flow-tube mass spectrometry,* Rap. Commun. Mass Spectrom. **20,** 61–68 (2006).

[20] C. Turner, P. Spanel, D. Smith, *A longitudinal study of methanol in the exhaled breath of 30 healthy volunteers using selected ion flow tube mass spectrometry, SIFT-MS,* Physiol. Meas. **27,** 637–648 (2006).

[21] J. Taucher, A. Hansel, A. Jordan, W. Lindinger, *Analysis of Compounds in Human Breath after Ingestion of Garlic Using Proton-Transfer-Reaction Mass Spectrometry,* J. Agric. and Food Chem. **44,** 3778-3782 (1996).

[22] C. Warneke, J. Kuczynski, A. Hansel, A. Jordan, W. Vogel, W. Lindinger, *Proton transfer reaction mass spectrometry (PTR-MS): propanol in human breath,* Int. J. Mass Spec. Ion Proc. **154,** 61-70 (1996).

[23] J. Taucher, A. Lagg, A. Hansel, W. Vogel, W. Lindinger, *Methanol in Human Breath,* Alcohol. Clin. Exp. Res. **19,** 1147-1150 (1995).

[24] A. Hansel, A. Jordan, R. Holzinger, P. Prazeller, W. Vogel, W. Lindinger, *Proton transfer reaction mass spectrometry: on-line trace gas analysis at the ppb level,* Int. J. Mass Spec. Ion Proc**. 149,** 609-619 (1995).

[25] D. Smith, P. Spanel, *The Novel Selected-ion Flow Tube Approach to Trace Gas Analysis of Air and Breath,* Rap. Comm. Mass Spec. **10,** 1183-1198 (1996).

[26] Y. Lin, S. R. Dueker, A. D. Jones, S. E. Ebeler, A. J. Clifford, *Protocol for collection and HPLC analysis of volatile carbonyl compounds in breath,* Clin. Chem. **41,** 1028-1032 (1995).

[27] S. Mendis, P. A. Sobotka, D. E. Euler, *Pentane and isoprene in expired air from humans: gas-chromatographic analysis of single breath,* Clin. Chem. **40,** 1485-1488 (1994).

[28] M. Phillips, J. Greenberg, *Method for the collection and analysis of volatile compounds in the breath,* J. Chrom. **564,** 242-249 (1991).

[29] D. Gelmont, R. A. Stein, J. F. Mead, *Isoprene-The main hydrocarbon in human breath,* Biochem. Biophys. Res. Comm. **99,** 1456-1460 (1981).

[30] J. P. Conkle, B. J. Camp, B. E. Welch, *Trace Composition of Human Respiratory Gas,* Arch. Environ. Health. **30,** 290-295 (1975).

[31] C. Grote, J. Pawliszyn, *Solid-Phase Microextraction for the Analysis of Human Breath,* Anal. Chem. **69,** 587-596 (1997).

[32] A. W. Jones, V. Lagesson, C. Tagesson, *Origins of breath isoprene,* J. Clin. Pathol. **48,** 979-980 (1995).

[33] R. Huo, A. Agapiou, V. Bocos-Bintintan, L. J. Brown, C. Burns, C. S. Creaser, N. A. Devenport, B. Gao-Lau, C. Guallar-Hoyas, L. Hildebrand, A. Malkar, H. J. Martin, V. H. Moll, P. Patel, A. Ratiu, J. C. Reynolds, S.; Sielemann, R. Slodzynski, M. Statheropoulos, M. A. Turner, W. Vautz, V. E. Wright, C. L. P. Thomas, *The trapped human experiment,* J. Breath Res. **5,** 1-12 (2011).

[34] M. Callagher, C. J. Wysocki, J. J. Leyden, A. I. Spielman, X. Sun, G. Preti, *Analyses of volatile organic compounds from human skin,* Brit. J. Dermatol. **159,** 780-791 (2008).

[35] R. C. Smallegange, N. O. Verhulst, W. Takken, *Sweaty skin: an invitation to bite?,* Trends Parasitol. **27,** 143-148 (2011).

[36] P. J. H. Jackman, W.C. Noble, *Normal axillary skin in various populations,* Clin. Exp. Dermatol. **8,** 259–268 (1983).

[37] R. B. Jacoby, J. C. Brahms, S. A. Ansari, J. Mattai, *Detection and quantification of apocrine secreted odor-binding protein on intact human axillary skin,* Int. J. Cosmet. Sci **26,** 37–46 (2004).

[38] F. Kuhn, A. Natsch, *Body odour of monozygotic human twins: a common pattern of odorant carboxylic acids released by a bacterial aminoacylase from axilla secretions contributing to an inherited body odour type,* J. R. Soc. Interface **6,** 377–392 (2009).

[39] A. M. Curran, S. I. Rabin, P. A. Prada, K. G. Furton, *Comparison of the Volatile Organic Compounds Present in Human Odor Using Spme-GC/MS,* J. Chem. Ecol. **31,** 1607-1619 (2005).

[40] F. Kanda, E. Yagi, M. Fukuda, K. Nakajima, T. Ohta, O. Nakata, *Elucidation of chemical compounds responsible for foot malodour*, Br. J. Dermatol. **122,** 771-776 (1990).

[41] X. Zeng, J. J. Leyden, H. J. Lawley, K. Sawano, I. Nohara, G. Preti, *Analysis of characteristic odors from human male axillae,* J. Chem. Ecol. **17,** 1469-1492 (1991).

[42] X. Zeng, J. J. Leyden, J. G. Brand, A. I. Spielman, K. J.; McGinley, G. Preti, *An investigation of human apocrine gland secretion for axillary odor precursors,* J. Chem. Ecol. **18,** 1039-55 (1992).

[43] X. Zeng, J. J. Leyden, A. I. Spielman, G. Preti, *Analysis of characteristic human female axillary odors: Qualitative comparison to males,* J. Chem. Ecol. **22,** 237-257 (1996).

[44] S. Munk, P. Munch, L. Stahnke, J. Adler-Nissen, P. Schieberle, *Primary odorants of laundry soiled with sweat/sebum: Influence of lipase on the odor profile,* J. Surfact. Deterg. **3,** 505-515 (2000).

[45] S. Haze, Y. Gozu, S. Nakamura, Y. Kohno, K. Sawano, H. Ohta, K. Yamazaki, *2-Nonenal Newly Found in Human Body Odor Tends to Increase with Aging,* J. Invest. Dermatol. **116,** 520-524 (2001).

[46] A. Ostrovskaya, P. A. Landa, M. Sokolinsky, A. D. Rosalia, D. Maes, *Study and identification of volatile compounds from human skin,* J. Cosmet. Sci. **53,** 147-148 (2002).

[47] U. R. Bemnier, D. L. Kline, D. R. Barnard, C. E. Schreck, R. A. Yost, *Analysis of Human Skin Emanations by Gas Chromatography/Mass Spectrometry. 2. Identification of Volatile Compounds That Are Candidate Attractants for the Yellow Fever Mosquito (Aedes aegypti),* Anal. Chem. **72,** 747-756 (2000).

[48] A. Amman, G. Poupart, S.; Tesler, M.; Ledochowski, A.; Schmid, S. Mechtcheriacov, *Applications of breath gas analysis in medicine,* Int. J. Mass Spectrom. **239,** 227-233 (2004).

[49] D. Smith, P. Spanel, S. Davies, *Trace gases in breath of healthy volunteers when fasting and after a protein-calorie meal: a preliminary study,* J. Appl. Physiol. **87,** 1584-1588 (1999).

[50] I. Marquez-Sillero, E. Aguilera-Herrador, S. Cardenas, M. Valcarcel, *Ion-mobility spectrometry for environmental analysis,* Trends Anal. Chem. **30,** 677-690 (2011).

[51] S. Armenta, M. Alcala, M. Blanco, *A review of recent unconventional applications of ion mobility spectrometry (IMS),* Anal. Chim. Acta **703,** 114– 123 (2011).

[52] C. D. Natale, A. Macagnano, R. Paolesse, E. Tarizzo, A. Mantini, A. D'Amico, *Human skin odor analysis by means of an electronic nose,* Sens. Act. B **65,** 216-219 (2000).

[53] C. Wang, P. Sahay, *Breath Analysis Using Laser Spectroscopic Techniques: Breath Biomarkers, Spectral Fingerprints, and Detection Limits,* Sensors **9,** 8230-8262 (2009).

[54] J. Wojtas, Z. Bielecki, T. Stacewicz, J. Micolajczyk, M. Nowakowski, *Ultrasensitive laser spectroscopy for breath analysis,* Opto-Electron. Rev. **20,** 26-39 (2012).

[55] D. J. Penn, E. Oberzaucher, K. Grammer, G. Fischer, H. A. Soini, D. Wiesler, M. V. Novotny, S. J. Dixon, Y. Xu, R. G. Brereton, *Individual and gender fingerprints in human body odour,* J. R. Soc. Interface **4,** 331-340 (2007).

[56] X. Zeng, J. J. Leyden, H. J. Lawley, K. Sawano, I. Nohara, G. Preti, *Analysis of characteristic odors from human male axillae,* J. Chem. Ecol. **17,** 1469-1492 (1991).

[57] T. Kotiaho, F. R. Lauritsen, T. K. Choudhury, R. G. Cooks, G. T. Tsao, *Membrane introduction mass spectrometry,* Anal. Chem. **63,** 875A-883A (1991).

[58] R. C. Johnson, R. G. Cooks, T. M. Allen, M. E. Cisper, P. H. Hemberger, *Membrane introduction Mass Spectrometry: Trends and applications,* Mass Spectrom. Rev. **19,** 1-37 (2000).

[59] M. A. Mendes, R. S. Pimpim, T. Kotiaho, M. N. Eberlin, *A Cryotrap Membrane Introduction Mass Spectrometry System for Analysis of Volatile Organic Compounds in Water at the Low Parts-per-Trillion Level,* Anal. Chem. **68,** 3502-3506 (1996).

[60] L. S. Riter, B. C. Laughlin, E. Nikolaev, R. G. Cooks, *Direct analysis of volatile organic compounds in human breath using a miniaturized cylindrical ion trap mass spectrometer with a membrane inlet,* Rap. Comm. Mass Spec. **16,** 2370-2373 (2002).

[61] R. A. Ketola, T. Kotiaho, M. E. Cisper, T. M. Allen. *Environmental applications of membrane introduction mass spectrometry.* J. Mass Spectrom. **2002,** *37*, 457-476.

[62] I. Cotte-Rodrıguez, E. Handberg, R. J. Noll, D. P. A. Kilgour, R. G. Cooks, *Improved detection of low vapour pressure compounds in air by serial combination of single-sided membrane introduction with fiber introduction mass spectrometry (SS-MIMS-FIMS),* Analyst **130**, 679-686 (2005).

[63] A. J. Thompson, A. S. Creba, R. M. Ferguson, E. T. Krogh, C. G. Gill, *A coaxially heated membrane introduction mass spectrometry interface for the rapid and sensitive on-line measurement of volatile and semi-volatile organic contaminants in air and water at parts-per-trillion levels,* Rap. Comm. Mass Spec. **13,** 2000-2008 (2006).

[64] E. Boscaini, M. L. Alexander, P. Prazeller, T. D. Mark, *Investigation of fundamental physical properties of a polydimethylsiloxane (PDMS) membrane using a proton transfer reaction mass spectrometer (PTRMS),* Int. J. Mass Spectrom. **239,** 179-186 (2004).

[65] F. L. Overney, C. G. Enke, *A mathematical study of sample modulation at a membrane inlet mass spectrometer-Potential application in analysis of mixtures*, J. Mass Spectrom. **7,** 93-100 (1996).

[66] M. A. LaPack, J. C. Tou, C. G. Enke, *Membrane mass spectrometry for the direct trace analysis of volatile organic compounds in air and water,* Anal. Chem. **62,** 1265-1271(1990).

[67] The International Dermal Institute, http://www.dermalinstitute.com/us/.

[68] Collin Singer, Wagtail UK Ltd, private communication.

Chapter 4

Threat compound detection using membrane inlet mass spectrometry

4.1. Introduction

In addition to human trafficking (described in the previous chapter), border control and customs services, civil defence and homeland security authorities also frequently experience problems related to illicit or hazardous materials' smuggling [1-3]. Threat compounds include: drugs, explosives, weapons, chemical warfare agents (CWAs) as well as their precursor or breakdown products. Terrorists and transnational criminal organizations use various inventive scenarios for the illegal transportation of the above substances through all type of borders [1]. These cases contain clandestine chemical threats concealed in trucks, barrels, cleverly packed boxes, shipping containers, passenger bags, ship bunkers, car seats, baggage cars, etc. Most of these situations are investigated by specialized personnel, police officers and by detection canines [4-7]. Some of the narcotics, explosives and chemical weapons even their very low vapour pressure values, release specific types of distinctive odours. These scents act as characteristic chemical ''odourprints'' or volatile chemical signatures, and act as markers of the parent compounds. They can therefore testify to the presence of illegal goods [7-9].

Border checkpoint ambient environments are mainly composed of nitrogen, oxygen, argon, trace gases, water vapours, fine ($P.M_{2.5}$) and dust particles, and volatile organic compounds (VOCs) emitted from various anthropogenic activities or other sources [10]. Due to the complex nature of the chemical environment of such border checkpoints, various analytical and sample introduction technologies have been developed for the early detection and monitoring of restricted goods. Existing mainstream technologies for threat detection in the laboratory and on-site utilize techniques based on ion

detection, vibrational spectroscopy, optical spectroscopy, nanotechnology, various types of sensors and pattern recognition based techniques. Ion detection techniques include mass spectrometry (MS) [11,12], gas chromatography combined with mass spectrometry (GC-MS) [13], liquid chromatography - mass spectrometry (LC-MS) [14, 15], low temperature plasma (LTP) ambient MS [16-17], ion mobility spectrometry (IMS) [18-25], solid phase microextraction-ion mobility spectrometry (SPME-IMS) [26] and field asymmetric ion mobility spectrometry (FAIMS) based techniques [27-29]. Atmospheric pressure chemical ionization (APCI) [30], desorption electrospray ionization (DESI) [31-37] and direct analysis in real time (DART) [38] MS present high selectivity and sensitivity with no pre-concentration of the samples required prior to analysis. Vibrational spectroscopy technologies comprise laser spectroscopy [39], light detection and ranging (LIDAR) [40, 41], X-radiation [42], terahertz spectroscopy (THz) [43-45], infra-red spectroscopy (IR) [46], Fourier-transform infra-red spectroscopy (FTIR) [47], Raman spectroscopy [48], surface enhanced Raman scattering (SERS) [49], and cavity ring down spectroscopy (CRDS) [50] based techniques. Moreover, electronic noses (EN) [51] which are intelligent chemical sensor array systems, typically consisting of two major components: (a) gas sensors and (b) a pattern recognition system have been used for explosives detection. A wide variety of sensors e.g. chemical [52] (e.g. colorimetry based devices), immunochemical [53] and electrochemical [54] (potentiometric, amperometric or conductimetric) sensors have been successfully applied in homeland security applications. Nanotechnology [55] includes molecularly imprinted polymers, nanoparticles and nanotubes and can assist other analytical techniques for improved threat detection and identification. Moore categorizes explosives detection methods according to their sampling procedure [8]. This categorization leads to contact and non contact sampling techniques. Contact sampling techniques are sorted in swipe based techniques (e.g. IMS, MS, GC-MS, FTIR, optical sensors, etc.), in place (e.g. colorimetry) and in vaporization techniques (e.g. thermal etc.). The non-contact sampling procedures are separated in standoff technologies (e.g. Raman, THz, IR, etc.) and near to the field such as IMS, MS, animals usage, electrochemical sensors, etc.

Special trained sniffer dogs can easily detect and locate illicit drugs, explosives, weapons, and tobacco in the field [4-7]. Researchers at Los Alamos National Laboratory worked closely with honey bees and trained them to detect explosives and different

types of bombs at very low concentrations (ppt levels) both in the lab and in field trials [40]. Nematodes *Caenorhabditis elegans* have a very well developed chemosensory system that allows them to provide olfactory detection of explosives or precursors from different chemical classes at various concentration levels [56]. Moreover, moths have been trained to respond to specific chemical odour signatures emitted from explosives or landmines [57]. Rats have also been used in the lab to search and alarm on vapours from explosives and drugs (e.g. cocaine) [58].

Mass spectrometry constitutes the gold standard for chemical analysis, detection and identification of illicit substances. In comparison with other instrumental analytical methods, MS is a versatile and precise technique offering unique data for both trace (crucial for explosives and CWAs early detection) and bulk analysis in threat detection operations. For instance, X-ray imaging can mainly be applied in bulk explosive detection. Recent rapid developments in miniaturization of individual MS components (pumping system, electronics unit, sampling inlet, ion source, mass analyzer, and detector) and in power consumption (low) make the whole device ideal for field applications and transfer lab to the sample. MS eliminates by far potential false alarms (usually man caused) or operational restrictions (size, weight, purchase and maintenance costs, detection times, limited or absence of portability, health risks during usage of rays releasing devices, background interferences or interactions etc.) that can be raised by alternative processes based on other technologies (e.g. X-ray, LIDAR based techniques, IMS).

To overcome limitations and portability issues of the existing analytical technology for *in situ* chemical analysis, membrane introduction mass spectrometry (MIMS) [3, 59-65] coupled to a portable mass spectrometer can be used both for gaseous and aqueous analysis and monitoring in real time with no sample preparation requirements. The operating principle of MIMS (already described in section 3.2) is based on pervaporation separation through thin polymer membranes [63]. A membrane sampling inlet is connected with a MS system allowing selective permeability of organic compounds in gas or liquid phase while blocking water or air molecules [64]. In this way the instrument is protected from high humidity and high concentrations of inorganic gases. At the same time organic compounds may pass through the membrane to the ion source for ionization and then to the mass analyzer for spectral analysis. The rate of transfer of targeted compounds in the MS and thus sensitivity enhancement

depends on the solubility and diffusivity properties of these compounds in the membrane material [60]. Porosity and thickness of the membrane material have also shown to play an important role in sensitivity maximization and detection of a wider range of VOCs and SVOCs in complex matrices [61, 64]. The mass spectra produced can be subsequently processed for both qualitative and quantitative analysis.

Compared to other large size and weight laboratory or even integrated on a vehicle MS based systems (e.g. PTR-MS, LC-MS [14, 15], GC-MS [13, 66], etc.) for threat detection, fully man portable MIMS offers very good sensitivity (low detection limits – ppt / ppb levels), rapid (in some seconds) and reliable analysis, accuracy, robustness, user friendliness (small size and weight) with low maintenance costs. The utility of an entirely portable device with the above characteristics addressing all the requirements of harsh environment operations for threat substance detection (e.g. CWAs) is currently of great interest and necessity to homeland security and transport security authorities.

This chapter reports the use of a man portable MIMS system with total weight less than 18 kg for monitoring characteristic odour chemical signatures emitted from narcotics, explosives, chemical weapons and their precursor or breakdown products from low ppb to low ppm concentration levels.

4.2. Experimental section

4.2.1. Concept

The main concept of this work was the mass spectrometric detection of characteristic odour signatures emitted from illegal drugs, explosives and CWAs and thus the further detection of the parent substances in real situations (e.g. border checkpoints, cargo services). Simulant compounds that were examined are presented in Table 4.1 and are closely related to the parent compounds. A sampling probe was connected to a portable membrane inlet quadrupole mass spectrometer (MIMS) to perform the detection of the described compounds.

Field tests followed the laboratory experiments to examine and demonstrate the usage of MIMS to detect scents from real illegal substances. Drug simulant compounds that were selected to be tested and simulate the real illicit substances include: methyl benzoate as a volatile signature for cocaine (dominant volatile chemical that was

identified in cocaine scent and also widely used in detection dog training), terpenes such as limonene, α-pinene, β-myrcene as volatile chemical signatures of tetrahydrocannabinol (THC) in marijuana, piperidine that is a precursor in the clandestine manufacture of phencyclidine (PCP) as well as a breakdown product when PCP is smoked, and acetic acid as odour signature for heroin [67-69].

Table 4.1: Summary of the simulant compounds used in the MIMS experiments and classification according to the threat family that they belong to.

substance	**parent compound**	**molecular weight**	**vapour pressure (Torr) at 20ºC**	**simulant compound**	**molecular weight**	**vapour pressure (Torr) at 20ºC**
drugs	Cocaine	303	~10^{-8}	Methyl benzoate	136	0.28
	THC in marijuana	314	4.6×10^{-8}	Limonene	136	3
				α-pinene	136	2
				β-myrcene	136	7
	Phencyclidine	243	2.5×10^{-2}	Piperidine	85	23
	Heroin	369	0	Acetic acid	60	11
explosives	TNT	227	6.7×10^{-6}	2-nitrotoluene	137	0.1
	Naphthalene	128	0.08	Naphthalene	128	0.08
	C4	N.A.	N.A.	Cyclohexanone	94	3.4
CWAs	Nerve agents (e.g. Sarin, Soman)	140, 182 respectively	2.10, 0.40	Dimethyl methylphosphonate (DMMP)	124	<0.6
	Mustard gas	159	0.069	2-chloroethyl ethyl sulfide (CES)	124	3.4
				Methyl salicylate	152	0.1

Explosive simulants that were examined include: 2-nitrotoluene (an intermediate component in the synthesis of explosives as well as a breakdown product of TNT), naphthalene (used in the production of black smoke and explosives) and finally cyclohexanone (the most abundant compound found in the headspace area of C4 and other plastic explosives) [68, 70]. To mimic chemical weapons, the following simulant compounds were chosen: dimethyl methylphosphonate (DMMP) that is used in the

production of nerve agents such as sarin and soman, and the methyl salicylate and 2-chloroethyl ethyl sulphide (CES) as simulant compounds for mustard gas [71]. All the experiments were replicated three times to ensure reproducibility and consistency of the results. Trials led to a repeatable degree of agreement and precision between the three experimental series. Natural and commercial products of daily life that may contain the selected analytes and can interfere with volatile emissions from restricted goods were also investigated and are presented in Table 4.2.

Table 4.2: List of well-known compounds that can interfere with volatile emissions from drugs, explosives and CWAs [72, 73].

compound	**natural and commercial products which may contain the targeted examined compounds**
Methyl benzoate	Perfumes, flavourings, solvents, pesticides
Limonene	Foods (e.g. lemons, citrus fruits, soft drinks), household products, fragrances, shampoos (as active ingredient), in spray products applied to domestic animals for fleas and ticks control
α-pinene	Foods (e.g. grapefruit juice, carrots, tomato, walnut, ginger, celery), potpourri, parquets floor coverings, wood-based furniture
β-myrcene	Foods, flavourings, aromas, medicine
Piperidine	Building block & chemical reagent in pharmaceutical compounds synthesis
Acetic acid	Foods (e.g. chips), photographic film, cleaning products
2-nitrotoluene	Agricultural chemical products, photographic chemical products, pigments
Naphthalene	Cigarette smoke, car exhaust, pest repellent
Cyclohexanone	Solvent in oil extract, dry cleaning, lacquers, resins, paints, varnish removers, fuel for camp stoves
DMMP	Flame retardant, additive to solvents and hydraulic fluids
CES	N.A.
Methyl salicylate	Foods (e.g. gums, mints), fragrances, beverages, antiseptic in mouthwash products, pesticides

4.2.2. Chemicals

Methyl benzoate (99%) was obtained from Fisher Scientific Ltd., U.K. All the other chemicals were bought from Sigma Aldrich Co. LLC., U.K. at the following purities: limonene (97%), α-pinene (98%), β-myrcene (analytical standard), piperidine (99%), acetic acid (99.7%), 2-nitrotoluene (≥ 99%), naphthalene (5000μg/mL in methanol), cyclohexanone (≥ 99%), dimethyl methylphosphonate (97%), 2-chloroethyl ethyl sulfide (98%) and methyl salicylate (≥ 99%), methanol (99.93%). All purchased chemicals were provided in liquid phase.

Real substances that were tested in the field were provided by Wagtail UK Ltd, a specialist dog handling company based in North Wales, UK [74]. Both explosives and drugs were supplied in solid form (as flakes, powder, cord, or resin). Supplied explosives were the following: TNT (UN number 0209) and Eurodyn^{TM} 2000 (UN number 0081). The drug provided for test was ecstasy (MDMA). Drug standard phencyclidine (1mg/ml in methanol) that was bought from Sigma-Aldrich by the University of Liverpool was also tested on-site.

4.2.3. Experimental setup

The experimental system used for the tests of threat compounds was essentially the same membrane inlet QMS as described in chapter 3. The main difference is that the vacuum system was replaced by a TURBOVAC SL80 turbomolecular pump bought from Oerlikon Leybold Vacuum (Chessington, UK). This was done for weight reduction purposes (from 23 kg down to 18 kg) and for achieving robustness and portability of the device. The main parts of Liverpool portable MIMS are a) the membrane sampling probe that allows to the gas samples to pass through the membrane and enter into the MS for analysis, b) the QMS (see section 3.3.5), c) the vacuum system and d) a computer for data acquisition. Figure 4.1 (adapted from Figure 3.2 in chapter 3) shows a schematic diagram for the Liverpool MIMS experimental setup that was applied for illegal and/or hazardous substances detection and monitoring.

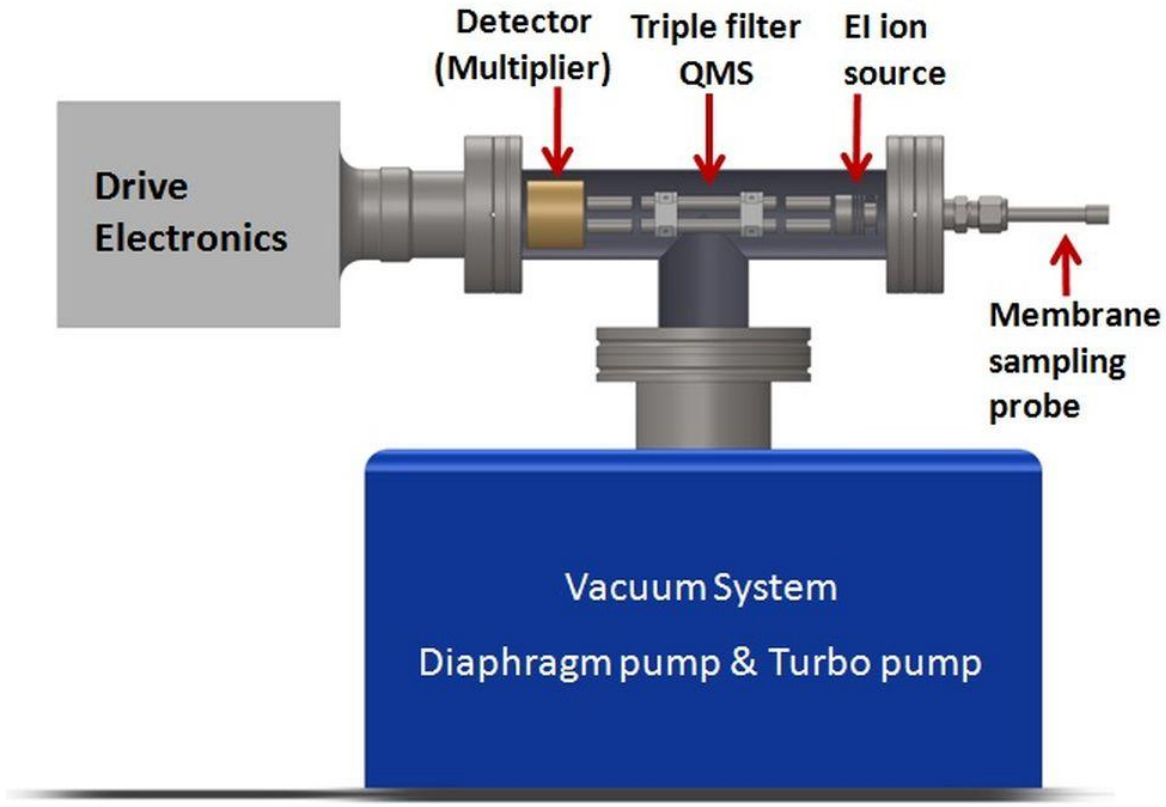

Figure 4.1: Schematic diagram for the MIMS system used for monitoring characteristic chemical odour signatures emitted from drugs, explosives and CWAs.

4.2.4. Test environments

The experiments for monitoring odour markers emitted from threat substances using a MIMS system were performed in the facilities of the University of Liverpool, UK. Field experiments took place and completed in Wagtail UK Ltd, which holds a UK Home Office License to store and keep explosives and drugs for sniffer dog training. The MIMS system was transported and set up in the Wagtail training terrain in order to evaluate its performance with real illegal compounds on-site (simulated environment similar to security checkpoints).

4.2.5. Sample preparation

MIMS linearity during online monitoring of the targeted VOCs was determined using gas standards. The procedure that was followed for gas standard production was based

on McClennen et al. [75] and on Naganowska-Nowak et al [76]. Stock standard solutions of the simulant compounds were prepared by volumetric serial dilution in methanol at concentrations of 1000 ppm and 100 ppm. Appropriate quantities of the stock solutions were injected with a high precision micropipetter (Brand GmbH, Germany) in 1.1 L and 2.8 L narrow-neck glass flasks (Sigma Aldrich Co. LLC., U.K.) filled with atmospheric air, carefully covered and left for 3 hours at room temperature (25 ºC) to evaporate and reach equilibrium. The flask tops were covered with several layers of parafilm M wrapping film. Gas standards of methyl benzoate, limonene, α-pinene, β-myrcene, piperidine, acetic acid, 2-nitrotoluene, naphthalene, cyclohexanone, DMMP, CES and methyl salicylate were prepared at the following concentrations: 50ppb, 100 ppb, 200 ppb, 400 ppb, 900 ppb, 4 ppm, 9 ppm and 18 ppm.

Before and among individual testing series, the glass flasks were carefully purged with odour-free soap and water and rinsed with deionised water (ReAgent Chemical Services Ltd, Cheshire, UK) in order to remove and eliminate interferences with other volatile compounds. They were left overnight uncovered at 50^{o}C, so that the remaining water drops would evaporate. The standard gases were tested with the following sequence: from the lowest concentration level to the highest. This was done to reduce potential memory effects between distinctive measurements and sample to sample carryover errors. Blank flasks containing only atmospheric air were also prepared following the above described process for examination of potential exogenous VOC contaminations prior to the start of the experimental series. Moreover, the covered with parafilm flasks containing the prepared gas standards were peripherally (outer surrounding area) tested with the MIMS system before experiments to examine any volatile leakage through the wrapping film.

During the field tests, a simple sample preparation procedure was followed to simulate real transportation conditions of threat substances. Field tests were done in order to confirm MIMS ability to detect selected threat analytes out of the lab and not to produce calibration curves or to determine detection limits. A small quantity sample ($\leq$ 0.5 g) from each individual solid substance was used for the tests. The solid drugs and explosives that were examined were placed in 1.1 L glass flasks, covered with parafilm and after 3 hours of enclosure and quiescence at room temperature (25^{o}C), measurements were taken by inserting the membrane inlet sampling probe directly inside into the flask through a small hole made on the parafilm surface. In this way, gas traces inside the flasks were continuously being monitored and recorded.

4.2.6. Sample introduction

During tests, a sheet polydimethylsiloxane (PDMS) membrane probe connected to the vacuum valve was directly inserted into the dilution bottles and was sampling the prepared standard gases. The same procedure was followed during the real substances detection tests in Wagtail's facilities. The membrane probe assembly consists of 100 mm stainless steel tubing coupled with a membrane sheet supported in the one end side with a 6.35 mm Swagelok stainless steel vacuum fitting union. The non sterile PDMS membrane sheeting was provided by Technical Products, Inc. of Georgia, USA. The membrane probe and subsequently the membrane were not heated. Moreover, none analyte enrichment procedures (e.g. usage of carrier gas) were used. Although PDMS membrane was the leading membrane used for the measurements, other membrane materials [polypropylene (PP), polyethersulfone (PES), polytetrafluoroethylene (PTFE), nylon] were also tested to examine their ability to detect the targeted compounds and to optimize detection and monitoring methodology. Table 4.3 shows all the membranes that were tested with different materials, porosities and wall thicknesses.

Table 4.3: Membranes tested with MIMS system to evaluate their ability to detect selected volatile compounds emitted from illegal drugs, explosives and chemical weapons.

no	membrane name	material	form	hydrophobicity/ hydrophilicity	pore size (μm)	thickness (mm)
1	GH Polypro	PP	sheet	hydrophilic	0.2	0.101
2	Supor®-100	PES	sheet	hydrophilic	0.1	0.1016
3	Mitex	PTFE	sheet	hydrophobic	10	0.13
4	Nylon	nylon	sheet	hydrophilic	0.45	NA
5	SIL-TEC	PDMS	sheet	hydrophobic	NA	0.12

4.2.7. Mass spectral analysis

Mass spectral analysis of the ionized gas sample was done using a triple filter QMS system provided by Q-Technologies Ltd, UK as described in the section 3.3.5. During data acquisition, 10 acquisition points were recorded per unit mass with average number of 10 scans per measurement throughout the whole mass range. Data were recorded on a laptop computer, plotted, and compared with reference mass spectra, using the NIST Chemistry WebBook as reference database for spectral peaks of each compound.

4.2.8. Vacuum system

The QMS was housed in a stainless steel chamber pumped by a vacuum system consisting of an Oerlikon oil-free DIVAC 0.8 T diaphragm pump and a TURBOVAC SL 80 turbomolecular pump. The diaphragm pump provides pressure down to 1×10^{-2} Torr, while the turbomolecular pump gives base pressure of 7.5×10^{-8} Torr. The system pressure was continuously being monitored by a highly accurate digital pressure gauge supplied by Pfeiffer (MRT 100, DN 25 ISO-KF) that uses a Pirani/Cold cathode method of measurement. The TURBOVAC SL 80 turbomolecular pump offered a lower ultimate pressure value for the same chamber volume compared to the Pfeiffer Balzers turbomolecular pump that was used in chapter 3. This turbomolecular pump replacement affected the overall system operation and membrane's performance as the new suction flow rate applied on the membrane material was higher. Thus the diffusion of the selected analytes across the membrane was positively affected, allowing a larger number of molecules to enter into the MS system. Operating pressure for mass analysis with the PDMS sheet membrane sampling probe attached and sample inlet valve fully open was varying between 3.5×10^{-6} Torr and 1.0×10^{-5} Torr depending on the concentration of the under analysis standard gas sample and on the nature (chemical structure, vapour pressure, etc.) of the under examination component that affect permeability through the PDMS membrane.

4.3. Results and discussion

4.3.1. Drug simulant experiments

This experimental series was done to investigate the chemical detection and monitoring of characteristic odour signatures emitted from narcotics, which can be found in their headspace gases. A PDMS MIMS was initially used to examine if the selected simulant compounds, corresponding to our specific application, could be detected with a membrane inlet sampling probe. Representative mass spectra for methyl benzoate, limonene, α-pinene, β-myrcene, piperidine and acetic acid corresponding to 900 ppb distinct gas standards are presented in Figure 4.2. After confirmation that detection with MIMS was achievable, gas standards of the selected volatile components were prepared for on-line monitoring at the following concentration levels: blank, 50 ppb, 100 ppb. 200 ppb, 400 ppb, 900 ppb, 4 ppm, 9 ppm and 18 ppm. Calibration curves of our MIMS instrument for drug simulant gas standards at concentrations from 50 ppb to 18 ppm exhibited good linearity with R^2 values in the range from 0.9598 to 0.9988 as shown in Table 4.4. Weak molecular weight fragments apparent in Figure 4.2 compared to NIST Chemistry WebBook can be explained by the fact that the membrane inlet used in the experiments allows selective permeation of molecules which depends upon the molecules' chemical structures, polarity, solubility and vapour pressure values. Membrane and membrane probe temperature may have affected the obtained spectra. As explained in the sample introduction section for the experiments, a non heated sampling probe was used. Higher membrane temperatures (e.g. > 70ºC) may lead to increased permeation rates and higher mass peaks in the mass spectra.

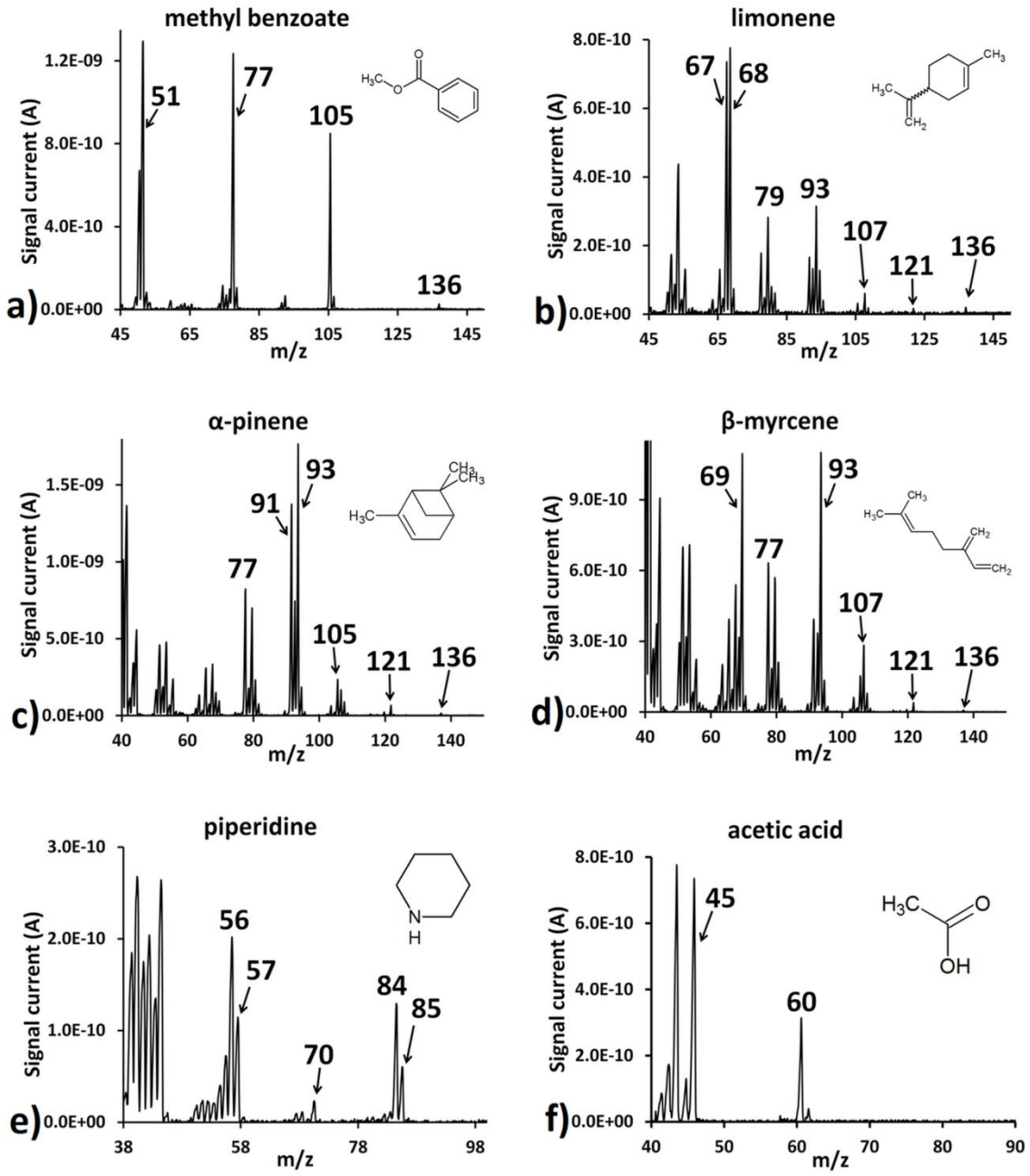

Figure 4.2: Representative experimental drug simulant mass spectra at 900 ppb obtained with MIMS for a) methyl benzoate, b) limonene, c) α-pinene, d) β-myrcene, e) piperidine and f) acetic acid.

4.3.2. Explosive simulant experiments

This subsection describes the mass spectrometric detection of distinctive volatile emissions from explosive materials. Representative mass spectra for 2-nitrotoluene, naphthalene and cyclohexanone corresponding to 900 ppb separate gas standards are

shown in Figure 4.3. As mentioned previously, gas standards of selected volatile compounds which emulate explosive odours were prepared for on-line monitoring at the following concentration levels: blank, 50 ppb, 100 ppb. 200 ppb, 400 ppb, 900 ppb, 4 ppm, 9 ppm and 18 ppm. Calibration curves of the MIMS instrument for explosive simulant analytes at concentrations from 50 ppb to 18 ppm also exhibited good linearity with R^2 values in the range from 0.9848 to 0.9987 as shown in Table 4.4.

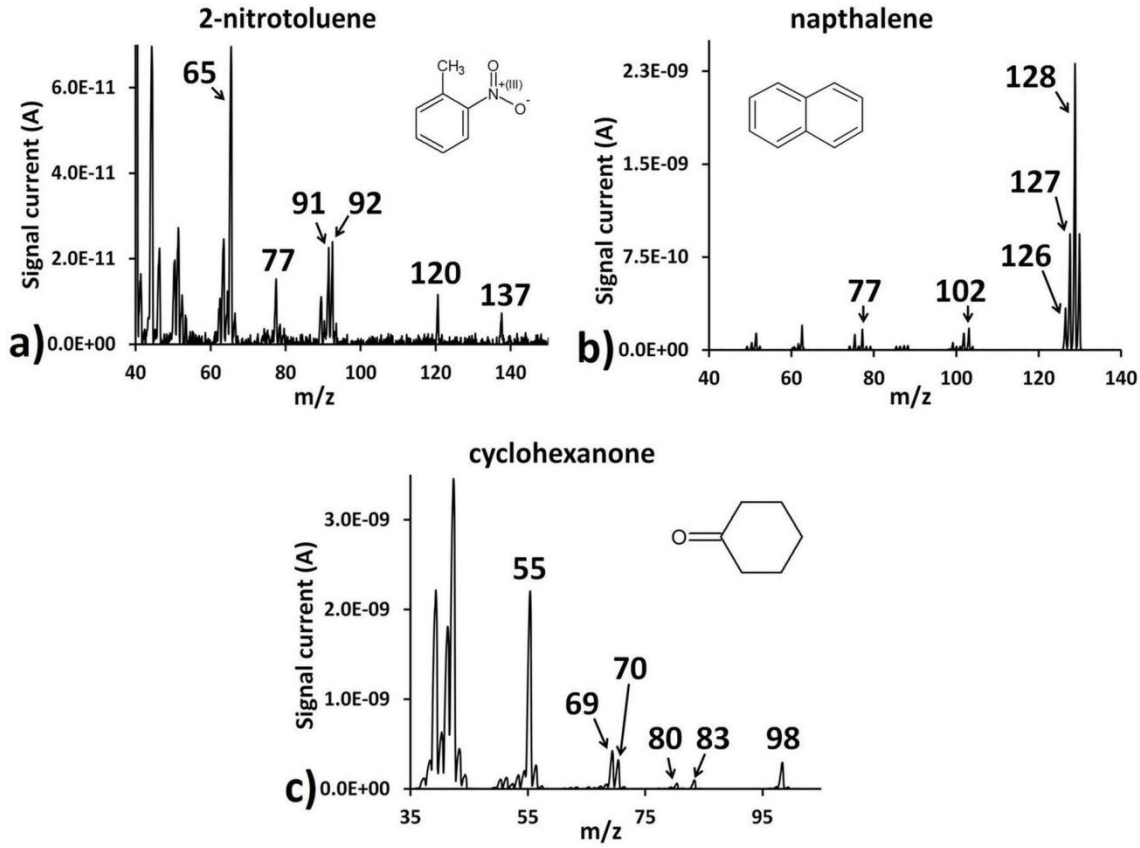

Figure 4.3: Representative experimental explosive simulant mass spectra at 900 ppb obtained with our MIMS for a) 2-nitrotoluene, b) naphthalene and c) cyclohexanone.

4.3.3. Chemical weapon simulant experiments

The experiments done in this section illustrate the mass spectrometric monitoring of distinctive odour emissions from CWAs. As for drug and explosive simulants, gas standards of characteristic odours which mimic CWAs were prepared for analysis at the following concentrations: blank, 50 ppb, 100 ppb, 200 ppb, 400 ppb, 900 ppb, 4 ppm, 9 ppm and 18 ppm. Representative mass spectra for DMMP, CES and methyl salicylate

corresponding to 900 ppb gas standards are shown in Figure 4.4. Calibration curves of our MIMS instrument for the CWA simulant compounds tested at concentrations from 50 ppb to 18 ppm exhibited linearity with R^2 values in the range from 0.9817 to 0.9982. During tests, methyl salicylate showed very slow response rise times.

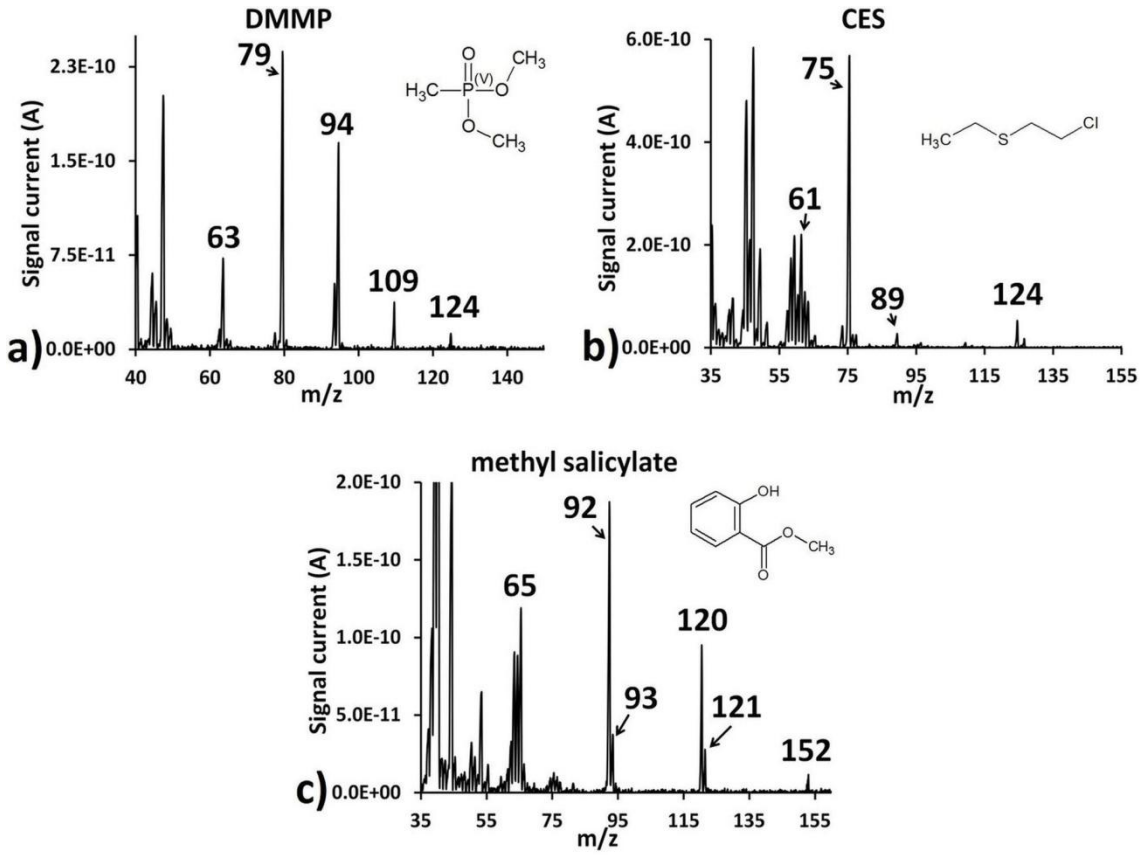

Figure 4.4: Representative experimental CWAs simulant mass spectra at 900 ppb obtained with our MIMS for a) DMMP, b) CES and c) methyl salicylate.

4.3.4. Membrane experiments and evaluation of the method

Five membranes made from different materials and with various properties (porosity, hydrophilicity, and thickness) were tested. However, membranes no. 1 – 4 (Table 4.3) were unsuitable for our application as detection of the targeted threat simulant compounds was not achieved. The SIL-TEC membrane gave the best performance, optimum selectivity, low detection limits and fast response times. Rise and fall response times are presented in Table 4.4. For the volatile compounds tested, the average rise time was 22 sec, while the average fall time was 55 sec. The 90% rise response time was the time required for the signal intensity to reach the 90% of its maximum value

(optimum sensitivity) after membrane sampling probe was inserted into the flasks containing the gas standards [3, 60]. The fall response time represents the time required for the PDMS membrane to purge and peaks signals return to base level. Rise and fall response times can be significantly improved by heating the membrane sampling probe, as heating affects diffusion of molecules through the membrane material. Linear regression coefficient R^2 and limits of detection obtained from the calibration curves produced from the experiments for each individual component are also shown in Table 4.4.

Table 4.4: Summary of the PDMS membrane rise and fall times, R^2 values and limits of detection for the simulant compounds that were examined using the MIMS system.

compound name	**characteristic mass fragments (*m/z*)**	**rise time (sec)**	**fall time (sec)**	**R^2**	**LOD (ppb)**
Methyl benzoate **(*m/z* 136)**	50, 51, 77, 105, 136	17	34	0.9810	0.98
Limonene **(*m/z* 136)**	53, 67, 68, 79, 93, 107, 121, 136	18	36	0.9875	9.3
α-pinene **(*m/z* 136)**	77, 79, 91, 93, 105, 121, 136	18	50	0.9931	1
β-myrcene **(*m/z* 136)**	51, 53, 69, 77, 79, 93, 107, 121, 136	18	54	0.9598	3
Piperidine **(*m/z* 85)**	56, 57, 70, 84, 85	29	88	0.9868	8.15
Acetic acid **(*m/z* 60)**	43, 45, 60	12	16	0.9988	5
2-nitrotoluene **(*m/z* 137)**	63, 65, 77, 89, 91, 92, 120, 137	23	36	0.9987	16
Naphthalene **(*m/z* 128)**	62, 75, 77, 101, 102, 126, 127, 128	19	43	0.9848	3.4
Cyclohexanone **(*m/z* 98)**	42, 55, 69, 70, 80, 83, 98	12	32	0.9886	0.86
DMMP **(*m/z* 124)**	63, 79, 93, 94, 109, 124	16	44	0.9982	4
CES **(*m/z* 124)**	47, 59, 61, 75, 89, 124	17	57	0.9817	2.7
Methyl salicylate **(*m/z* 152)**	63, 64, 65, 92, 93, 120, 121, 152	67	168	0.9927	6.5

Calculated R^2 values correspond to the molecular weight peak (characteristic mass fragment) for each simulant compound for the following concentration range: 50 ppb to

18 ppm. Limit of detections (LOD) were calculated from the calibration plots and are estimated in the range from 860 ppt for cyclohexanone to 16 ppb for 2-nitrotoluene. LOD estimates were based on signal current values obtained from experimentally tested in our lab 50 ppb simulant gas standards. In each case, LOD values were determined at least three times above the noise level. Analytical instruments of large size and weight (e.g. PTR-MS devices) have detection limits for threat compound analysis and monitoring in the sub-ppt levels. However, the existing MIMS system offers a good sensitivity (high ppt levels) for a portable instrument that can be further improved e.g. by the use of advanced signal processing algorithms.

4.3.5. Field experiments

Field tests took place in Wagtail UK Ltd. facilities to examine MIMS performance with real threat substances. Two drugs (MDMA and phencyclidine) and two explosives (Eurodyn^{TM}2000 and TNT) were tested with our MIMS attached to a PDMS sampling probe. Eurodyn^{TM}2000 (with vapour pressure equal to 0.05 Torr at 20^{o}C) is a nitroglycol based explosive with a molecular weight (M.W.) of 152 g/mol. Its mass spectrum (EI) has mainly 2 characteristic mass fragments: *m/z* 46 and *m/z* 76. Even though detection of the Eurodyn^{TM}2000 explosive was successful and rapid, only some low mass fragments of TNT (M.W.: 227 g/mol), MDMA (M.W.: 193 g/mol) and phencyclidine (M.W.: 243 g/mol and vapour pressure equal to 2.5×10^{-2} Torr at 25^{o}C) were observed. The obtained mass spectra corresponded partially with the reference electron ionization mass spectra supplied by the NIST Chemistry WebBook. This can be explained by the fact that parent compounds more readily pass through the membrane material and also because of the limited mass to charge range (*m/z* 1-200) of the existing QMS instrument used. Membrane response rise time for Eurodyn^{TM}2000 was 24 sec and for phencyclidine was 48 sec. Figure 4.5 shows the Liverpool portable MIMS system in operation during field trials. Figure 4.6 shows representative experimental mass spectra for one explosive (Eurodyn^{TM}2000) and one drug (phencyclidine).

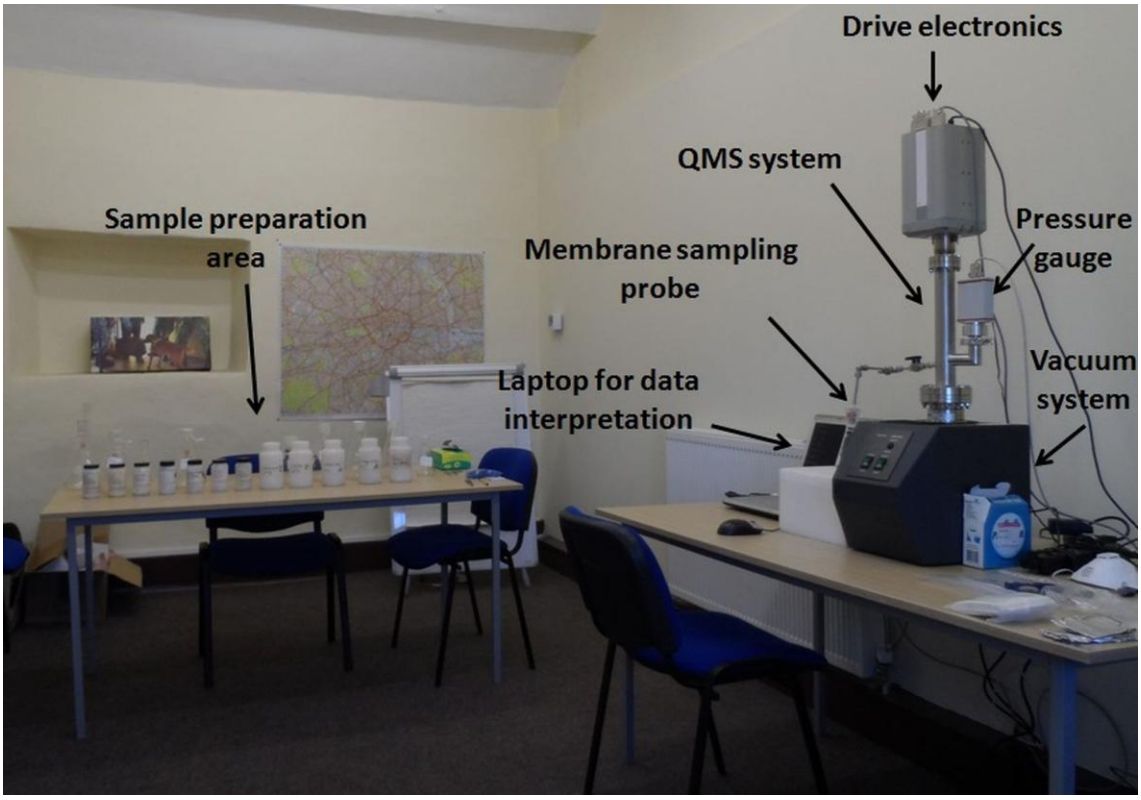

Figure 4.5: Liverpool portable MIMS system in Wagtail facilities during field experiments.

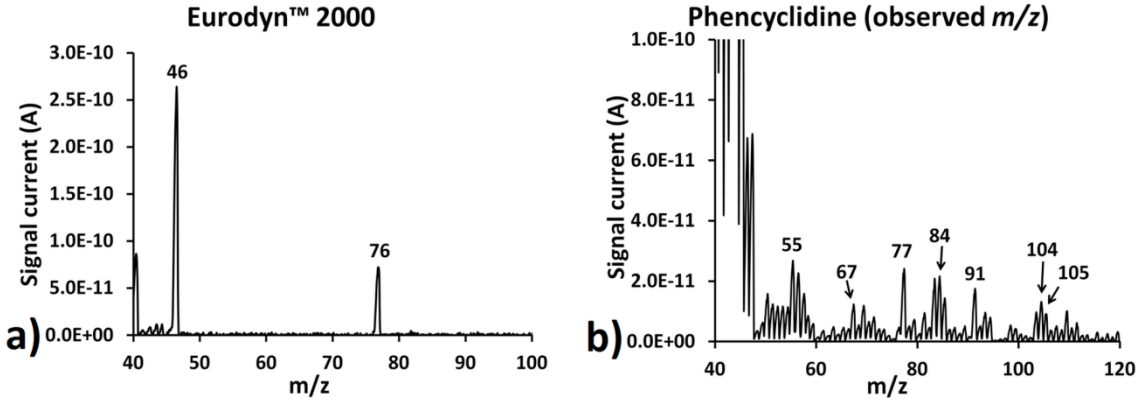

Figure 4.6: Mass spectra of a) Eurodyn^{TM}2000 (ethylene glycol dinitrate based explosive) and b) 5 ppm phencyclidine (recreational drug) acquired by the MIMS system during field tests.

4.3.6. Optimization experiments

4.3.6.1. Methodology description

In order to achieve sensitivity enhancement (lowest LOD values) and fastest response times for our technique a series of experiments including use of a heated flat PDMS membrane sampling probe coupled to the Liverpool portable MIMS system was performed. Drug simulant compounds examined to simulate the real illicit compounds included methyl benzoate and piperidine. Explosive simulants that were tested include: 2-nitrotoluene and cyclohexanone. In order to emulate chemical weapon threats, the following two simulant compounds were chosen: dimethyl methylphosphonate (DMMP) and 2-chloroethyl ethyl sulfide (CES). Table 4.1 gives further detail on the examined substances. Gaseous standards of the selected analytes were prepared (as described above in the sample preparation subsection) at the following concentrations: blank, 1 ppb, 5 ppb, 10 ppb, 25 ppb, 50 ppb, and 100 ppb. The standard gases were tested from the lowest concentration level to the highest. The membrane probe assembly was externally heated at 70°C using an electrical heating wire controlled by a dual digital PID temperature controller (model: TA4-SNR+K). The temperature of the membrane material was additionally monitored using a digital ATC-800 temperature control unit with temperature measuring range from -20°C to 99°C to ensure operational temperature stability. Once again, experimental trials were replicated three times to ensure repeatability and consistency of the results. Mass spectral analysis was done as described previously in the sections 3.3.5 and 4.2.7.

4.3.6.2. Drug simulant experiments

This subsection investigates the mass spectrometric monitoring of methyl benzoate and of piperidine using Liverpool portable MIMS system coupled to a heated at 70 ºC PDMS membrane inlet sampling probe. Gas standards of the selected volatile compounds were prepared for on-line monitoring at the following concentration levels: blank, 1 ppb, 5 ppb, 10 ppb, 25 ppb, 50 ppb, and 100 ppb. Representative mass spectra for methyl benzoate and for piperidine corresponding to 50 ppb gas standards are presented in Figure 4.7.

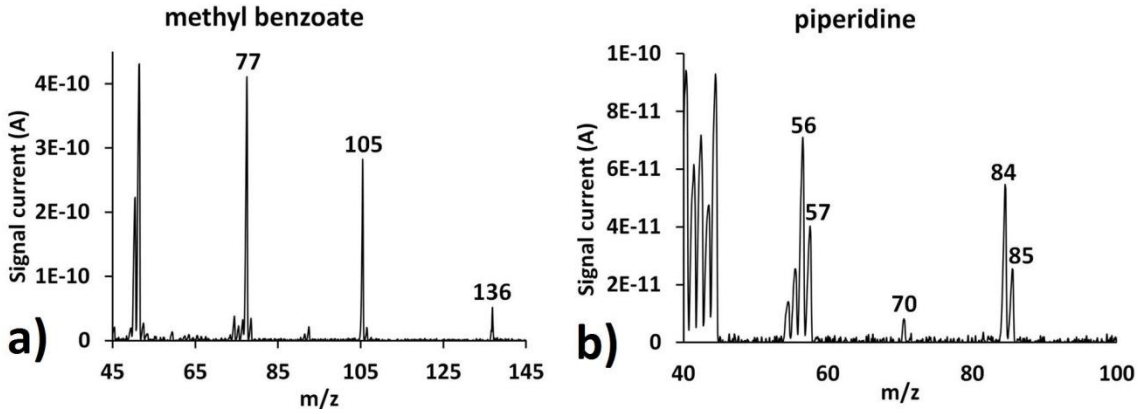

Figure 4.7: Representative experimental drug simulant mass spectra at 50 ppb for a) methyl benzoate and b) piperidine using the Liverpool portable MIMS system.

Calibration plots were generated to evaluate the performance of the method. As shown in Figure 4.8, in order to produce calibration curves, two characteristic mass fragments for each targeted compound were chosen. This was done to confirm that their signal intensities were closely dependent on the gas samples concentrations. Calibration curves of our MIMS instrument for the two drug associated gas standard compounds at the concentration area from 1 ppb to 100 ppb exhibited excellent linearity with the following R^2 values: 0.9975 for mass 136 and 0.9972 for mass 105 of methyl benzoate and 0.9994 for mass 85 and 0.9991 for mass 84 of piperidine. The system response times were in the level of few seconds (Table 4.5).

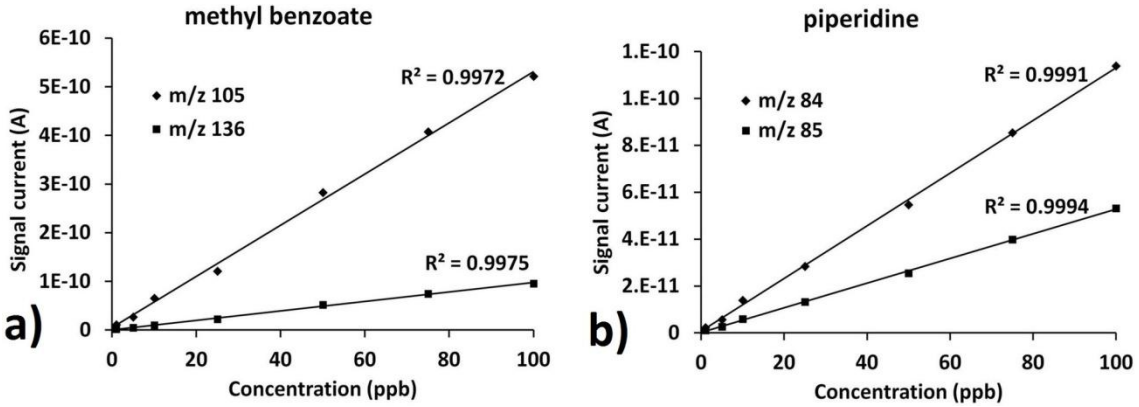

Figure 4.8: Calibration curves for a) methyl benzoate and b) piperidine using the Liverpool portable MIMS system.

Figure 4.9 presents typical membrane rise and fall response times for mass 136 of methyl benzoate at 50 ppb. A stable sampling period with duration 30 sec is also shown.

Rise response time represents the time required for the signal intensity to reach its maximum value, whereas fall time shows the time needed for the membrane material to purify and peaks signals return to baseline level. Limits of detection (LOD) were calculated (based on signal current comparisons with the 1 ppb mass spectrum) and are shown in Table 4.5. As previously described, detection limits were based on the signal to noise ratio (S/N=3). LOD estimates were calculated, so that they will have three times greater signal intensities compared to the baseline (blank/noise) signal levels. Slight differences in mass fragments' relative abundances between reference (NIST Chemistry WebBook) and experimental mass spectra can be explained by the fact that the membrane inlet used in the experiments allows selective permeation of molecules according to their molecular structure and on their physical and chemical properties such as polarity, solubility and vapour pressure.

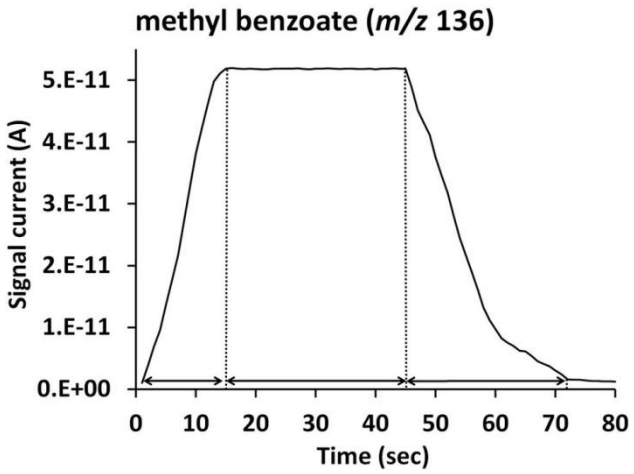

Figure 4.9: Typical rise and fall response profile for mass 136 of methyl benzoate at 50 ppb as a function of time.

4.3.6.3. Explosive simulant experiments

The mass spectral investigation and on-line monitoring of volatile compounds associated with explosive materials is presented in this subsection. Representative mass spectra (obtained with a heated membrane sampling probe coupled to Liverpool MIMS system) for 2-nitrotoluene and cyclohexanone corresponding to 50 ppb gas standards are shown in Figure 4.10. Calibration curves (Figure 4.11) of our MIMS instrument for explosive simulant analytes at concentrations from 1 ppb to 100 ppb exhibited excellent

linear performance with R^2 values of 0.9977 for mass 137 and 0.9972 for mass 120 of 2-nitrotoluene and 0.9993 for mass 98 and 0.9991 for mass 55 of cyclohexanone as presented in Table 4.5. Limits of detection of our technique for the targeted explosive stimulant compounds were calculated (as described above) at high ppt concentration levels.

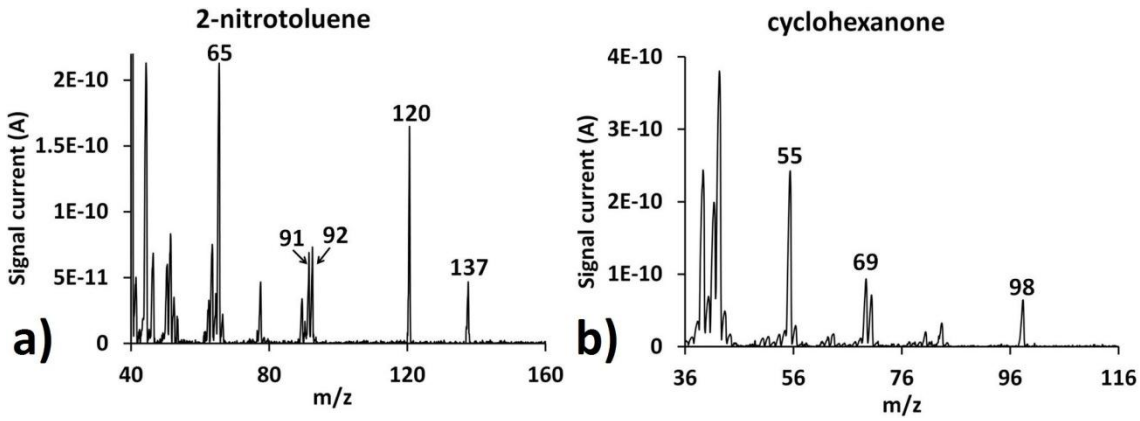

Figure 4.10: Representative experimental explosive simulant mass spectra at 50 ppb for a) 2-nitrotoluene and b) cyclohexanone using the Liverpool portable MIMS system.

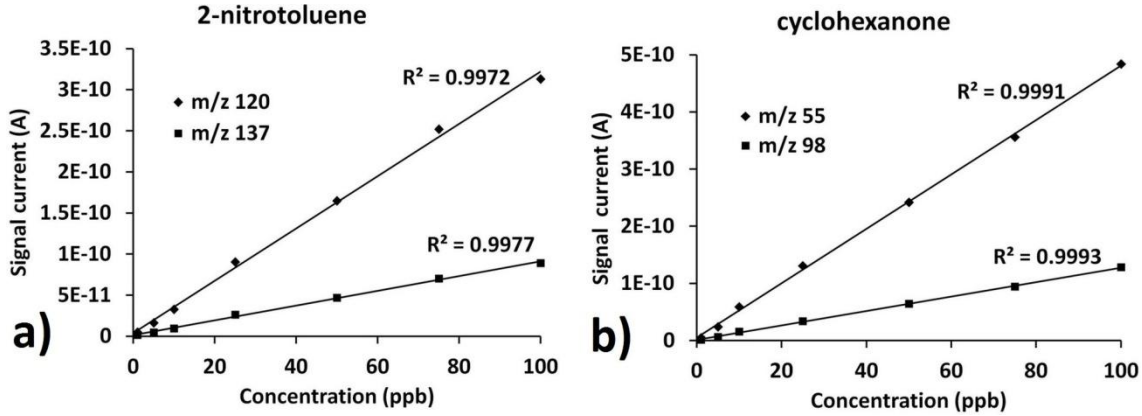

Figure 4.11: Calibration curves for a) 2-nitrotoluene and b) cyclohexanone using the Liverpool portable MIMS system.

4.3.6.4. CWAs simulant experiments

The mass spectrometric monitoring of distinctive odours emitted from CWAs is examined in this section. Gas standards of characteristic odorous compounds (DMMP and CES) which simulate chemical weapons were prepared for on line monitoring at the following concentration levels: blank, 1 ppb, 5 ppb, 10 ppb, 25 ppb, 50 ppb, and 100

ppb. Representative mass spectra for DMMP and CES corresponding to 50 ppb gas standards are presented in Figure 4.12. Once again our MIMS instrument exhibited fast response times and very good linearity for the targeted substances with the following R^2 values: 0.9987 for mass 124 and 0.9986 for mass 109 of DMMP and 0.9984 for mass 124 and 0.9984 for mass 75 of CES as shown in Figure 4.13 and Table 4.5.

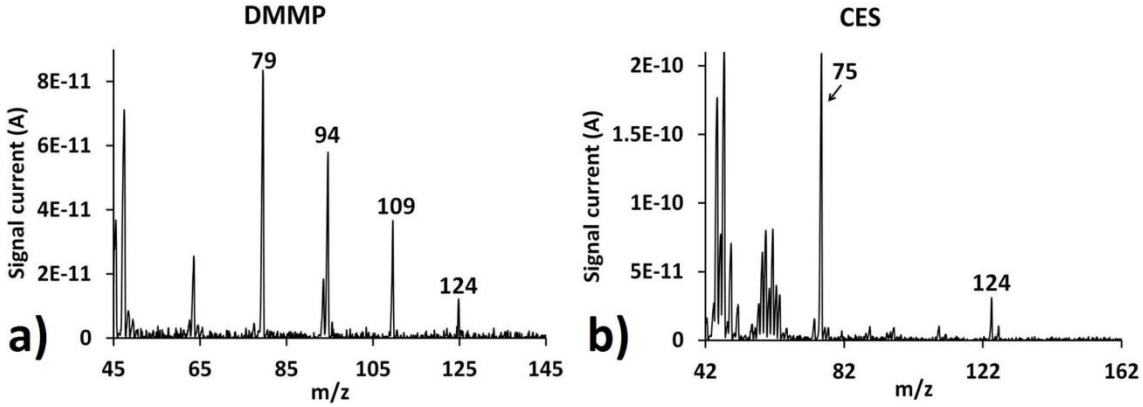

Figure 4.12: Representative experimental chemical weapon simulant mass spectra at 50 ppb for a) DMMP and b) CES using the Liverpool portable MIMS system.

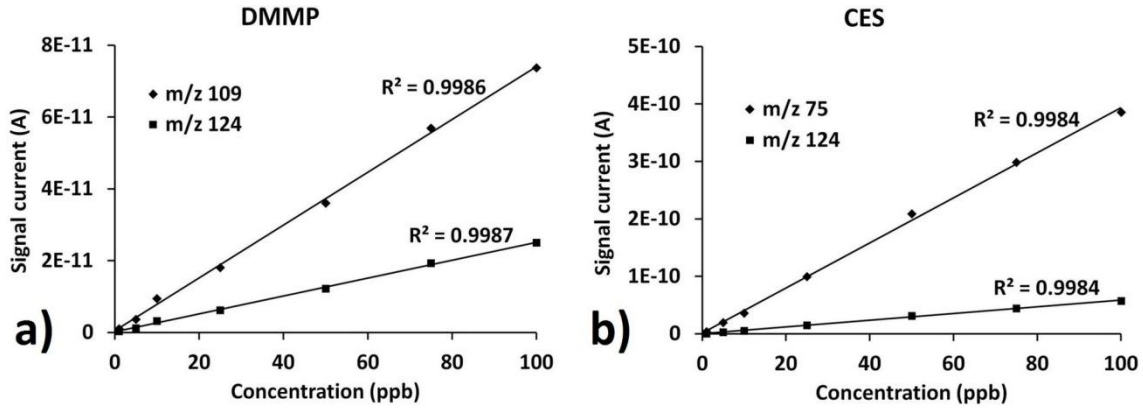

Figure 4.13: Calibration curves for a) DMMP and b) CES using the Liverpool portable MIMS system.

4.3.6.5. Evaluation of the method

In order to further improve sensitivity (achievement of even lower concentration analyzed) and gain fastest response times (both rise and fall times) a thin sheet PDMS membrane sampling probe heated at 70°C was used during experiments to monitor selected threat simulant compounds. For the volatile compounds tested, the average rise

time was 15.1 sec, while the average fall time was 34.8 sec. Rise and fall response times were significantly improved by heating the membrane sampling probe. This was done because heating affects diffusion of molecules through the membrane material. Heating of the sampling probe has also significant suction effects (quantitative and qualitative) of the molecules from the membrane material to the vacuum system. Moreover, linear regression coefficient R^2 values and low limits of detection (high ppt) obtained from the calibration curves produced from the experiments for each individual component are shown in Table 4.5. LOD estimates were based on signal current values obtained from experimentally tested in our lab 1 ppb simulant gas standards. LOD values were determined to be at least three times above the noise level, as for previous experiments.

Table 4.5: Liverpool MIMS system performance (response times, linearity and LOD) with the examined simulant compounds.

compound name	**rise time (sec)**	**fall time (sec)**	**R^2**	**LOD (ppb)**
Methyl benzoate **(*m/z* 136)**	15	27	0.9975	0.68
Piperidine **(*m/z* 85)**	22	58	0.9994	0.96
2-nitrotoluene **(m/z 137)**	18	27	0.9977	0.80
Cyclohexanone **(m/z 98)**	10	28	0.9993	0.61
DMMP **(m/z 124)**	14	28	0.9987	0.85
CES **(m/z 124)**	12	41	0.9984	0.70

4.4. Conclusions

A portable membrane inlet mass spectrometer was used to monitor odour chemical signatures found in the gas surrounding area of illegal and hazardous substances. This chapter demonstrated proof of principle for trace detection and on-line monitoring of volatile chemical markers emitted from drugs, explosives and chemical warfare agents. In the examined compounds list, intermediate, precursor and breakdown products were also included. Different membranes were tested to achieve maximum sensitivity enhancement whereas minimum sample preparation requirements were needed. Fast detection response times were observed. Field experiments with threat compounds followed the lab experiments to confirm detectability of real illicit components (drugs

and explosives). Positive preliminary results were obtained allowing future exploitation. Detection limits in the sub ppb range were obtained, with the possibility of further improvement in the future.

Future work will include further testing of our MIMS system in the field with more real threat and / or simulant compounds and experimental determination of detection limits. Moreover, it could be beneficial to replace the EI ion source with a chemical ionization ion source in order to produce clearer mass spectra and distinctive molecular species and fragments. To date no signal processing algorithms have been used: raw data only are presented. Future work will also address this issue and seek to enhance signal extraction from the background and/or from base (noise) level. Further sensitivity enhancement and lower LOD's are anticipated by using such techniques. The mass range of the mass analyzer will be expanded (e.g. up to 500 Da) in order to extend the range of detectable analytes. Further weight reduction (e.g. below 10 kg) is also planned. Field experiments in harsh environments such as airports, other security checkpoints or cargo services are needed for *in-situ* validation of our apparatus.

4.5. References

[1] U.S. Department of Homeland Security, www.dhs.gov.

[2] United Nations Office on Drugs and Crime, https://www.unodc.org/unodc/index.html.

[3] S. Giannoukos, B. Brkić, S. Taylor, N. France, *Monitoring of human chemical signatures using membrane inlet mass spectrometry,* Anal. Chem. **86,** 1106−1114 (2014).

[4] G. A. Schoon, J. C. De Bruin, *The ability of dogs to recognize and cross-match human odours,* Forensic Sci. Int. **69,** 111-118 (1994).

[5] G. A. Schoon, *A first assessment of the reliability of an improved scent identification line-up,* J. Forensic Sci. **43,** 70-75 (1998).

[6] D. Komar, *The use of cadaver dogs in locating scattered, scavenged human remains: preliminary field test results,* J. Forensic Sci. **44,** 405-408 (1999).

[7] N. Lorenzo, T. Wan, R. J. Harper, Y. L. Hsu, M. Chow, S. Rose, K. G. Furton, *Laboratory and field experiments used to identify Canis lupus var. familiaris active odor signature chemicals from drugs, explosives, and humans,* Anal. Bioanal. Chem. **376,** 1212-1224 (2003).

[8] D. S. Moore, *Recent Advances in Trace Explosives Detection Instrumentation,* Sens. Imaging **8,** 9-38 (2007).

[9] R. J. Harper, J. R. Almirall, K. G. Furton, *Identification of dominant odor chemicals emanating from explosives for use in developing optimal training aid combinations and mimics for canine detection,* Talanta **67,** 313-327 (2005).

[10] World Health Organization, http://www.who.int/en/.

[11] Z. Ouyang, R. J. Noll, R. G. Cooks, *Handheld miniature ion trap mass spectrometers,* Anal. Chem. **81,** 2421-2425 (2009).

[12] J. A. Contreras, J. A. Murray, S. E. Tolley, J. L. Oliphant, H. D. Tolley, S. A. Lammert, E. D. Lee, D. W. Later, M. L. Lee, *Hand-portable gas chromatograph-toroidal ion trap mass spectrometer (GC-TMS) for detection of hazardous compounds,* J. Am. Soc. Mass Spectrom. **19,** 1425–1434 (2008).

[13] A. Sambouli, A. El Bouri, T. Bouayoun, M. A. Bellimam, *Headspace-GC/MS detection of TATP traces in post-explosion debris,* Forensic Sci. Int. **146,** 191–194 (2004).

[14] D. Perret, S. Marchese, A. Gentili, R. Curini, A. Terracciano, E. Bafile, F. Romolo, *LC-MS-MS Determination of Stabilizers and Explosives Residues in Hand-Swabs,* Chromatographia **68,** 517-524 (2008).

[15] L. Widmer, S. Watson, K. Schlatter, A. Crowson, *Development of an LC/MS method for the trace analysis of triacetone triperoxide (TATP),* Analyst **127,** 1627-1632 (2002).

[16] P. I. Hendricks, J. K. Dalgleish, J. T. Shelley, M. A. Kirleis, M. T. McNicholas, L. Li, T. C. Chen, C. H. Chen, J. S. Duncan, F. Boudreau, R. J. Noll, J. P. Denton, T. A. Roach, Z. Ouyang, R. G. Cooks, *Autonomous in situ analysis and real-time chemical detection using a backpack miniature mass spectrometer: concept, instrumentation development, and performance,* Anal. Chem. **86,** 2900-2908 (2014).

[17] Y. Zhang, X. Ma, S. Zhang, C. Yang, Z. Ouyang, X. Zhang, *Direct detection of explosives on solid surfaces by low temperature plasma desorption mass spectrometry,* Analyst **134,** 176-181 (2009).

[18] R. G. Ewing, D. A. Atkinson, G. A. Eiceman, G. J. Ewing, *A critical review of ion mobility spectrometry for the detection of explosives and explosive related compounds,* Talanta **54,** 515-529 (2001).

[19] B. H. Clowers, W. F. Siems, H. H. Hill, S. M. Massick, *Hadamard Transform Ion Mobility Spectrometry,* Anal. Chem. **78,** 44–51 (2006).

[20] G. A. Buttigieg, A. K. Knight, S. Denson, C. Pommier, M. B. Denton, *Characterization of the explosive triacetone triperoxide and detection by ion mobility spectrometry,* Forensic Sci. Int. **135,** 53–59 (2003).

[21] I. Marquez-Sillero, E. Aguilera-Herrador, S. Cardenas, M. Valcarcel, *Ion-mobility spectrometry for environmental analysis,* Trends Anal. Chem. **30,** 677-690 (2011).

[22] S. Armenta, M. Alcala, M. Blanco, *A review of recent, unconventional applications of ion mobility spectrometry (IMS),* Anal. Chim. Acta **703,** 114-123 (2011).

[23] Z. Karpas, *Ion mobility spectrometry: A tool in the war against terror,* B. of the Israel Chem. Soc. **24,** 26-30 (2009).

[24] T. L. Buxton, P. B. Harrington, *Rapid multivariate curve resolution applied to identification of explosives by ion mobility spectrometry,* Anal. Chim. Acta **434,** 269-282 (2001).

[25] M. A. Mäkinen, O. A. Anttalainen, M. E. T. Sillanpää, *Ion Mobility Spectrometry and Its Applications in Detection of Chemical Warfare Agents,* Anal. Chem. **82,** 9594–960 (2010).

[26] J. M. Perr, K. G. Furton, J. R. Almirall, *Solid phase microextraction ion mobility spectrometer interface for explosive and taggant detection,* J. Separ. Sci. **28,** 177-183 (2005).

[27] G. A. Eiceman, E. V. Krylov, N. S. Krylova, E. G. Nazarov, R. A. Miller, *Separation of Ions from Explosives in Differential Mobility Spectrometry by Vapor-Modified Drift Gas,* Anal. Chem. **76,** 4937-4944 (2004).

[28] B. M. Kolakowski, Z. Mester, *Review of applications of high-field asymmetric waveform ion mobility spectrometry (FAIMS) and differential mobility spectrometry (DMS),* Analyst **132,** 842-864 (2007).

[29] M. J. Pollard, C. K. Hilton, H. Li, K. Kaplan, R. A. Yost, H. H. Hill Jr, *Ion mobility spectrometer-field asymmetric ion mobility spectrometer-mass spectrometry,* Int. J. Ion Mobil. Spectrom. **14,** 15-22 (2011).

[30] Y. Takada, H. Nagano, M. Suga, Y. Hashimoto, M. Yamada, M. Sakairi, K. Kusumoto, T. Ota, J. Nakamura, *Detection of Military Explosives by Atmospheric Pressure Chemical Ionization Mass Spectrometry with Counter-Flow Introduction,* Propell. Explos. Pyrotech. **27,** 224-228 (2002).

[31] I. Cotte-Rodriguez, H. Hernandez-Soto, H. Chen, R. G. Cooks, *In Situ Trace Detection of Peroxide Explosives by Desorption Electrospray Ionization and*

Desorption Atmospheric Pressure Chemical Ionization, Anal. Chem. **80,** 1512–1519 (2008).

[32] I. Cotte-Rodriguez, Z. Takats, N. Talaty, H. W. Chen, R. G. Cooks, *Desorption Electrospray Ionization of Explosives on Surfaces: Sensitivity and Selectivity Enhancement by Reactive Desorption Electrospray Ionization,* Anal. Chem. **77,** 6755–6764 (2005).

[33] D. R. Justes, N. Talaty, I. Cotte-Rodriguez, R. G. Cooks, *Detection of explosives on skin using ambient ionization mass spectrometry,* Chem. Commun. **21,** 2142–2144 (2007).

[34] J. T. Kauppila, N. Talaty, T. Kuuranne, T. Kotiaho, R. Kostiainen, R. G. Cooks, *Rapid analysis of metabolites and drugs of abuse from urine samples by desorption electrospray ionization-mass spectrometry,* Analyst **132,** 868–875 (2007).

[35] R. G. Cooks, Z. Ouyang, Z. Takats, J. M. Wiseman, *Ambient Mass Spectrometry, Science* **311,** 1566–1570 (2006).

[36] Z. Takats, J. M. Wiseman, B. Gologan, R. G. Cooks, *Mass Spectrometry Sampling Under Ambient Conditions with Desorption Electrospray Ionization, Science* **306,** 471–473 (2004).

[37] I. Cotte-Rodriguez, R. G. Cooks, *Non-proximate detection of explosives and chemical warfare agent simulants by desorption electrospray ionization mass spectrometry,* Chem. Comm. **28,** 2968–2970 (2006).

[38] R. B. Cody, J. A. Laramee, H. D. Durst, *Versatile New Ion Source for the Analysis of Materials in Open Air under Ambient Conditions,* Anal. Chem. **77,** 2297-2302 (2005).

[39] J. L. Gottfried, F. C. De Lucia Jr, C. A. Munson, A. W. Miziolek, *Laser-induced breakdown spectroscopy for detection of explosives residues: a review of recent advances, challenges, and future prospects,* Anal. Bioanal. Chem. **395,** 283-300 (2009).

[40] J. A. Shaw, N. L. Seldomridge, D. L. Dunkle, P. W. Nugent, L. H. Spangler, J. J. Bromenshenk, C. B. Henderson, J. H. Churnside, J. J. Wilson, *Polarization lidar measurements of honey bees in flight for locating land mines,* Opt. Express **13,** 5853-5863 (2005).

[41] P. Weibring, H. Edner, S. Svanberg, *Versitile mobile lidar system for environmental monitoring,* Appl. Opt. **42,** 3583–3594 (2003).

[42] K. Wells, D. A. Bradley, *A review of X-ray explosives detection techniques for checked baggage*, Appl. Radiat. Isotopes **70,** 1729-1746 (2012).

[43] Y. C. Shen, T. Lo, P. F. Taday, B. E. Cole, W. R. Tribe, M. C. Kemp, *Detection and identification of explosives using terahertz pulsed spectroscopic imaging,* Appl. Phys. Lett. **86,** 241116 (2005).

[44] F. Huang, B. Schulkin, H. Altan, J. F. Federici, D. Gary, R. Barat, D. Zimdars, M. H. Chen, D. B. Tanner, *Terahertz study of 1,3,5-trinitro-s-triazine by time domain and Fourier transform infrared spectroscopy,* Appl. Phys. Lett. **85,** 5535–5537 (2004).

[45] H. B. Liu, Y. Chen, G. J. Bastiaans, X. C. Zhang, *Detection and identification of explosive RDX by Thz diffuse reflection spectroscopy,* Opt. Express **14,** 415-423 (2006).

[46] J. Oxley, J. Smith, J. Brady, F. Dubnikova, R. Kosloff, L. Zeiri, Y. Zeiri, *Raman and infrared fingerprint spectroscopy of peroxide-based explosives,* Appl Spectrosc. **62,** 906-915 (2008).

[47] O. M. Primera-Pedrozo, Y. M. Soto-Feliciano, L. C. Pacheco-Londoño, S. P. Hernández-Rivera, *Detection of High Explosives Using Reflection Absorption Infrared Spectroscopy with Fiber Coupled Grazing Angle Probe/FTIR,* Sensing and Imaging **10,** 1-13 (2009).

[48] J. C. Carter, S. M. Angel, M. Lawrence-Snyder, J. Scaffidi, R. E. Whipple, J. G. Reynolds, *Standoff detection of high explosive materials at 50 meters in ambient light conditions using a small Raman instrument,* Appl. Spectrosc. **59,** 769-775 (2005).

[49] D. A. Stuart, K. B. Biggs, R. P. Van Duyne, *Surface-enhanced Raman spectroscopy of half-mustard agent,* Analyst **131,** 568–572 (2006).

[50] C. Ramos, P. J. Dagdigian, *Effect of photochemistry on molecular detection by cavity ringdown spectroscopy: a case study of an explosive-related compound,* Appl. Optics **46,** 6526-6532 (2007).

[51] J. Yinon, *Detection of Explosives by Electronic Noses,* Anal. Chem. **75,** 98-105 (2003).

[52] F. Wang, W. Wang, B. Liu, Z. Wang, Z. Zhang, *Copolypeptide-doped polyaniline nanofibers for electrochemical detection of ultratrace trinitrotoluene,* Talanta **79,** 376-382 (2009).

[53] D. R. Shankaran, K. Matsumoto, K. Toko, N. Miura, *Development and comparison of two immunoassays for the detection of 2,4,6-trinitrotoluene (TNT) based on surface Plasmon resonance,* Sens. Actuators B **114,** 71–79 (2006).

[54] P. Rabenecker, K. Pinkwart, *A Look Behind Electrochemical Detection of Explosives,* Propellants Explos. Pyrotech. **34,** 274-279 (2009).

[55] L. Senesac, T. G. Thundat, *Nanosensors for trace explosive detection,* materialstoday **11,** 28-36 (2008).

[56] C. Liao, A. Gock, M. Michie, B. Morton, A. Anderson, S. Trowell, *Behavioural and Genetic Evidence for C. Elegans' Ability to Detect Volatile Chemicals Associated with Explosives,* PLOS ONE **5,** 1-9 (2010).

[57] T. L. King, F. M. Horine, K. C. Daly, B. H. Smith, *Explosives Detection With Hard-Wired Moths,* IEEE Transactions on Instrumentation and Measurement **53,** 1113-1118 (2004).

[58] J. Otto, M. F. Brown, W. Long, *Training rats to search and alert on contraband odors,* Appl. Anim. Behav. Sci. **77,** 217–232 (2002).

[59] R. C. Johnson, R. G. Cooks, T. M. Allen, M. E. Cisper, P. H. Hemberger, *Membrane introduction mass spectrometry: trends and applications,* Mass Spectrom. Rev. **19,** 1-37 (2000).

[60] E. Boscaini, M. L. Alexander, P. Prazeller, T. D. Mark, *Investigation of fundamental physical properties of a polydimethylsiloxane (PDMS) membrane using proton transfer reaction mass spectrometer (PTRMS),* Int. J. Mass Spectrom. **239,** 179-186 (2004).

[61] A. J. Thompson, A. S. Creba, R. M. Ferguson, E. T. Krogh, C. G. Gill, *A coaxially heated membrane introduction mass spectrometry interface for the rapid and sensitive on-line measurement of volatile and semi-volatile organic contaminants in air and water at parts-per-trillion levels,* Rap. Comm. Mass Spec. **13,** 2000-2008 (2006).

[62] L. S. Riter, B. C. Laughlin, E. Nikolaev, R. G. Cooks, *Direct analysis of volatile organic compounds in human breath using a miniaturized cylindrical ion trap mass spectrometer with a membrane inlet,* Rap. Comm. Mass Spec. **16,** 2370-2373 (2002).

[63] R. A. Ketola, T. Kotiaho, M. E. Cisper, T. M. Allen, *Environmental applications of membrane introduction mass spectrometry,* J. Mass Spectrom. **37,** 457-476 (2002).

[64] I. Cotte-Rodrıguez, E. Handberg, R. J. Noll, D. P. A. Kilgour, R. G. Cooks, *Improved detection of low vapor pressure compounds in air by serial combination of single-sided membrane introduction with fiber introduction mass spectrometry (SS-MIMS-FIMS),* Analyst **130**, 679-686 (2005).

[65] L. S. Riter, Z. Takáts, R. G. Cooks, *Single-sided membrane introduction mass spectrometry for on-line determination of semi-volatile organic compounds in air,* Analyst **126,** 1980-1984 (2001).

[66] B. A. Eckenrode, *The application of an integrated multifunctional field-portable GC/MS system,* Field Analytical Chemistry and Technology, **2,** 3–20 (1998).

[67] M. S. Macias, R. J. Harper, K. G. Furton, *A comparison of Real Versus Contraband VOCs for Reliable Detector Dog Training Utilizing SPME-GC-MS,* Am. Lab. **40,** 16-19 (2008).

[68] H. Lai, A. Leung, M. Magee, J. R. Almirall, *Identification of volatile chemical signatures from plastic explosives by SPME-GC/MS and detection by ion mobility spectrometry,* Anal. Bioanal. Chem. **396,** 2997-3007 (2010).

[69] E. B. Russo, *Taming THC: potential cannabis synergy and phytocannabinoid-terpenoid entourage effects,* Br. J. Pharmacol. **163,** 1344-1364 (2011).

[70] P. Guerra, H. Lai, J. R. Almirall. Analysis of the volatile chemical markers of explosives using novel solid phase microextraction coupled to ion mobility spectrometry. *J. Sep. Sci.* **2008,** *31,* 2891-2898.

[71] J. E. Riviere, C. E. Smith, K. Budsaba, J. D. Brooks, E. J. Olajos, H. Salem, N. A. Monteiro-Riviere, *Use of methyl salicylate as a simulant to predict the percutaneous absorption of sulphur mustard,* J. Appl. Toxicol. **21,** 91–99 (2001).

[72] U.S. Department of Health & Human Services, http://www.hhs.gov/.

[73] U.S National Library of Medicine, Toxicology Data Network, http://toxnet.nlm.nih.gov/index.html.

[74] Wagtail UK Ltd., http://www.wagtailuk.com/.

[75] W. H. McClennen, C. L. Vaughn, P. A. Cole, S. N. Sheya, D. J. Wager, T. J. Mott, J. P. Dworzanski, N. S. Arnold, H. L. C. Meuzelaar, *Roving GC/MS: Mapping VOC gradients and trends in space and time,* Field Anal. Chem. Technol. **1,** 109−116 (1996).

[76] A. Naganowska-Nowak, P. Konieczka, A. Przyjazny, J. Namiesnik, *Development of Techniques of Generation of Gaseous Standard Mixtures,* Crit. Rev. Anal. Chem. **35,** 31−55 (2005).

Part II

Chapter 5

Linear ion trap mass spectrometry

5.1. Introduction

The growing trend towards miniaturised mass spectrometry has already brought portable systems for environmental [1, 2] and security [3, 4] applications. The main driver for hardware realization of portable systems has been a miniaturization of the mass analyzer – the key component of every mass spectrometer. A smaller analyzer can operate at higher pressures due to shorter ion mean free path, requiring less robust vacuum system, which reduces size and weight of a system. Miniaturization also enables analyzer operation at lower voltages, which reduces power consumption necessary for a portable system. The three types of mass analyzers that have been successfully miniaturized include quadrupole mass filter [5-7], ion trap [8-10] and time-of-flight [11-13]. The ion trap is the most commonly used analyzer in portable systems due to its capability to perform mass analysis at higher pressures than other analyzers and it offers a relatively high mass range (m/z to 2000).

In this chapter an ideal linear ion trap (LIT) with a coupled ion source lens system (ISLS) for ion injection and focusing is simulated. The LIT in this case is considered to be a 2D trap with linear quadrupole electric field along axial (z) direction. The field linearity provides better performance for an LIT than for 3D types of ion traps (e.g., quadrupole ion trap) [14]. The main advantages include better sensitivity and faster mass scanning. This is because a linear axial field enables ‘smoother’ forward and backward ion oscillations, which results in more ions remaining stable during trapping and allows faster ejection during scanning [15-17]. Sensitivity in portable LIT mass spectrometers is commonly optimized with the design of a mass analyzer and signal-to-noise ratio of the detector (usually electron multiplier). Optimization of geometry and increase in the size of an analyzer, increase the capacity to store ions leading to higher sensitivity. Likewise, higher gain multiplier detectors further improve sensitivity.

However, both of these factors have their limitations. The LIT size can be increased to the level determined by electrode voltages required to achieve the targeted mass range for a given size. In a similar way, multiplier gain can only be increased to a level where signal is clearly distinguished from the noise. Another option for sensitivity enhancement is to improve ion injection and focusing to further increase the number of trapped and ejected ions. This can be done through optimized design of an ISLS, which is investigated in this chapter. A LIT mass analyser similar to the one simulated was constructed and tested. Also presented in this chapter are preliminary experimental results.

The following sections describe characteristics of a non-scanning LIT, modelling method and ISLS with simulation results presented for ion injection, trapping and ejection. The advantage of using a non-scanning LIT to achieve high sensitivity for targeted substances is explained with experimental results shown for the Liverpool LIT. The accuracy and suitability of the boundary element method for the simulation study are discussed. The functionality of the ISLS is explained with modelling parameters given. Simulation results are shown for cocaine (m/z 182 and 304) ions for a range of geometric parameters of the ISLS including ion trajectories for commercial and simulation-optimized lens systems. High impact of the ISLS geometry on sensitivity of the mass analyzer is demonstrated, showing significant potential for sensitivity enhancement through optimized ion injection and focusing.

5.2. Non-scanning linear ion trap mass spectrometry

Mass analysis in ion traps is usually achieved through voltage scanning on the trap electrodes. In this way, confined ions are selectively ejected from the trap from lowest to highest mass-to-charge ratio (m/z) to generate mass spectrum across the defined mass range. In LITs, voltage scanning is done by ramping the RF voltage amplitude on the trap electrodes in sequence with ramped bias voltages [18, 19]. Bias voltages are either low value DC or low amplitude AC held at a constant ratio with the RF voltage and used to isolate individual ion masses. Fine mass resolution of spectral peaks is achieved by varying the scan time, where longer scan times give higher resolutions.

In portable applications for which only specific substances have to be monitored (e.g., few spectral peaks), mass analysis through scanning may not be the best choice. The main reasons are lower sensitivity and more complicated drive electronics due to

the voltage scanning circuitry involved. All scanning methods begin at one fixed RF voltage (low cut-off point) to trap all the ions across the defined mass range. This trapping RF voltage may be optimal for a few ion masses, but it will not be optimal for most other masses, which can cause a significant loss of ions during trapping and reduce sensitivity. Apart from ion losses during trapping, many ejected ions are lost during scanning when the RF trapping voltage is ramped. This is because of the nature of the mass scanning, where the trade-off between trapping and scanning voltages is created to maintain higher ion masses confined during ejection of a lower ion mass.

An alternative mass analysis scheme for portable sensing is to use a non-scanning method, where no voltage ramping is performed [20]. In a non-scanning method, for each run, only one specific targeted ion mass is confined and ejected at a time. In this way, every mass that is monitored can have optimal discrete trapping and ejection voltages applied, which increases instrument sensitivity. Removal of scanning circuits also simplifies circuitry design, reduces power consumption and overall cost of the drive electronics.

Figure 5.1 shows a schematic diagram of a non-scanning ideal LIT with hyperbolic electrodes designed at University of Liverpool. It operates by axially injecting ions into the trap using the ISLS, where one specific ion mass is trapped and axially ejected at a time. Selective ion trapping is performed by applying suitable positive RF voltage to the *y*-axis quadrupole rods (*y*-electrodes), and negative and positive DC biases to the *x*- and *y*-axes rods (*x*,*y*-electrodes) respectively. Ion extraction of positive ions is achieved by switching the positive DC voltage on the exit endplate (exit *z*-electrode) to a suitable negative value, enabling maximum number of ions at the target mass to be ejected.

To isolate a single ion mass, the LIT must be operating near the tip of its stability diagram. Figure 5.2 shows the stability diagram for an ideal 2D LIT, which is identical to the one for a quadrupole mass filter [21]. The stability diagram is mathematically represented with dimensionless parameters a_u and q_u, whose values for single mass trapping are slightly below 0.706 and 0.237 respectively. The DC and RF voltages required for isolation of a single charged positive ion mass for the LIT in Figure 5.1 are given by the following equations (5.1 and 5.2) [21]:

$$U = a_u m r_0^2 \Omega^2 / 8e \tag{5.1}$$

$$V = q_u m r_0^2 \Omega^2 / e \tag{5.2}$$

where U is the total DC bias applied to x- and/or y-electrodes, m is the ion mass, r_0 is the inscribed radius of electric field, Ω is the angular frequency (equal to $2\pi f$, where f is the frequency of the RF field), e is the elementary charge of an electron and V is peak-to-peak RF amplitude applied to y-electrodes.

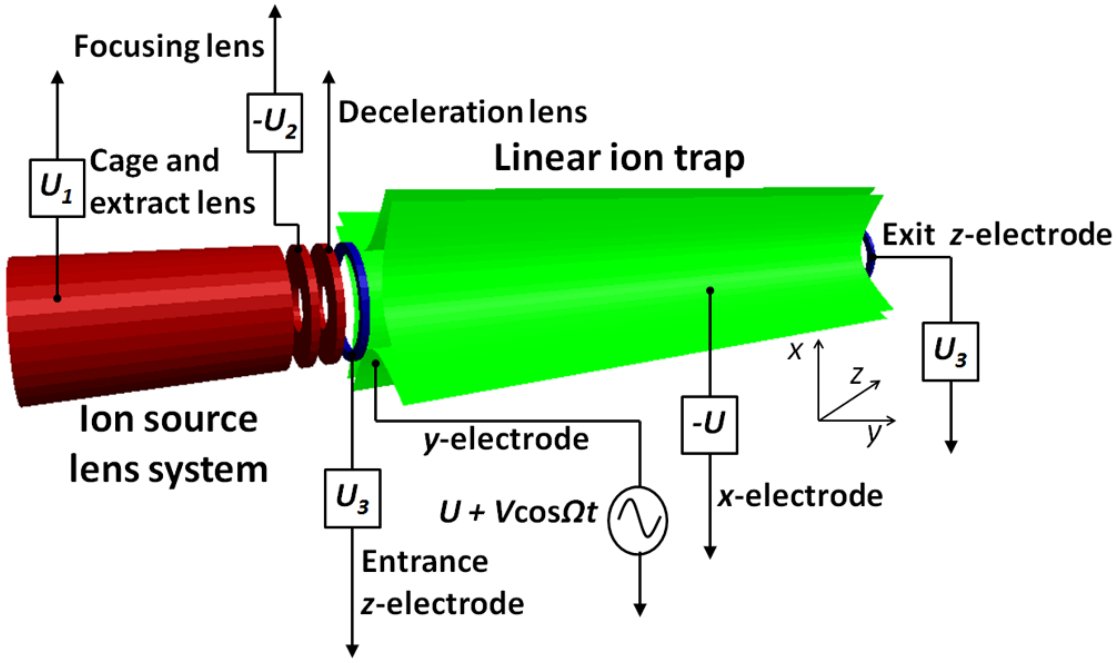

Figure 5.1: Schematic diagram of a non-scanning linear ion trap with a coupled ion source lens system.

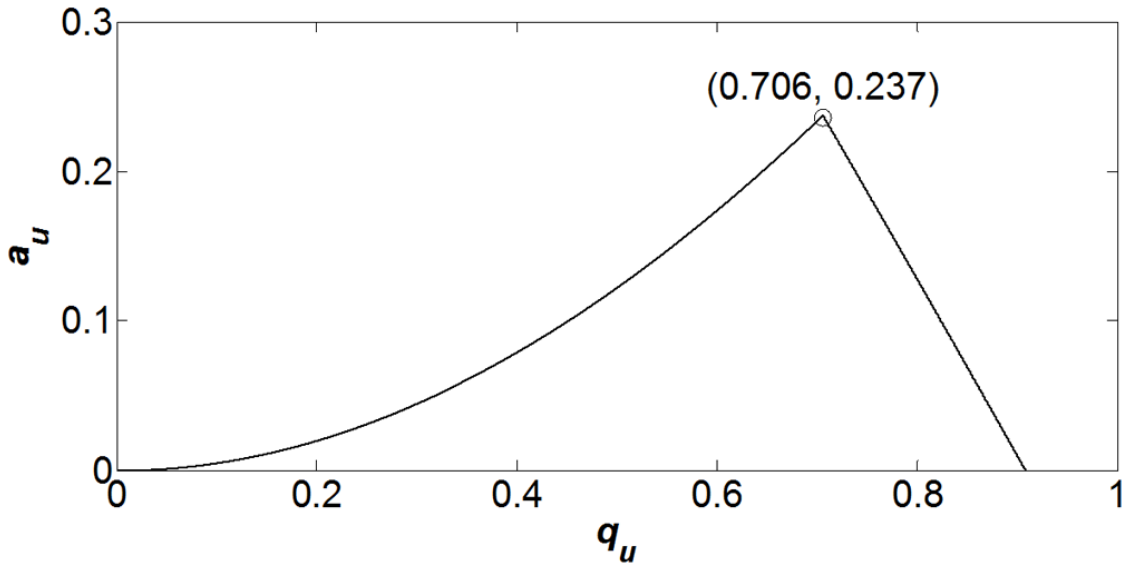

Figure 5.2: Stability diagram for an ideal 2D linear ion trap.

5.3. Non-scanning LIT simulations

5.3.1. CPO simulation software

Numerical modelling can be very useful when designing mass spectrometers because the effects on ion motion from electrode geometry alterations can be investigated much quicker and cheaper than in experiments. The simulation results presented here for the ISLS coupled to the non-scanning LIT were done using a 3D version of a commercial software simulation program: Charged Particle Optics (CPO) [22]. CPO is based on the boundary element method (BEM), which was previously shown to be highly accurate for modelling ion motion in miniature ion traps [23]. CPO also supports space charge simulation, which allows closer approximation to experimental conditions.

The BEM works by numerically solving the charge distribution on the electrode surfaces. The values of these surface charges are used to compute the electrostatic fields and potentials at any point in 3D space between the electrodes. The electrodes drawn using the BEM are divided into small segments, which are usually represented by a triangular mesh. Each triangular segment in CPO is assumed to have uniformly distributed amount of constant charge. Segmentation is done only on conducting surfaces rather than complete electrode volumes as in other methods (e.g., finite element and finite difference methods). Because of this feature, BEM is also called surface charge method [24]. Finally, CPO offers high accuracy near the electrode edges, which made it a logical choice for modelling mass spectrometer components.

5.3.1.1. Simulation set-up

In the model described here, a lens system for an external ionization ion source was coupled to an ideal linear ion trap operating in a non-scanning mode (Figure 5.1). The lens system consists of ion extract lens, focusing lens and deceleration lens, which can be used for any type of ion source where ions are created outside of mass analyzer. The system in Figure 5.1 is adapted for an electron impact ion source where positive ions are created inside a cylindrical cage after sample neutrals were bombarded with electrons from the hot filament. Upon creation, ions are extracted from the cage using the extract lens that is connected to the cage with same positive DC voltage applied. Extracted ions

are then focused and accelerated using focusing lens held at negative DC voltage. To increase the ability of focused ions to be confined within the trap, their energies are reduced using a grounded deceleration lens.

Figure 5.3 shows the equipotential lines within the ISLS with strong controlling effect from the ion focusing lens.

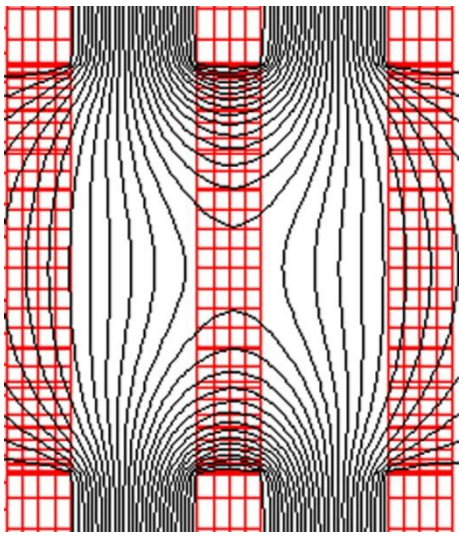

Figure 5.3: Equipotential lines within the ion source lens system.

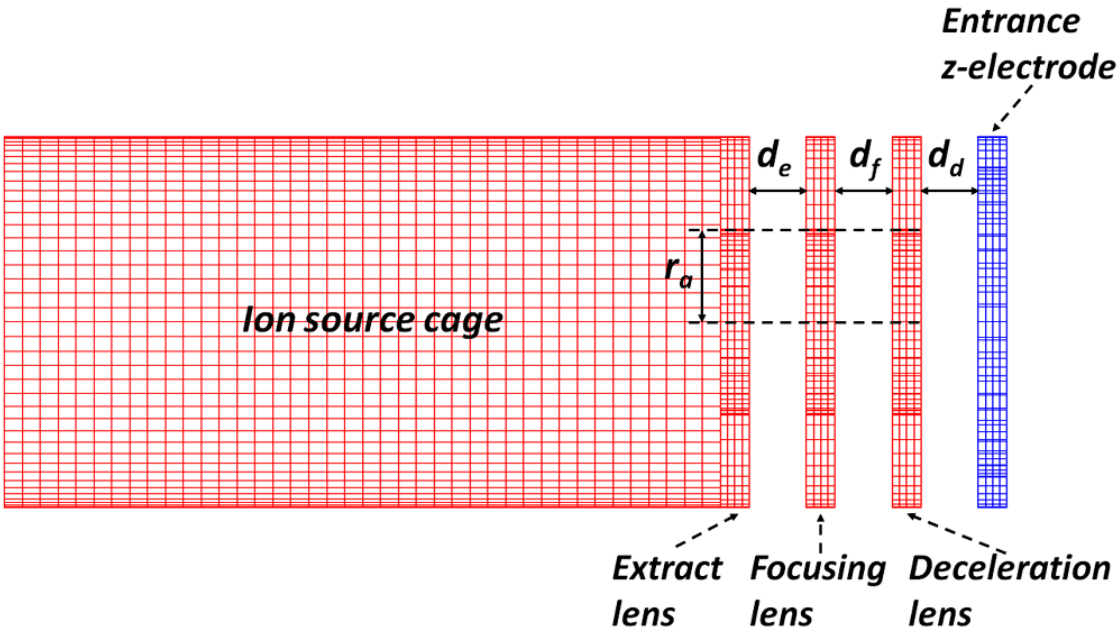

Figure 5.4: Geometrical parameters of the ion source lens system varied in the simulation study.

Figure 5.4 shows the ISLS geometrical parameters that were varied in our simulation study for optimizing the sensitivity of an LIT. These include:

a. aperture radius (r_a) of the lenses,
b. distance between the deceleration lens and entrance *z*-electrode (d_d) using the optimal r_a value,
c. distance between focusing and deceleration lenses (d_f) using optimal r_a and d_d,
d. distance between extract and focusing lenses (d_e) using optimal r_a, d_d and d_f.

The dimensions for the ISLS geometrical parameters are the following:

- ion source cage: 3 mm radius and 10 mm length,
- lens aperture radius (r_a): varied from 0.25 mm ($0.1r_0$) to 2.5 mm (r_0),
- lens thicknesses (d): 0.4 mm,
- inter-lens distances (d_d, d_f and d_e): varied between 0.8 mm ($2d$) to 4 mm ($10d$).

Note that 0.4 mm lens thickness is a typical thickness of commercially available electrostatic lenses for electron impact ion sources. Likewise, the inter-lens distance step of 0.8 mm corresponds to the width of standard commercial ceramic spacers. The defined values for LIT geometrical parameters are therefore:

- *x*,*y*-electrodes: 40 mm electrode length with 2.5 mm r_0,
- *z*-electrodes: 0.4 mm thickness, 2.5 mm aperture radius with 0.8 mm separation from *x*,*y*-electrodes.

Simulations were done for most distinguished cocaine fragment masses at m/z 182 and 304 since cocaine detection is a potential application for a portable LIT mass spectrometer. 8,000 randomly distributed ions at m/z 182 and 304 were defined within the whole cage area with their initial energy set to 0.01 eV. For each variation of geometrical parameters, three phases of ion motion were simulated: injection, trapping and ejection. Successful ions in each phase were the ones that satisfied the following conditions:

✓ injection: successful ions must pass through the lens system and enter the LIT,
✓ trapping: successful ions must remain trapped within the LIT for 1 ms,
✓ ejection: successful ions must exit the LIT through the aperture on the exit *z*-electrode.

Note that trapping times in a real portable LIT system would even be shorter in order to maximize sensitivity and detection speed for a targeted substance. The ISLS voltages defined in the model were:

- cage and extract lens: 3 V,
- focusing lens: -70 V,
- deceleration lens: 0 V.

Voltages on the LIT electrodes were chosen as follows:

- *x*-electrodes: 0 V during injection and trapping with bias voltages during ejection of -6.9 V DC for m/z 182 and -11.5 V DC for m/z 304,
- *y*-electrodes: 329 Vp-p and 549 Vp-p at 1 MHz with bias voltages of 6.9 V DC and 11.5 V DC for m/z 182 and 304 respectively,
- entrance *z*-electrode: 0 V during injection and 20 V during trapping and ejection,
- exit *z*-electrode: 20 V during injection and trapping, and -20 V during ejection.

RF and DC voltages were calculated from equations (5.1) and (5.2). The DC biases on *x*,*y*-electrodes were adjusted to create DC potential differences (*U* voltages), required for trapping specific ion masses.

5.3.1.2. Simulation results for cocaine characteristic ions

Figure 5.5 shows the effect of lens aperture variation on ion injection, trapping and ejection from the total number of defined cocaine *m/z* 182 ions. As can be seen, the optimum lens r_a value is 0.75 mm ($0.3r_0$). To further improve ion focusing and maximize LIT sensitivity, distances between extract, focusing and deceleration lenses were also varied using optimal lens aperture radius. Effect of distance variation between the deceleration lens and entrance *z*-electrode is shown in Figure 5.6, where the optimum d_d value was found to be 2.4 mm ($6d$). Figure 5.7 shows the effect of distance variation between the focusing and deceleration lenses with optimum d_f value of 1.6 mm ($4d$). Finally, the effect of distance variation between the extract and focusing lenses is shown in Figure 5.8 with optimum d_e value of 0.8 mm ($2d$). It can be seen from Figures 5.5-5.8 that ion injection, and particularly trapping efficiency and ion ejection have been greatly affected by altering the distances between the lenses. This is because

the change of distances between the lenses has high impact on ion focusing, particularly between the focusing lens and entrance *z*-electrode.

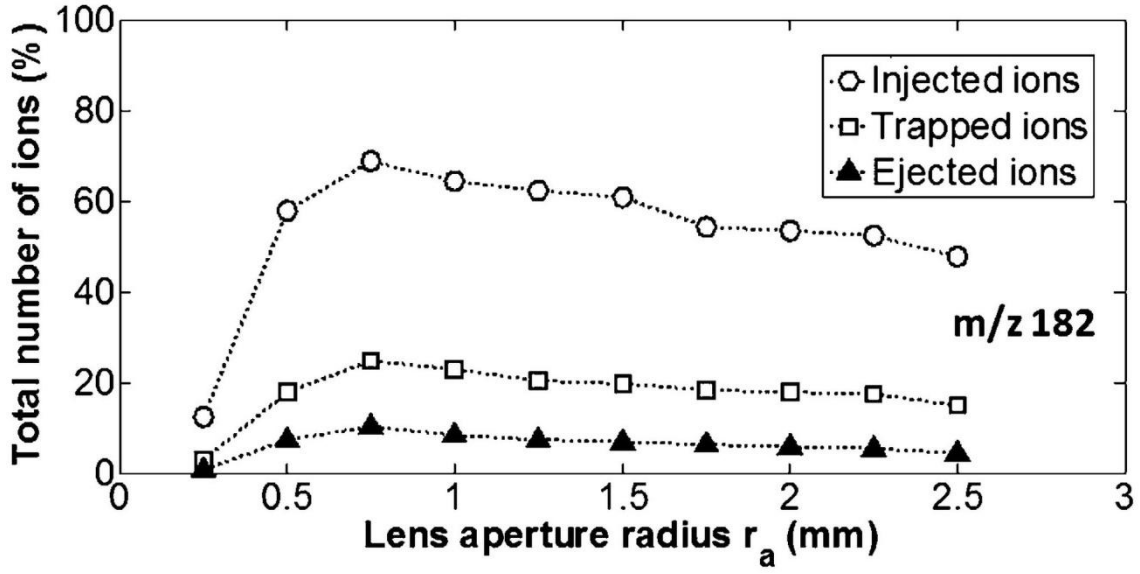

Figure 5.5: Total number of injected, trapped and ejected *m/z* 182 ions with variation of aperture radius of the EI source lens system.

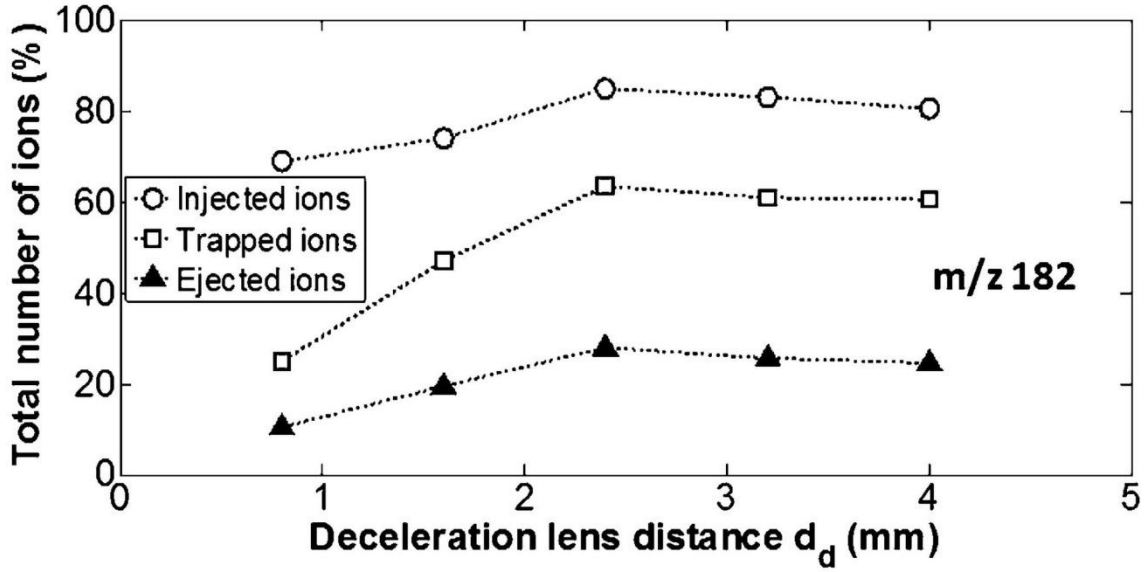

Figure 5.6: Total number of injected, trapped and ejected *m/z* 182 ions with variation of separation between deceleration lens and front *z*-electrode.

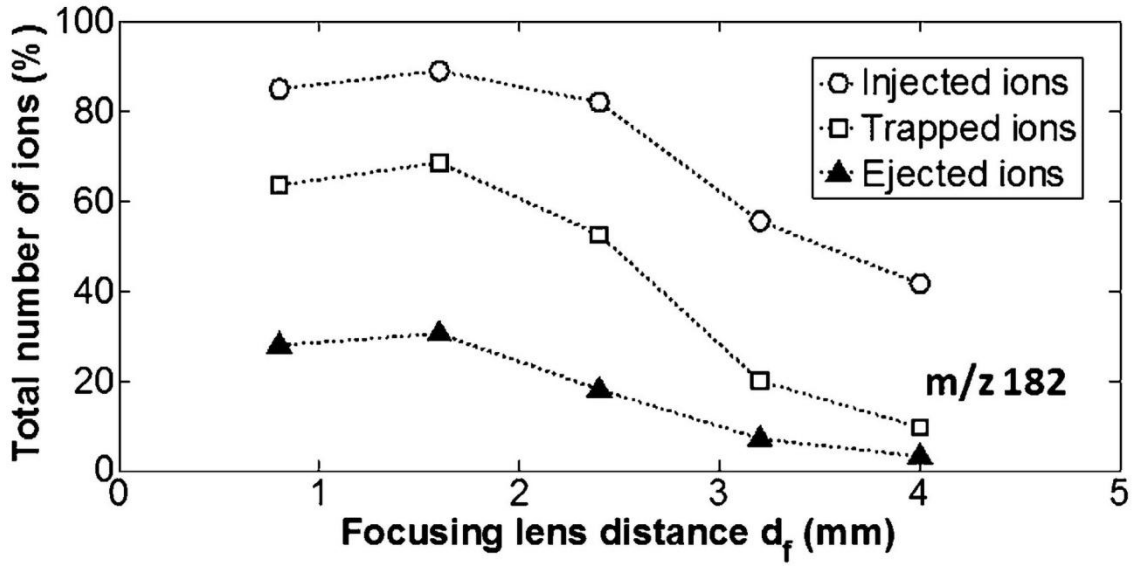

Figure 5.7: Total number of injected, trapped and ejected *m/z* 182 ions with variation of separation between focusing and deceleration lenses.

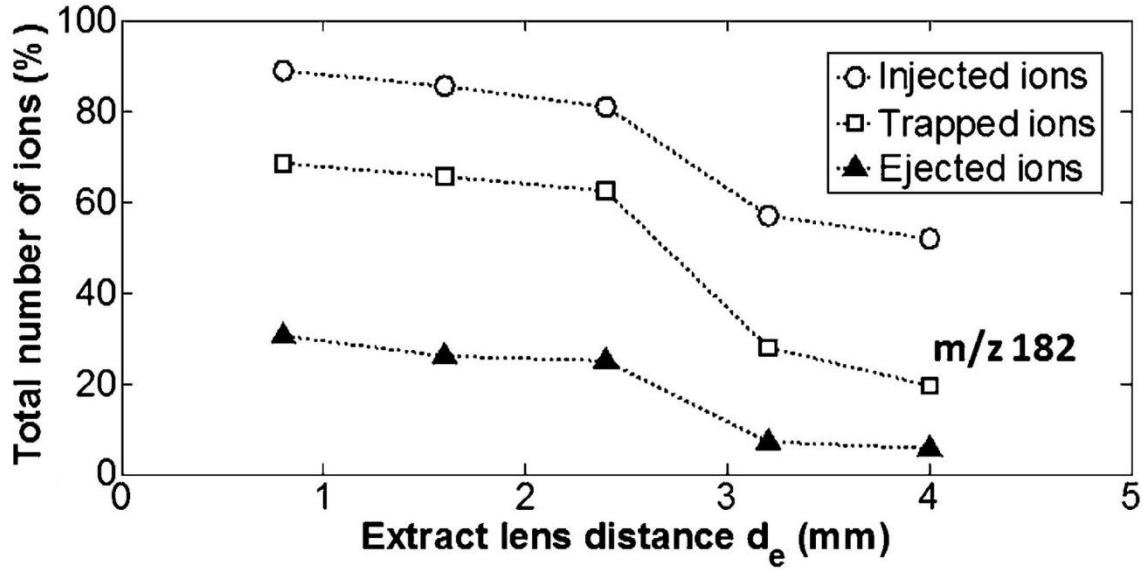

Figure 5.8: Total number of injected, trapped and ejected m/z 182 ions with variation of separation between extract and focusing lenses

Figures 5.9-5.12 show simulation results for cocaine m/z 304 ions with similar effects generated as for m/z 182. As can be seen, the optimal values for r_a, d_d, d_f and d_e are still the same as for m/z 182 with very similar output trends. More specifically, Figure 5.9 presents the results for varying aperture radius r_a of the EI ion source lens system for maximal injection, trapping and ejection of cocaine *m/z* 304 ions for an ideal

LIT in a non-scanning mode. Distance variation effects between the deceleration lens and the entrance z-electrode are shown in Figure 5.10 whereas distance variations effects between focusing and deceleration lenses can be found in Figure 5.11. Distance variation effects between extract and focusing lenses are presented in Figure 5.12.

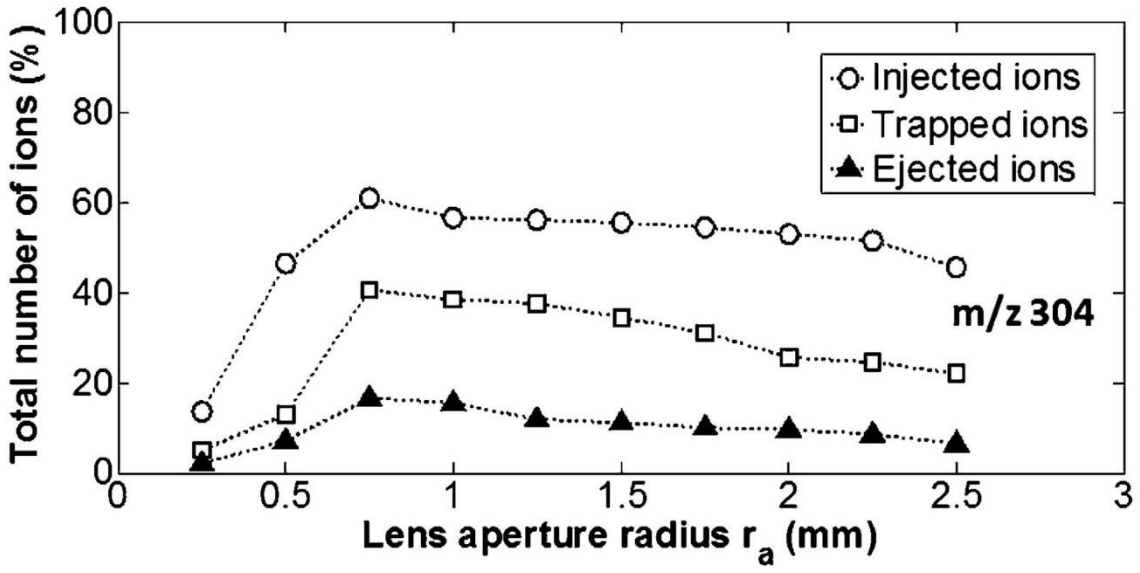

Figure 5.9: Total number of injected, trapped and ejected *m/z* 304 ions with variation of aperture radius of the EI source lens system.

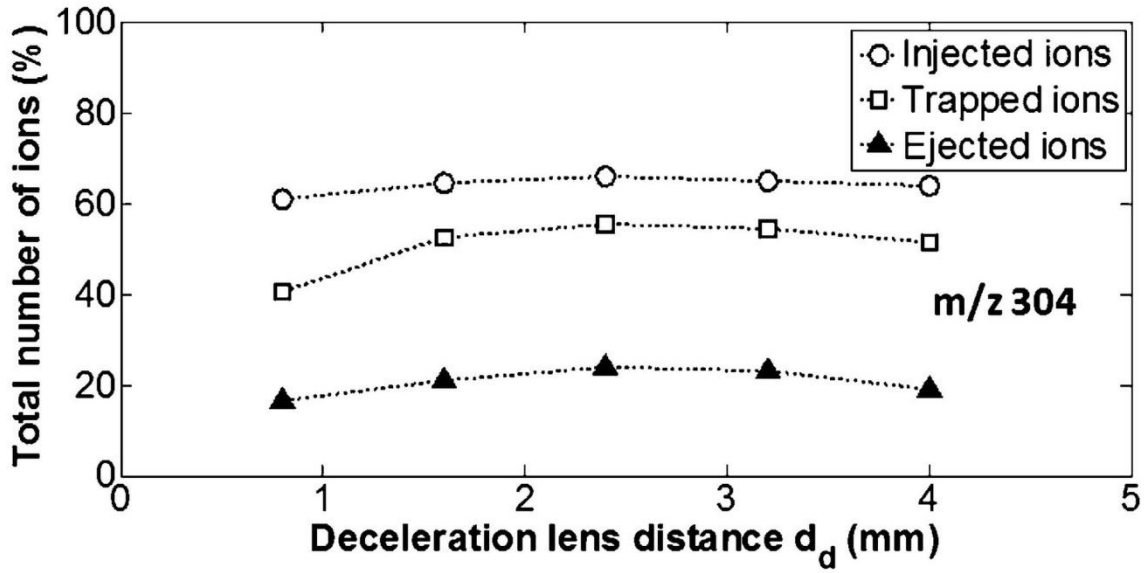

Figure 5.10: Total number of injected, trapped and ejected *m/z* 304 ions with variation of separation between deceleration lens and front *z*-electrode.

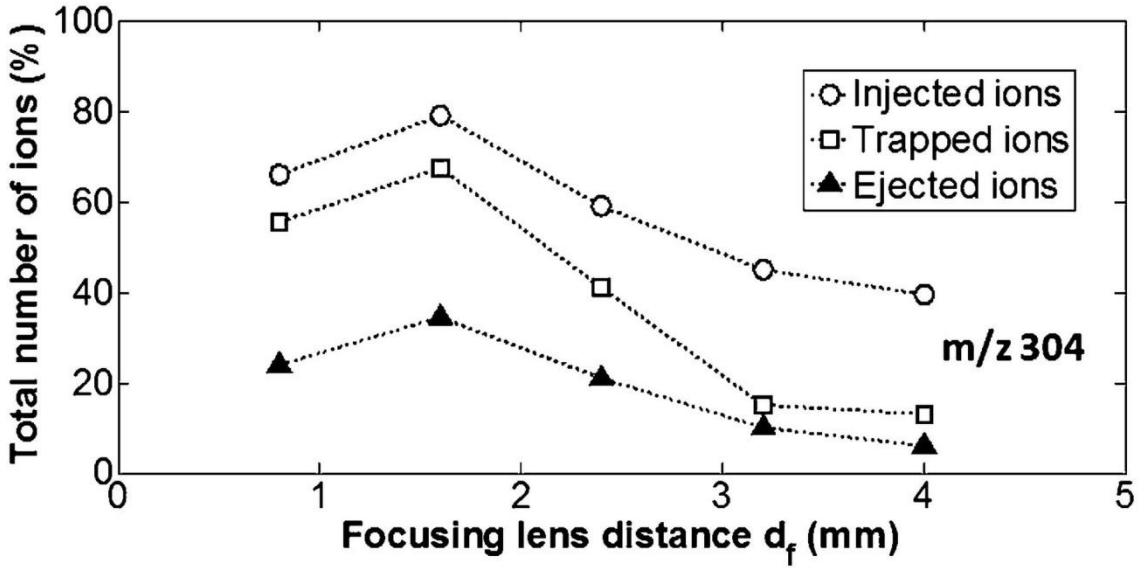

Figure 5.11: Total number of injected, trapped and ejected *m/z* 304 ions with variation of separation between focusing and deceleration lenses.

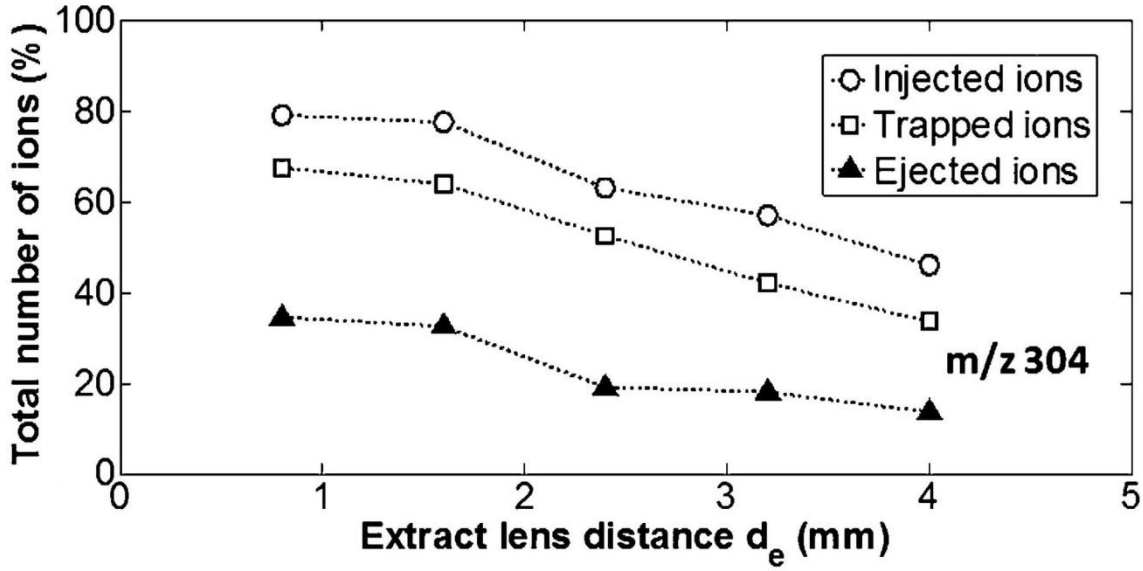

Figure 5.12: Total number of injected, trapped and ejected *m/z* 304 ions with variation of separation between extract and focusing lenses

As it can be found from Table 5.1, compared to standard lens system in a commercial ion source (SS Scientific Ltd, Sussex, UK), simulation optimized ISLS shows sensitivity improvement by a factor of 4. Note that trapping efficiency in a non-scanning LIT is reduced when DC voltage is applied to the rods to narrow the mass

window width, which reduces sensitivity. Also a number of ions are lost during ion ejection when a negative DC voltage is applied to exit z-electrode, which further reduces sensitivity. Therefore, the loss of ions during mass isolation and ion ejection from the LIT can be compensated for by improved ion injection through the optimized ISLS.

Table 5.1: Parameter and performance comparison between commercial and CPO enhanced ion source lens systems.

	Commercial lens system	**CPO enhanced lens system**
r_a (mm)	1.5	0.75
d_e (mm)	0.8	0.8
d_f (mm)	0.8	1.6
d_d (mm)	0.8	2.4
Ion injection (%)	61	89
Ion trapping (%)	20	68.5
Ion ejection (%)	**7**	**30.5**

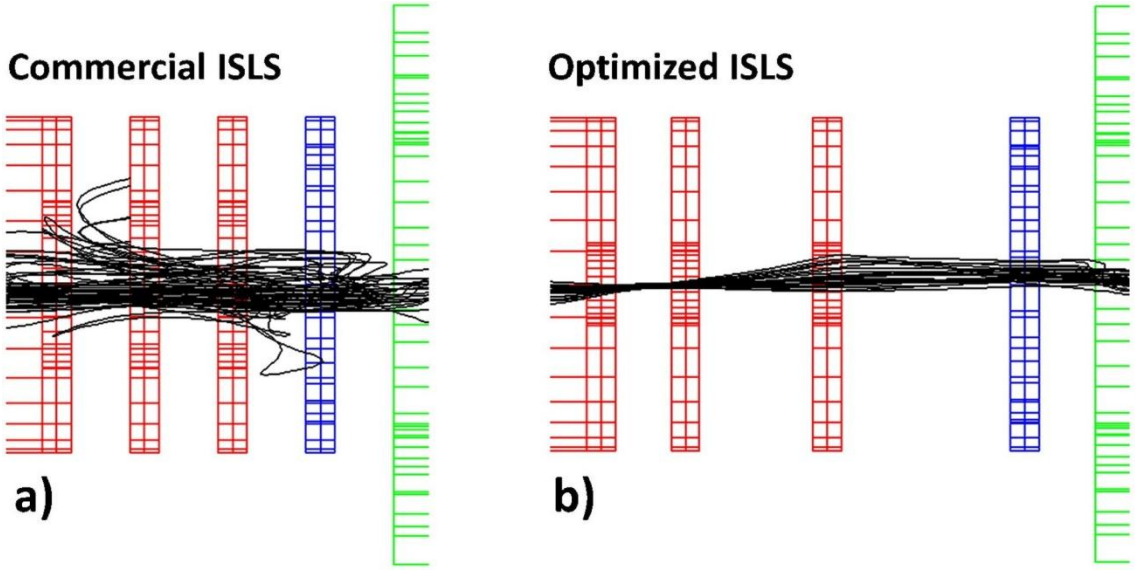

Figure 5.13: Simulated ion trajectories in CPO for cocaine at *m/z* 182 for a) commercial and b) optimized ISLS.

Space charge effects between ions were included in our simulations within the ISLS only, while no space charge was used within LIT. This is because CPO supports space charge for DC systems only, while no space charge effect is included for RF-driven

systems like LITs. Figures 5.13a and 5.13b show trajectories for cocaine *m/z* 182 ions for commercial and simulation-optimized lens systems respectively using identical drive parameters. As can be seen, an optimized lens system with smaller aperture size and suitable lens spacing provides significantly better ion injection and focusing, which results in higher sensitivity of the analyzer.

5.3.2. LIT2 simulation software

In order to numerically optimize ion trapping in a non scanning LIT mass analyser, a novel 3D simulation software package (LIT2) developed in the Mass Spectrometry Group, University of Liverpool to model linear ion traps (LITs) with axial ion injection and ejection with high accuracy using different features:

a) large number of sample ions (up to 500,000),

b) buffer gas collision effects for any given buffer gas mass,

c) support for different electrode geometries (hyperbolic, circular and square),

d) support for displaced electrodes due to manufacturing imperfections.

LIT2 uses the boundary element method (BEM) for field calculations. BEM has been previously demonstrated to be more accurate and faster than finite difference methods (FDM) and finite element methods (FEM) for modeling ion trajectories in miniature ion traps [23]. Moreover, LIT2 supports a much larger number of ions than commercial BEM electrostatic programs like CPO, and has user-friendly settings for buffer gas cooling and a separate field solving program that provides high computational efficiency. Figure 5.14 shows LIT2 the equipotential contours at the center of a hyperbolic LIT whereas Figure 5.15 presents the equipotential contours formation at the ends of a hyperbolic LIT.

Simulations using LIT2 software follow the below described operational steps:

1. Definition of system's geometry

This step includes the definition of the geometrical parameters of LIT electrodes and the number of charges on them.

2. Computation of electric fields

This step computes the 3D electric field grids within the electrode volumes.

3. Computation of ion motion:

Computation of ion motion for given masses and timings during injection, trapping and ejection periods using different voltage settings on LIT rods and endcaps take place in this simulation step.

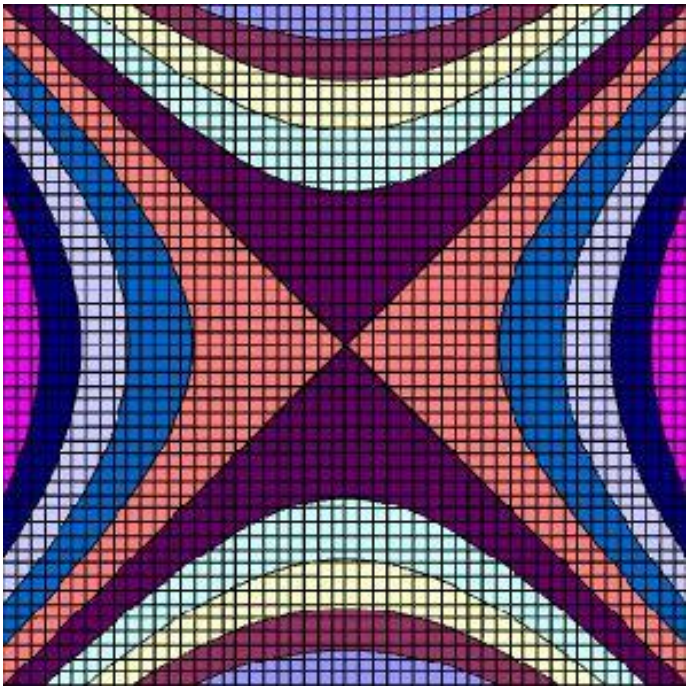

Figure 5.14: LIT2 equipotential contours at the center of a hyperbolic LIT.

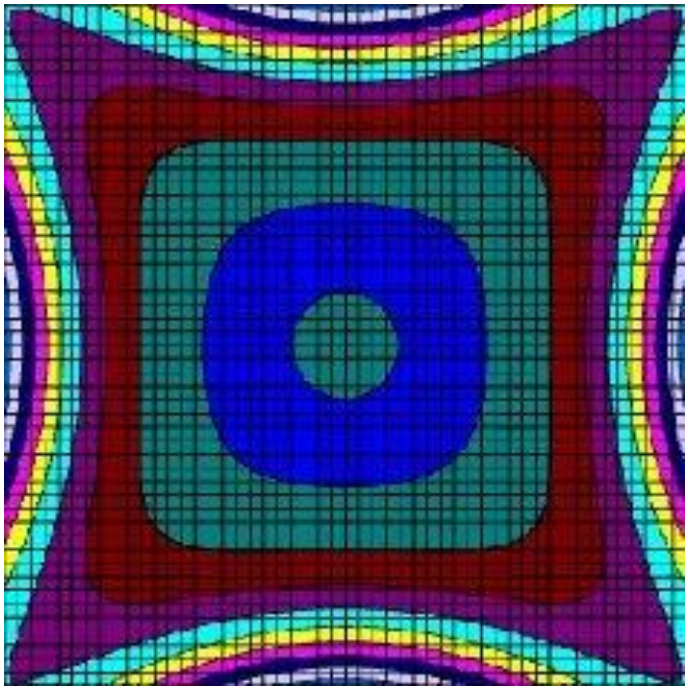

Figure 5.15: LIT2 equipotential contours at the ends of a hyperbolic LIT.

5.3.2.1. LIT2 simulations for cocaine and TNT characteristic ions

The LIT2 simulation work described in this subsection followed the below parameters for ion motion (Figure 5.16 presents the main LIT2 command window):

a. Ion masses: *m/z* 182 and 304 for cocaine; *m/z* 210 and 227 for TNT,
b. Total number of created ions: 100,000,
c. Average ion injection energy: 5 eV before the entrance endcap electrode,
d. Buffer gas: helium gas at room temperature (300 K),
e. LIT r_0: 2.5 mm with RF drive frequency at 1 MHz,
f. Timings: 1 ms ion injection, 1 ms ion trapping and 8 ms ion ejection,
g. Rod voltages: UV ratio at 60% for trapping and 99% for mass isolation,
h. Endcap voltages: 20V for injection/trapping, -100V on exit for ejection.

As it can be observed from the outcomes of this simulation work, small endcap electrode aperture radius (r_a=0.2*r_o) provide better ion trapping, which results in higher sensitivity (Figure 5.17). Moreover, as it is shown in Figure 5.18, the distance between endcap and rod electrodes has significant effect on LIT trapping efficiency.

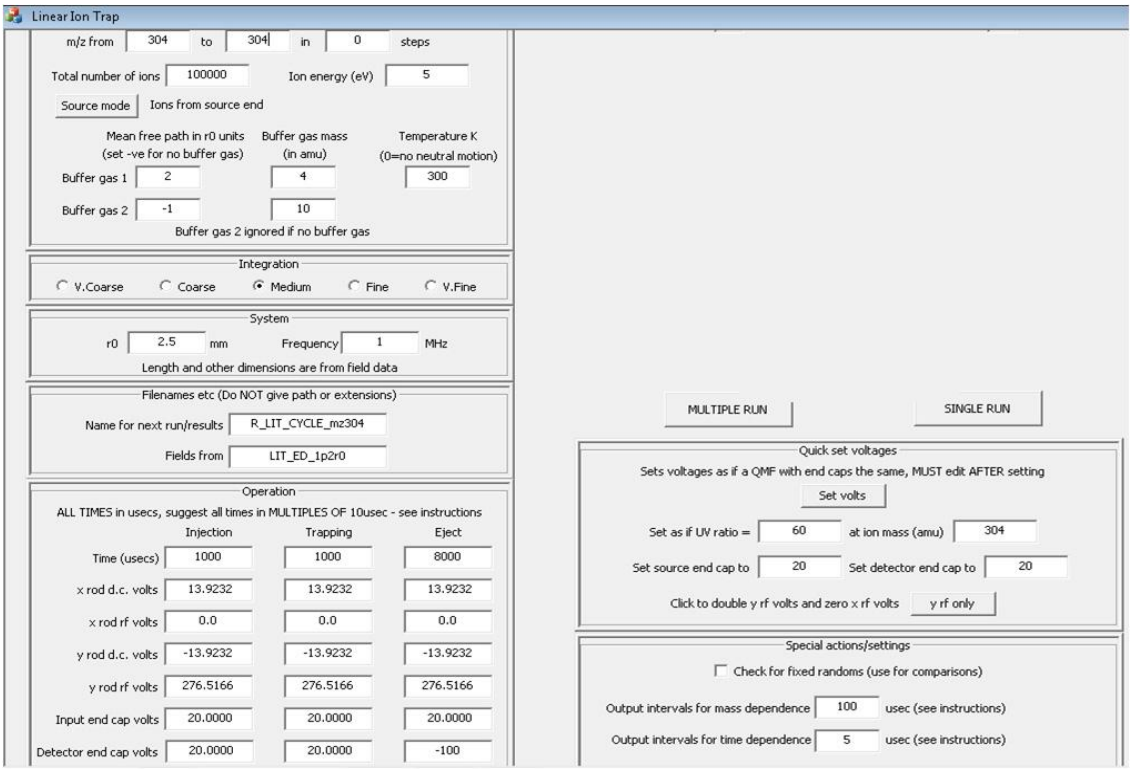

Figure 5.16: Sample screenshot of LIT2 main window for defining parameters for ion motion. Integration levels are also included and they range from very coarse to very fine.

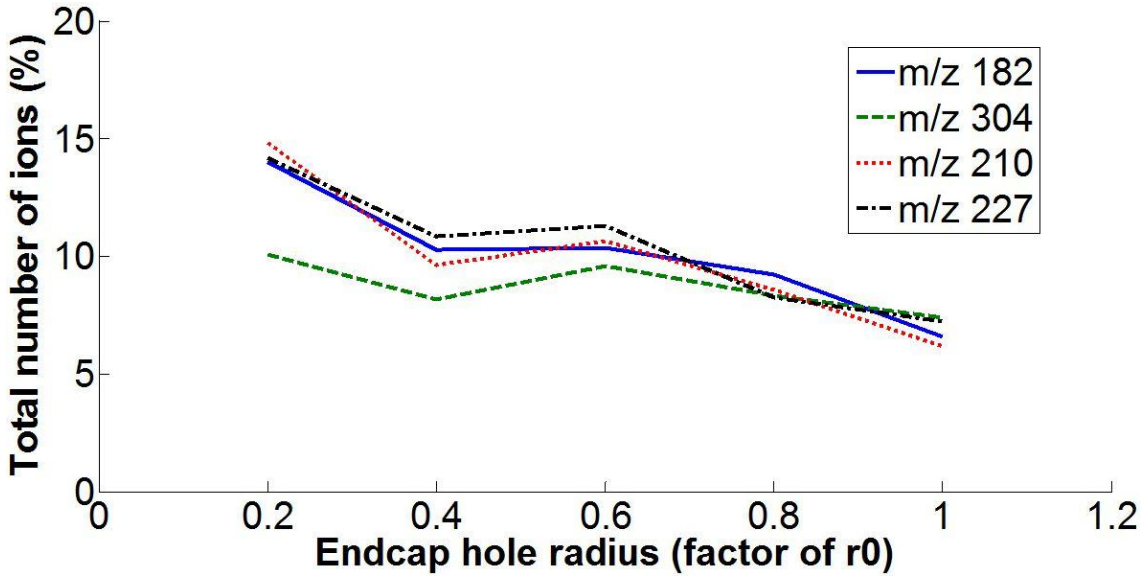

Figure 5.17: Total number of trapped ions for cocaine (*m/z* 182, 304) and TNT (*m/z* 210, 227) mass fragments, with variation of aperture radius on LIT endcap electrodes between $0.2r_0$ and r_0. UV ratio was at 60%.

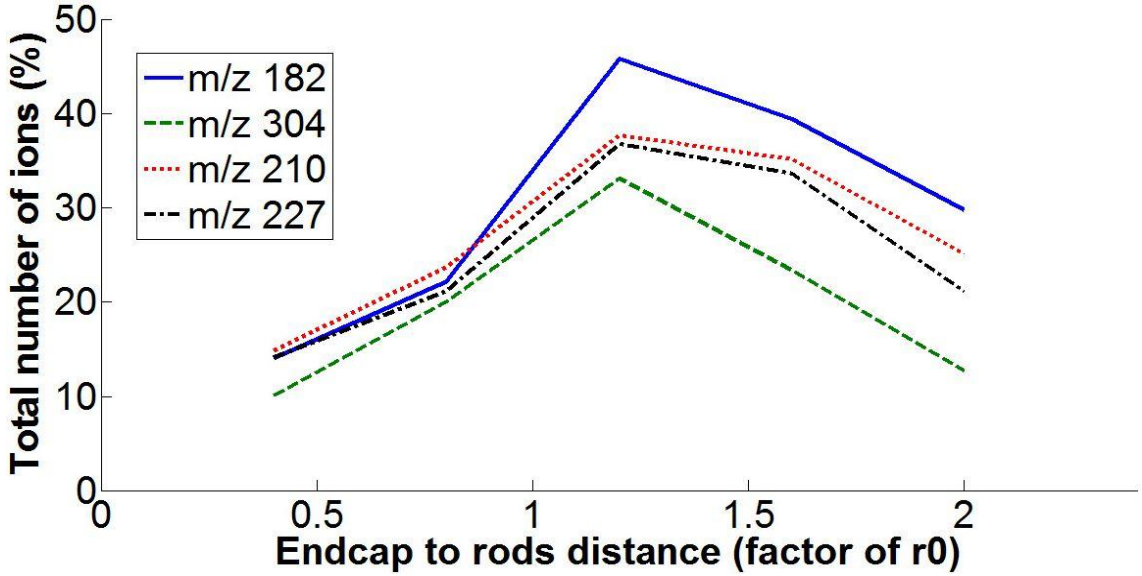

Figure 5.18: Total number of trapped ions for cocaine (*m/z* 182, 304) and TNT (*m/z* 210, 227) mass fragments, with variation of distances between endcap and rod electrodes between $0.4r_0$ and $2r_0$. UV ratio was at 60%.

From simulations investigating lengths variations of the LIT rod electrodes, it was found that longer LIT rod length is generally better for greater ion capacity and trapping efficiency. This can be observed in Figure 5.19 where optimum ion trapping for cocaine and TNT ions can be achieved by LIT rods longer than $48r_o$. This LIT rod length ($48r_0$ = 120mm) was then used to further calculate cocaine mass peak resolution at *m/z* 304.

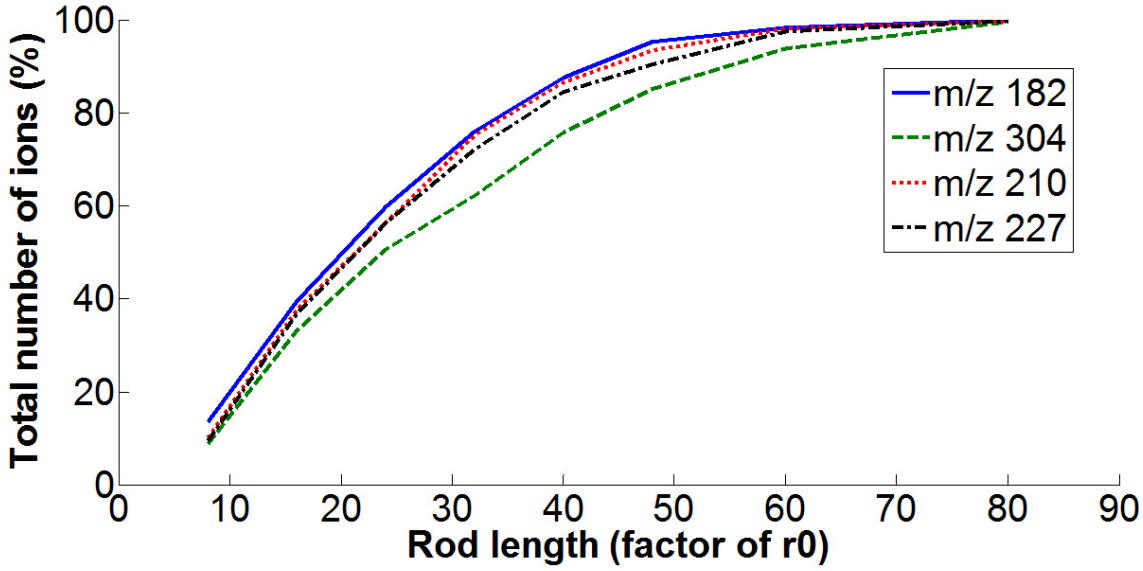

Figure 5.19: Total number of trapped ions for cocaine (*m/z* 182, 304) and TNT (*m/z* 210, 227) mass fragments, with variation of lengths of rod electrodes between $8r_0$ and $80r_0$. UV ratio was at 60%.

Results showed that 2 Th is currently the narrowest mass window width that can be achieved in a non-scanning LIT (Figure 5.20). Thomson unit (Th) was proposed by Prof Cooks and Rockwood, in honor of J. J. Thomson, as a unit of m/z ratio.

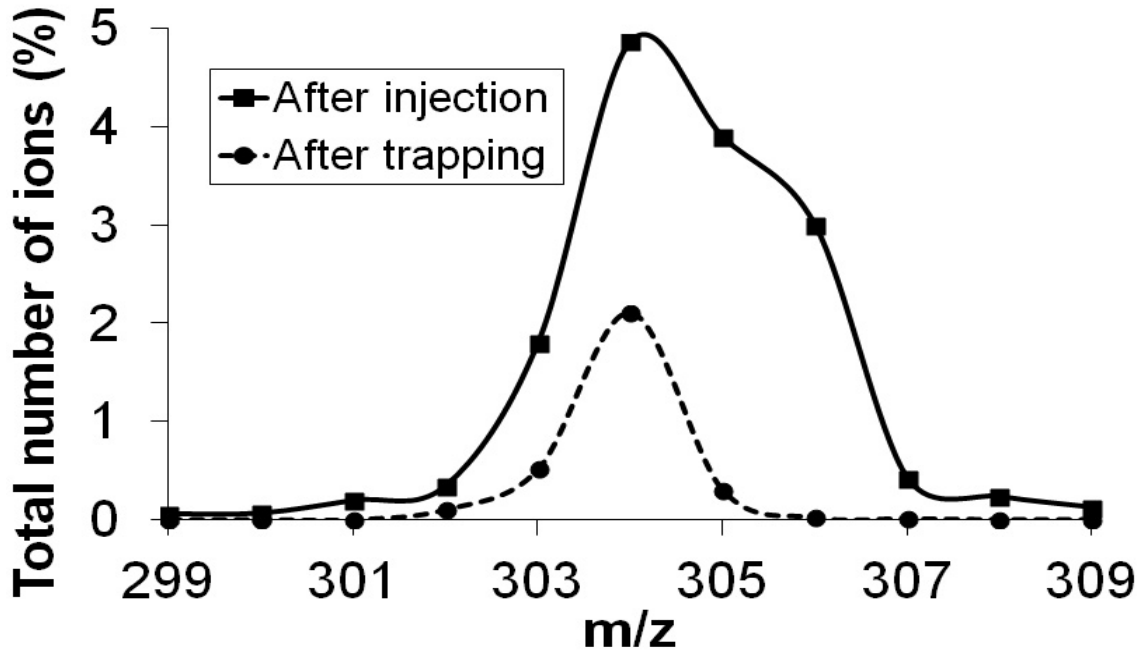

Figure 5.20: Mass window isolation of cocaine fragment *m/z* 304 after 1 ms injection time and 1 ms trapping time. UV ratio was at 99%. LIT rod length was $48r_0$

5.4. Non-scanning LIT experiments

5.4.1. Experimental setup

Selective mass isolation in a non-scanning mode has been done experimentally using hyperbolic LIT fabricated by the University of Liverpool with the design shown in Figure 5.1. The tested LIT was built using CNC machining with electrodes made from stainless steel and electrode holders made from ceramic resin (Figure 5.21). The length of *x*- and *y*-electrodes was 40 mm with 2.5 mm r_0. The z-electrodes were 0.4 mm thick discs separated from *x*,*y*-electrodes by 0.8 mm with 2.5 mm aperture radius. A commercial dual thoria filament electron impact ion source was used (SS Scientific Ltd, UK) that was close coupled to LIT providing external ion injection. The detector was a channeltron type electron multiplier (Burle, US). Data acquisition was obtained using in-house made charge amplifier connected to oscilloscope.

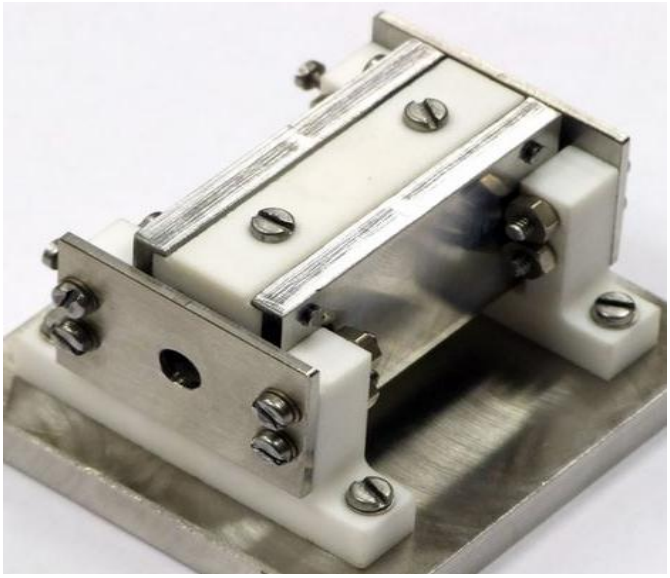

Figure 5.21: Hyperbolic LIT fabricated using computer numerical control (CNC) machining by University of Liverpool

5.4.2. Experimental results

For the experimental mass isolation of Kr-84 and Xe-131 ions, the following parameters were used:

- Ion source: 100 µA electron emission current with 2.2 A filament current and -20 V applied to the repeller/filament common; 100 ms ionization time.
- LIT: *x*-electrodes: negative DC bias of -4.2 V for Kr-84 and -6.5 V for Xe-131; y-electrodes: positive DC bias of 4.2 V for Kr-84 and 6.5 V for Xe-131, RF amplitude of 196 V_{p-p} for Kr-84 and 304 V_{p-p} for Xe-131 at 1.14 MHz RF drive frequency; *z*-electrodes: entrance endplate at 0 V during ion injection, and at 20 V during ion trapping and ejection, exit endplate at 20 V during ion injection and trapping, and at -100 V during ion ejection; 1 ms ion trapping time; 300 ms ion ejection time.
- Detector: multiplier voltage at -1000 V for isolation of both Kr-84 and Xe-131.
- Pressure: typically up to 10^{-4} Torr with a sample gas and helium buffer gas added for optimal signal intensity.

Figure 5.22 shows peak intensities for Kr-84 and Xe-131 with mass isolation window width of 6 Th. Upper and lower mass limits of the window were identified by increasing and decreasing RF/DC voltage levels until the mass peak disappeared. The time to completely eject trapped ion masses was 7.5 ms within specified ejection time of 300 ms. With further RF/DC fine adjustments, the mass window width could be reduced to 4 Th, but not much lower. This is because mass peak disappears when RF and DC voltages are very near the tip of the stability diagram. Sensitivity improvement through increase of ionization time could be seen up to 100 ms, while longer ionization times did not give any enhancement in sensitivity. Further enhancement of sensitivity is possible through maximising number of ions injected into LIT and better ion focusing.

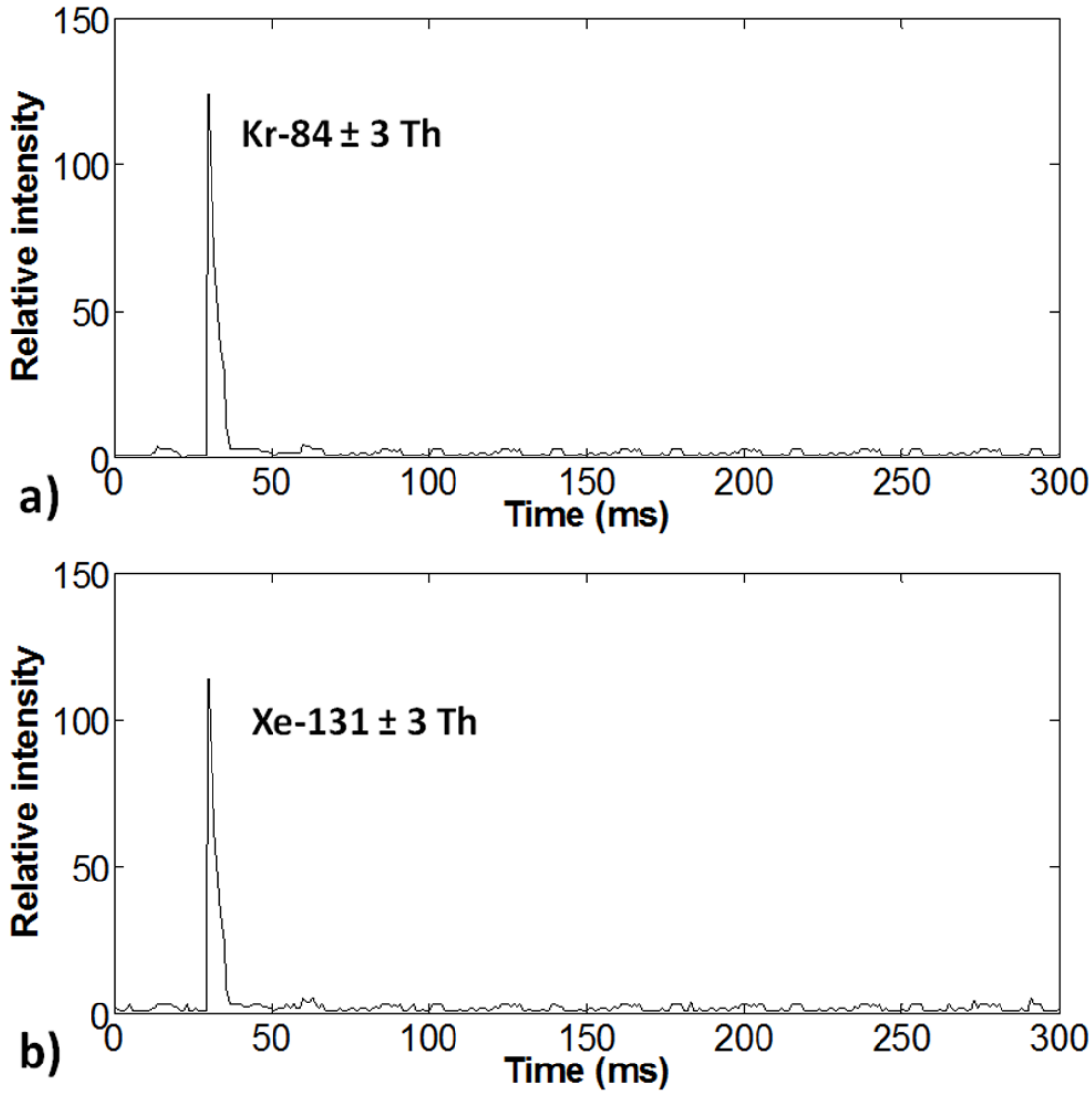

Figure 5.22: Experimental selective mass isolation for a) Kr-84 and b) Xe-131 within CNC linear ion trap operating in a non-scanning mode. The mass window width obtained is 6 Th.

5.5. Conclusions

Simulation results have shown considerable improvement in analyzer sensitivity by altering geometrical parameters of the ion source lens system coupled to a non-scanning linear ion trap. It was found that smaller lens aperture size was generally better for sensitivity, but not too small as ion transmission would be significantly reduced. Separation of the ion deceleration lens from the trap showed a moderate change in sensitivity. Distance alteration of the ion focusing lens had high impact on sensitivity

with moderate lens separation shown to be the optimal one. Extract lens separation showed considerable change in sensitivity with minimal separation proven to be the best. With optimized lens distances, lower focusing voltages will be required, which will lead to lower ion injection energies and higher sensitivity. An optimized lens system also shows improvement in sensitivity by a factor of 4 compared to standard lens systems that have larger aperture sizes and minimal lens separations.

A novel built in house simulation package (LIT2) for modeling linear ion traps with high accuracy was also described and demonstrated. Simulation results for optimization of ion trapping in linear ion traps by varying endcap electrodes hole radii, distances between endcaps and rod electrodes, and rod lengths have been presented. It was found that small endcap electrode aperture radius provides better ion injection and trapping and that the distance between endcap and rod electrodes has significant effect on LIT trapping efficiency. Moreover, LIT rods length affects ion capacity and trapping efficiency. Current simulation results showed that 2 Th is the narrowest mass window width that can be achieved in a non-scanning LIT whereas resolution improvement to 1 Th or less is planned to be done by adding a small DC ramp option to the software during trapping sequence. Future work will also involve LIT simulations with other rod geometries (circular and square) and electrode displacements.

5.6. References

[1] A. Keil, H. Hernandez-Soto, R. J. Noll, M. Fico, L. Gao, Z. Ouyang, R. G. Cooks, *Monitoring of toxic compounds in air using a handheld rectilinear ion trap mass spectrometer,* Anal. Chem. **80,** 734-741 (2008).

[2] B. Brkić, N. France, S. Taylor, *Oil-in-water monitoring using membrane inlet mass spectrometry,* Anal. Chem. **83,** 6230-6236 (2011).

[3] A. Keil, N. Talaty, C. Janfelt, R. J. Noll, L. Gao, Z. Ouyang, R. G. Cooks, *Ambient mass spectrometry with a handheld mass spectrometer at high pressure,* Anal. Chem. **79,** 7734-7739 (2007).

[4] N. Talaty, C. C. Mulligan, D. R. Justes, A.U. Jackson, R. J. Noll, R. G. Cooks, *Fabric analysis by ambient mass spectrometry for explosives and drugs,* Analyst **133,** 1532-1540 (2008).

[5] S. Taylor, R. F. Tindall, R. R. A. Syms, *Silicon based quadrupole mass spectrometry using microelectromechanical systems,* J. Vac. Sci. Technol. B **19,** 557-562 (2001).

[6] B. Brkić, N. France, A. T. Clare, C. J. Sutcliffe, P. R. Chalker, S. Taylor, *Development of Quadrupole Mass Spectrometers Using Rapid Prototyping Technology,* J. Am. Soc. Mass Spectrom. **20,** 1359-1365 (2009).

[7] K. Cheung, L. F. Velásquez-García, A. I. Akinwande, *Chip-scale quadrupole mass filters for portable mass spectrometry,* IEEE J. Microelectromech. Syst. **19,** 469-483 (2010).

[8] D. Cruz, J. P. Chang, M. Fico, A. J. Guymon, D. E. Austin, M. G. Blain, *Design, microfabrication, and analysis of micrometer-sized cylindrical ion trap arrays,* Rev. Sci. Instrum. **78,** 015107 (2007).

[9] A. T. Clare, L. Gao, B. Brkić, P. R. Chalker, S. Taylor, *Linear Ion Trap Fabricated Using Rapid Manufacturing Technology,* J. Am. Soc. Mass Spectrom. **21,** 317-322 (2010).

[10] J. D. Maas, P. I. Hendricks, Z. Ouyang, R. G. Cooks, W. J. Chappell, *Miniature monolithic rectilinear ion trap arrays by stereolithography on printed circuit board,* IEEE J. Microelectromech. Syst. **19,** 951-960 (2010).

[11] H. J. Yoon, J. H. Kim, E. S. Choi, S. S. Yang, K. W. Jung, *Fabrication of a novel micro time-of-flight mass spectrometer,* Sens. Actuators A **97-98,** 441-447 (2002).

[12] E. Wapelhorst, J. P. Hauschild, J. Müller, *Complex MEMS: a fully integrated TOF micro mass spectrometer,* Sens. Actuators A **138,** 22-27 (2007).

[13] S. Shimma, H. Nagao, J. Aoki, K. Takahashi, S. Miki, M. Toyoda, *Miniaturized high-resolution time-of-flight mass spectrometer MULTUM-S II with an infinite flight path,* Anal. Chem. **82,** 8456-8463 (2010).

[14] D. J. Douglas, A. J. Frank, D. Mao, *Linear ion traps in mass spectrometry,* Mass Spec. Rev. **24,** 1-29 (2005).

[15] Y. Hashimoto, H. Hasegawa, T. Baba, I. Waki, *Mass Selective Ejection by Axial Resonant Excitation from a Linear Ion Trap,* J. Am. Soc. Mass Spectrom. **17,** 685-690 (2006).

[16] J. W. Hager, *Off-Resonance Excitation in a Linear Ion Trap,* J. Am. Soc. Mass Spectrom. **20,** 443-450 (2009).

[17] M. Guna, T. A. Biesenthal, *Performance Enhancements of Mass Selective Axial Ejection from a Linear Ion Trap,* J. Am. Soc. Mass Spectrom. **20,** 1132-1140 (2009).

[18] J. C. Schwartz, M. W. Senko, J. E. P. Syka, *A two-dimensional quadrupole ion trap mass spectrometer,* J. Am. Soc. Mass Spectrom. **13,** 659-669 (2002).

[19] F. A. Londry, J. W. Hager, *Mass Selective axial ion ejection from a linear quadrupole ion trap,* J. Am. Soc. Mass Spectrom. **14,** 1130-1147 (2003).

[20] C. Zhang, H. Chen, A. J. Guymon, G. Wu, R.G. Cooks, Z. Ouyang, *Instrumentation and methods for ion and reaction monitoring using a non-scanning rectilinear ion trap,* Int. J. Mass Spectrom. **255-256,** 1-10 (2006).

[21] P. H. Dawson, *Quadrupole mass analyzers: Performance, design and some recent applications,* Mass Spec. Rev. **5,** 1-37 (1986).

[22] F. H. Read, N. J. Bowring, *The CPO programs and BEM for charged particle optics,* Nucl. Instr. Meth. Phys. Res. A **645,** 273-277 (2011).

[23] B. Brkić, S. Taylor, J. F. Ralph, N. France, *High-fidelity simulations of ion trajectories in miniature ion traps using the boundary-element method,* Phys. Rev. A **73,** 012326, 1-6 (2006).

[24] A. Renau, F. H. Read, J.N. H. Brunt, *The charge-density method of solving electrostatic problems with and without the inclusion of space-charge,* J. Phys. E: Sci. Instrum. **15,** 347-354 (1982).

Chapter 6
Optimised non-scanning linear ion trap mass spectrometer

6.1. Introduction

For in-field applications that require analysis of specific molecules, simple and low cost portable mass spectrometers are highly suitable [1-6]. When analysis of application-targeted molecules is required, the use of a non-scanning mass spectrometer is highly recommended. This is because a non-scanning mass spectrometer performs selective ion monitoring with optimal voltages for each ion mass without having to obtain a full mass spectrum [7, 8]. A result of such operation mode is higher sensitivity, simpler control electronics, smaller size, lower power consumption and cost.

Apart from simplicity and cost savings with electronics for a non-scanning mass spectrometer, manufacturing of mass analyzers can also be simplified at significantly lower cost than with conventional techniques. Previous work has demonstrated design, fabrication and proof of concept for using digital light processing (DLP) technique to implement polymer-based quadrupole mass filter (QMF) [9] and linear ion trap (LIT) [10] with hyperbolic rods. DLP is a rapid prototyping (RP) technique that uses dynamic masking capability to selectively cure a photosensitive polymer resin, which enables fabrication of complicated 3D structures. Modern DLP machines also have enhanced resolution mode (ERM) that further improves surface quality and can provide nanoscale surface roughness. Compared to stereolithography (SLA), another RP technique used for polymer-based rectilinear ion traps [11-13], DLP provides better manufacturing accuracy and surface smoothness. This is because DLP has much smaller volumetric pixels (≈ 15 μm x 15 μm x 25 μm) compared to SLA tracks width (≈ 200 μm) and ERM capability for improving surface quality. Due to these advantages, our work has focused on rapid manufacturing of analyzers with hyperbolic electrodes that provide the ideal quadrupole electric field and therefore optimal performance of an analyzer [14, 15].

Previous DLP QMF and LIT were made using polymethylmethacrylate (PMMA), which gave accurate and smooth electrodes. However, some level of outgassing under vacuum was noticed during previous QMF tests from PMMA [9], which resulted in an unwanted pressure increase. For those ion traps that operate at higher pressures than quadrupole mass spectrometers and use buffer gas for ion cooling, outgassing could be further increased and affect mass analysis. Therefore, PMMA has been replaced with ceramic-filled resin (HTM140), which has higher heat deflection temperature (HDT) and lower outgassing rate. The HDT for HTM140 is 140°C straight out of the machine without performing any UV and thermal post cure processes that would increase it further, while it is 75 °C for PMMA [16]. Another important issue for a polymer-based analyzer is high quality of metal coating on electrodes, which is essential for a commercial instrument. Types of coating used on previous analyzer prototypes are evaporative and sputter processes that deposit gold directly on polymer electrodes. Even though such coatings provided very good conductivity on the rods, gold deposits would start to wear out over time. This affects dielectric constant and capacitance between the RF rods, which could cause instability of RF voltages and errors in mass analysis. For these reasons, polymer electrodes were coated using specially adapted electroplating process for plastic structures. Coating included thick base layer of copper and nickel with thin layer of high gloss gold, which provided very firm attachment of metal layers to the rods and excellent electrical conductivity.

The following section describes experimental characteristics of a non-scanning LIT, DLP machining, electroplating process and experimental setup for tests with a non-scanning DLP LIT. Results and discussion are given for optimized DLP LIT prototype, outgassing tests with HTM140 polymer, and experiments with DLP LIT for detection of key mass fragments in simulants for cocaine, TNT and sarin.

6.2. Non-scanning linear ion trap

Theory of non-scanning LIT mass spectrometry has been described in detail in Chapter 5, section 5.2. The reader is referred to Figure 5.1 that shows a schematic diagram of a non-scanning LIT consisting of four hyperbolic rod electrodes for radial (x,y) ion confinement and two disc endcap electrodes for axial (z) confinement.

6.2.1. DLP manufacture

A typical fabrication procedure in a DLP machine (Figure 6.1) consists of the following steps:

a) CAD model is loaded into a machine and processed using its software,

b) Model is vertically sliced into a series of individual layers of 25 µm thickness,

c) Direct light projector projects a mask of the slice to be processed using a digital micromirror device (DMD),

d) Polymer resin is selectively cured to form cross section of part,

e) Build substrate moves up by 25 µm,

f) Procedure is repeated until all slices are processed.

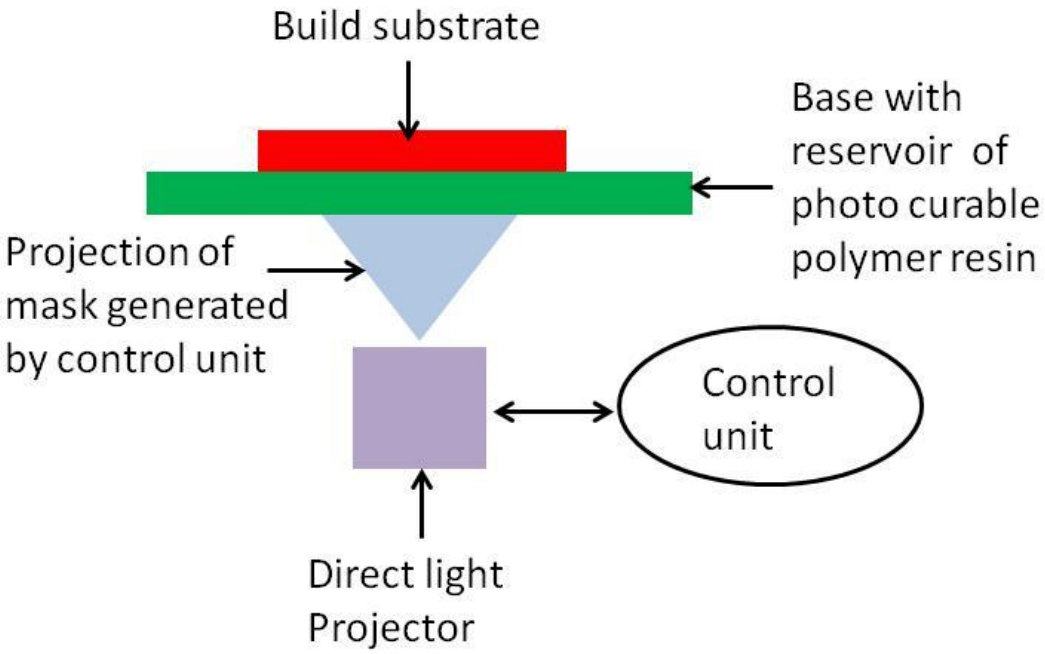

Figure 6.1: Main components of a DLP machine

The DLP machine used for LIT manufacturing was the Envisiontec Perfactory 3 Mini Multi Lens with ERM (Figure 6.2). It uses 700 mW/dm^2 of visible light at 25 µm layers. The smallest ERM voxel size is 16 µm and the maximum build envelope available is 84 mm x 63 mm x 230 mm. The build time of structures is not dependent on the number/size of parts, but only on the height of the parts. Manufacture of multiple DLP LIT parts (see Figure 6.4a) takes approximately 11 hours.

Figure 6.2: Envisiontec Perfactory Mini Type III for Multi Lens use with ERM

6.2.2. Electroplating process

The Metalise™ process from 3DDC Ltd, UK was used for the metallic coating of DLP LIT rod electrodes. This method has been specifically developed for plastic components that have been produced via additive manufacturing. The DLP electrodes were initially pre-processed using a fine sanding procedure. The surface roughness of the parts was further reduced to allow for the electroplating process to be carried out, and therefore achieving the best results. For the LIT electrode application, a thick layer of copper and nickel (130 μm) was first applied before the final coating with high gloss gold (0.3 μm). The hyperbolic top surfaces of the electrodes were then polished smooth for best performance. This coating technique is a specially adapted electroplating process, where electrical current is applied to an anode and cathode both placed into an electrolytic solution. In this case, the cathode is the DLP electrode and the anode would be either a sacrificial anode or an inert anode. Material is transferred from the anode to the cathode and over time the cathode is plated. The electroplating process is summarized in Figure 6.3.

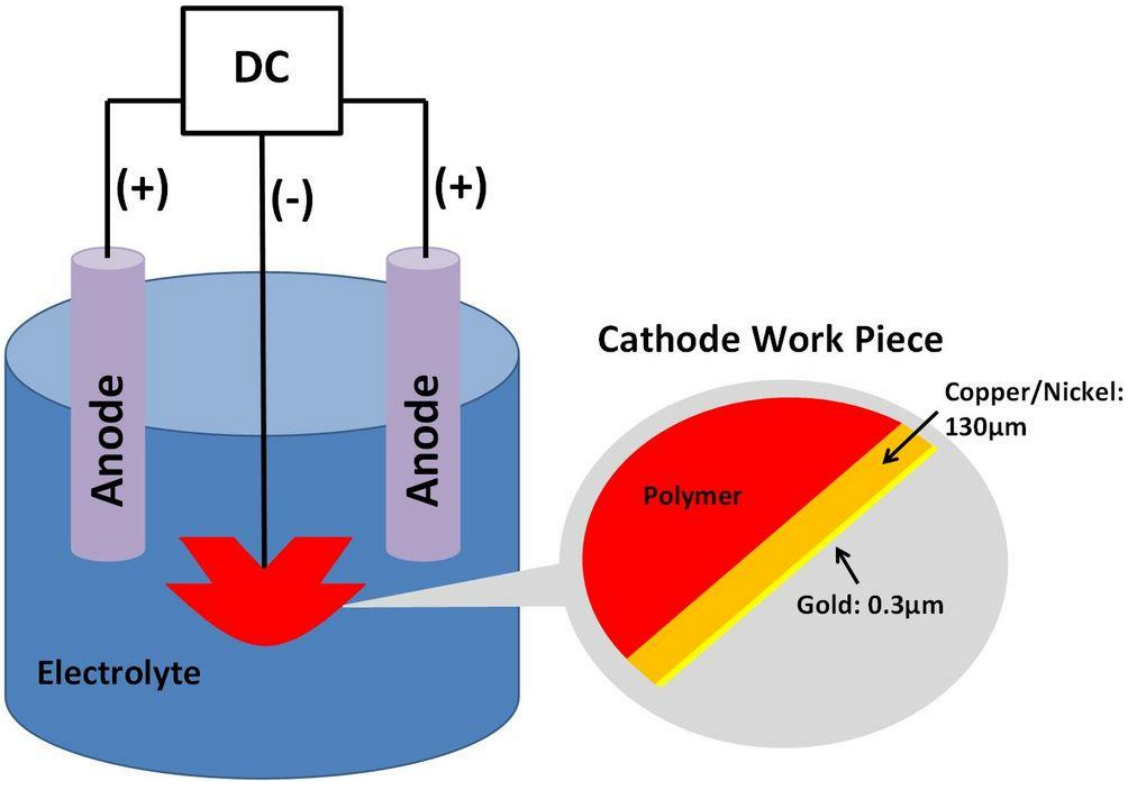

Figure 6.3: Schematic diagram of electroplating process used for enhanced coating of DLP linear ion trap.

6.2.3. DLP LIT fabrication

For accurate alignment and fitting of DLP LIT electrodes, a stack of rods and housings were designed and fabricated with different tolerances for choosing the right match. This is summarized in Figure 6.4a showing defined geometries for rods and housings on a build envelope of the DLP machine. Compared to conventional methods, this method is fast and cost effective for obtaining desired inter-electrode distance ($2r_0$) and alignment. As can be seen in Figure 6.4b, grooves in housing for the rods are made slightly larger to accommodate electroplated rods with thick coating and maintain their separation. Top part of the housing has slightly reduced outer diameter to accommodate base holder for entrance endcap and ion source. The bottom part of the housing has diameter adjusted to the size of insulating adaptor, which provides separation between the exit endcap and multiplier shielding tube. The length of DLP LIT rods is 40 mm with 2.5 mm r_0. Endcaps are 0.4 mm thick discs separated from the rods by 0.8 mm with 1.5 mm aperture radius. Due to low manufacturing costs for simple disc electrodes, endcaps are made from stainless steel using conventional engineering, while DLP is

kept for complicated electrode shapes and isolation parts. Figure 6.4c shows high quality electroplated LIT rods with thick layer of copper/nickel (130 μm) and thin layer of gold (0.3 μm). Rods are slid into the housing with a tight fit and additionally supported with miniature screws for electrical contact for which holes are made in the housing. Resistance on electroplated DLP rods from top to bottom is less than 0.01 Ω. Measured capacitance between *x* and *y*-electrodes is 13.6 pF.

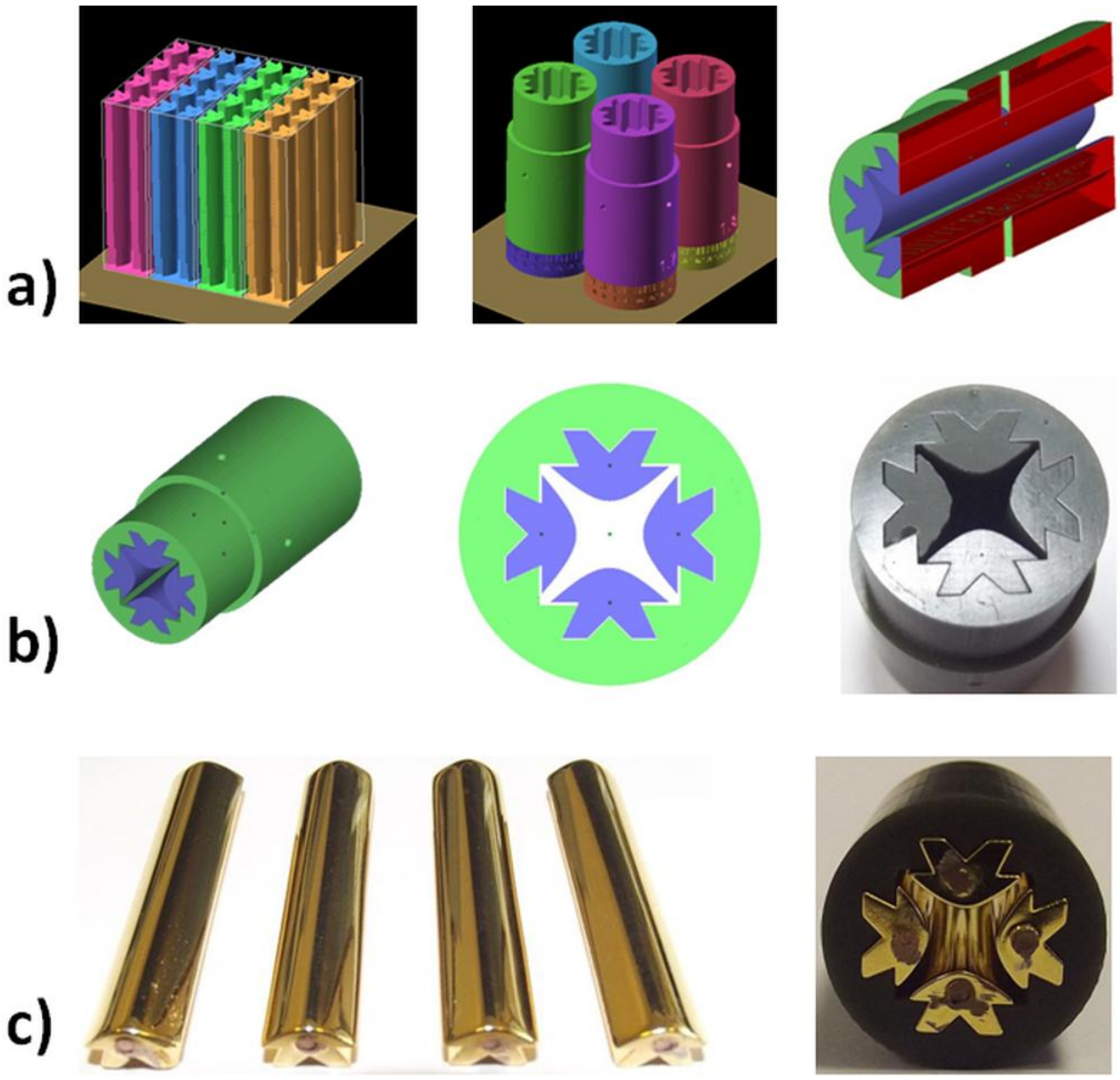

Figure 6.4: Design, fabrication and assembly of DLP linear ion trap: a) fabrication design stack of DLP LIT rods and housings on a machine build envelope with vertical cross section of LIT assembly, b) fabrication design of LIT assembly with non-coated prototype, c) electroplated LIT rods and final rod assembly in ceramic resin housing.

6.2.4. DLP LIT outgassing tests

Outgassing molecules from polymer resin materials mainly include water vapours and atmospheric gases [17]. The outgassing levels of these molecules change with different surrounding temperatures. Since the housing of the DLP LIT is always exposed to some level of heat (e.g. radiated from vacuum system or EI ion source), outgassing tests were performed with a DLP sample in a heated chamber. Tests were done at 50 and 100 °C temperatures, even though 100 °C is higher than the temperature to which DLP LIT is exposed during operation. Table 6.1 shows outgassing levels of typical air gases when HTM140 material is exposed to heat. Results are for a chamber with HTM140 after 30 min of degassing at 50 and 100 °C. Gas levels were measured using a single filter quadrupole mass spectrometer. After temperature exposure, no water levels were seen and very low levels of hydrogen were present.

Table 6.1: Outgassing tests with HTM140 material at 50 and 100 °C temperatures.

	Gas presence after 30 min of degassing at 50°C (%)	**Gas presence after 30 min of degassing at 100°C (%)**
H_2	0.79	1.15
He	0	0
CO	0	0
N_2	65.55	63.51
CH_4	0.27	0.47
H_2O	0	0
O_2	0	0
Ar	1.23	1.02
CO_2	32.16	33.85
Kr	0	0
TOTAL	100	100

As expected, nitrogen and carbon dioxide were the most abundant gases with argon and methane present in low amounts. No traces of helium, carbon monoxide, oxygen and krypton were seen after temperature degassing. It can be seen that there are minor differences between degassing of air molecules for 50 and 100 °C temperatures. When

it comes to pressure changes in the vacuum chamber, only a small rise in base pressure was seen – from 5 x 10^{-6} Torr with a blank chamber to 7 x 10^{-6} Torr with HTM140 LIT inside. On the other hand, base pressure with PMMA LIT went up to 2 x 10^{-5} Torr, which shows more significant outgassing and less room for adding sample and buffer gas. Therefore, in terms of analyzer sensitivity, overall operation and usage in a commercial system, HTM140 is a better choice than PMMA.

6.3. Portable pre-prototype LIT-MS system

6.3.1. Specification

The portable LIT-MS sniffer described in this subsection was developed in the framework of a EU funded research project entitled Sniffles [18]. Liverpool portable pre-prototype LIT-MS system (Figure 6.5) was designed to address the following technical characteristics:

a. Mass analyser: non-scanning LIT,
b. Mass range: up to m/z 500,
c. Resolution: 4 Th,
d. Power: 75 W,
e. Size: 62 cm x 49 cm x 22 cm,
f. Weight: 14 kg.

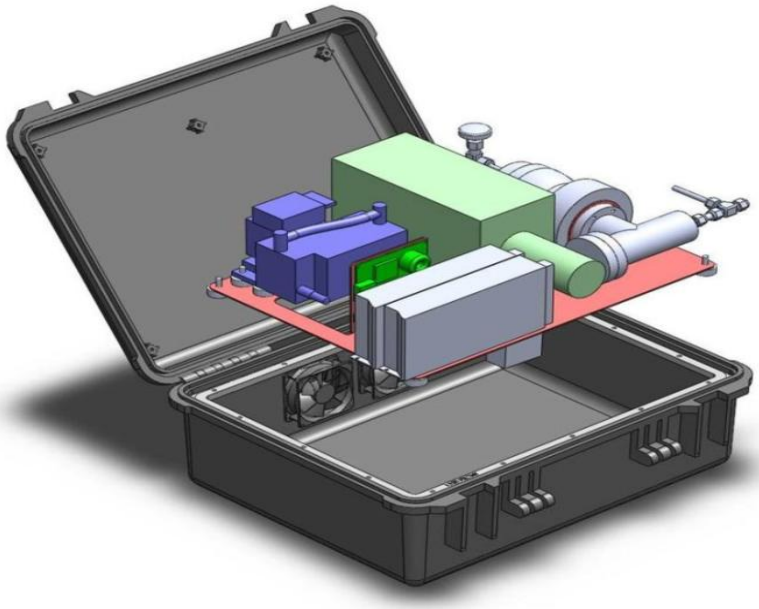

Figure 6.5: Schematic drawing of Liverpool's LIT-MS portable artificial sniffer.

Liverpool artificial sniffer aims to assist border control and civil defence authorities by offering high accuracy and high sensitivity field chemical analysis with fast response times, a user friendly graphical interface and low maintenance costs. The main target components for on-site detection and on-line monitoring include illegal or hazardous substances such as drugs, explosives and chemical warfare agents (CWAs).

6.3.2. System architecture

Figure 6.6 describes how the operator of our artificial sniffer communicates via the incorporated on the case tablet computer with our beta electronic control unit (ECU) and with the LIT-MS including the system's main support parts (sample inlet components e.g. preconcentrator, pulsed sampling system, etc.). The preconcentrator operating principle is based on two stage absorption/desorption process. Sample absorption takes place on a tube filled with sorbent material capable of collecting compounds of interest and then thermally desorb them into the MS vacuum chamber for analysis. The end user of the portable MS device can be informed of threat presence on the screen of the tablet by specific alarm signs.

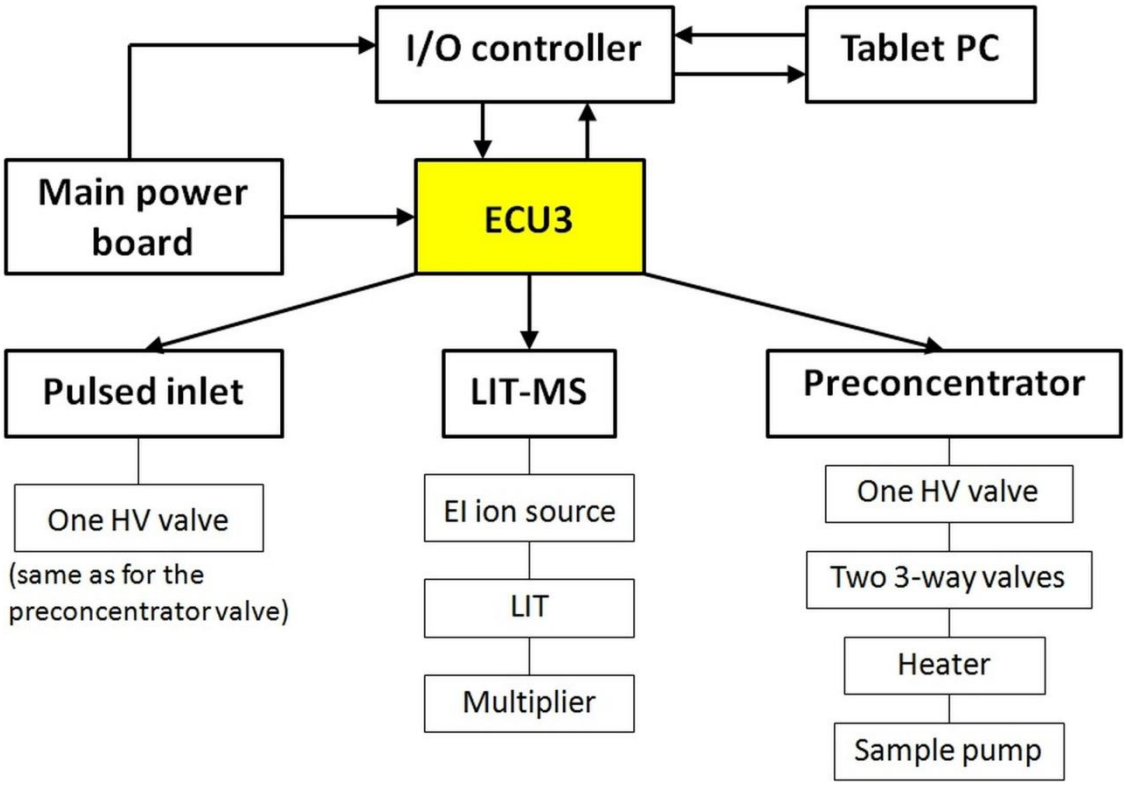

Figure 6.6: LIT-MS sniffer device general communication scheme with the operator.

6.3.3. System integration

The main parts of UoL's pre-prototype LIT-MS system are presented in Figure 6.7 and Figure 6.8. Our artificial sniffer consists of the following components (approximate weights are given in brackets next to each individual part):

a. Case: Peli case with dimensions 62 cm x 49 cm x 22 cm (6 kg),
b. LIT-MS: EI ion source, DLP LIT, EM detector, CF40 flange (0.5 kg),
c. Vacuum chamber: miniature tube and adaptor (1 kg),
d. Vacuum system: miniature Pfeiffer's diaphragm and turbo pumps (3.5 kg),
e. Electronics: flexible electronic control unit - ECU (1.5 kg),
f. Power supply: 24 V mains for vacuum system, electronics and pressure gauge (0.75 kg),
g. Support components: inlet, digital pressure gauge, cables (0.75 kg),

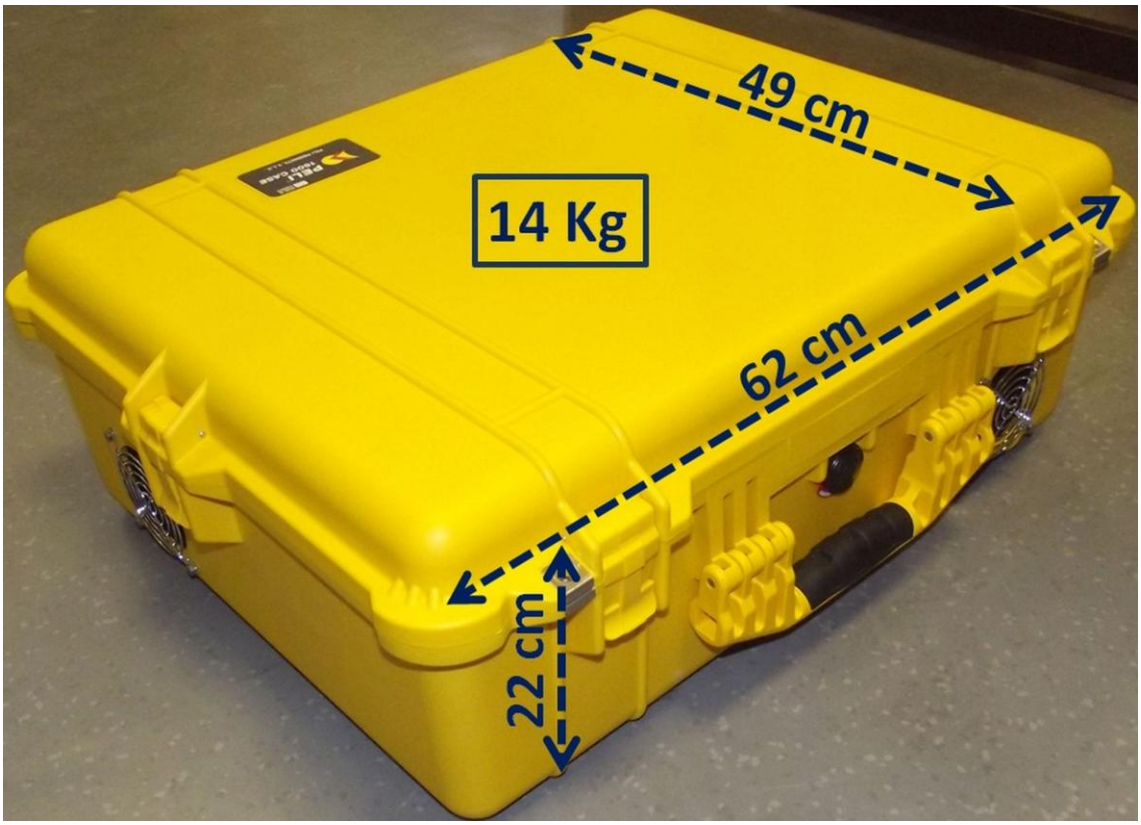

Figure 6.7: External view of the UoL's pre-prototype LIT-MS.

The main components of the LIT-MS are: the electron impact (EI) ion source, the DLP LIT and the electron multiplier (EM) detector on a CF40 flange (Figure 6.9).

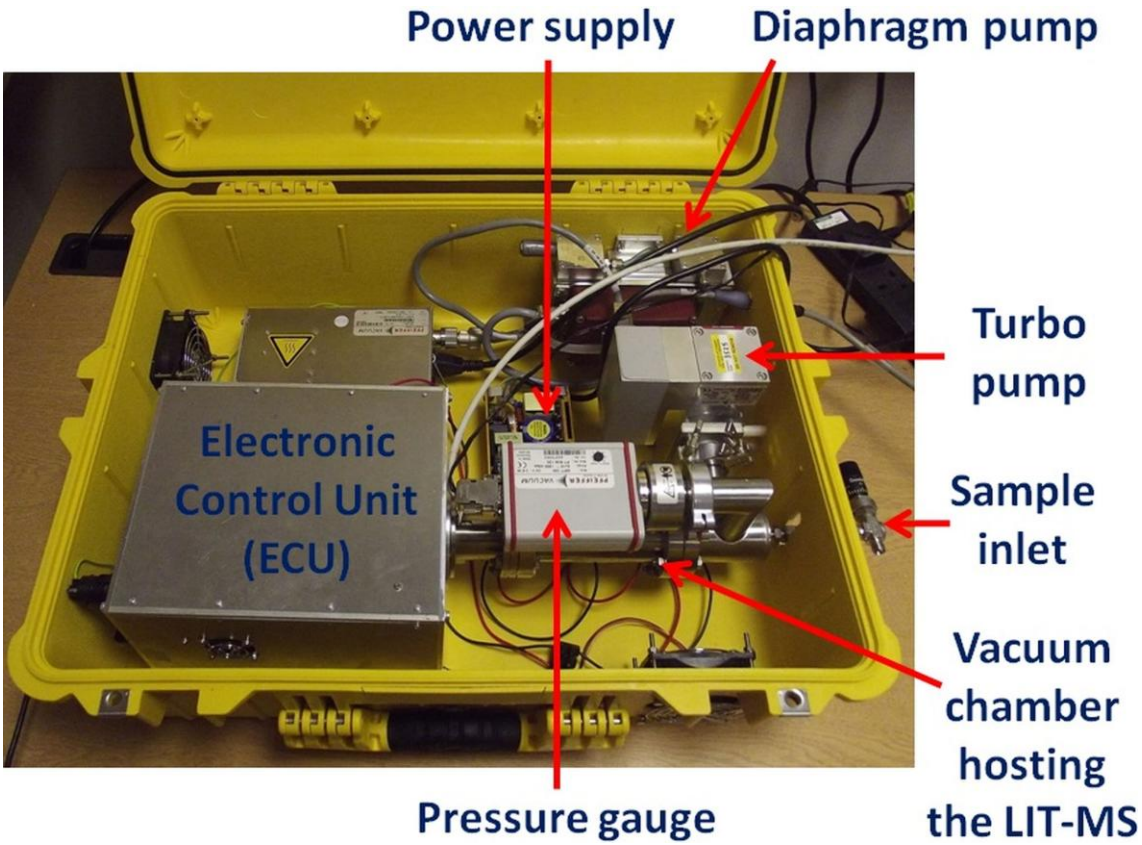

Figure 6.8: Internal view of the UoL's pre-prototype LIT-MS system operating in a non scanning mode.

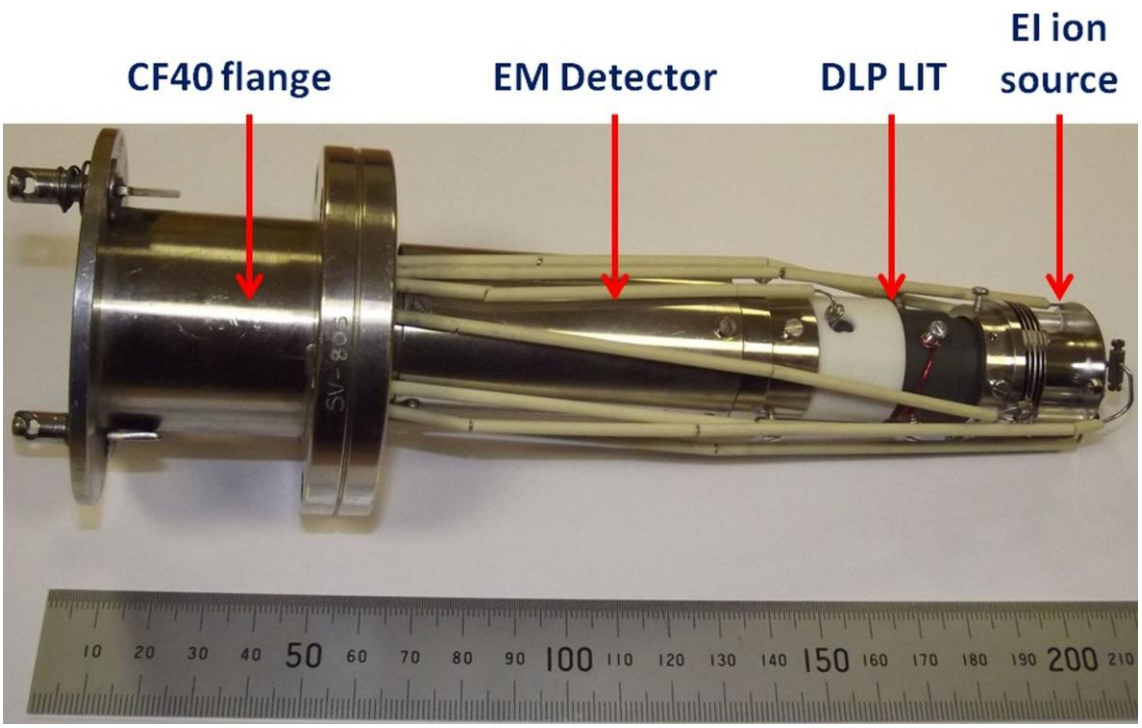

Figure 6.9: Assembly of UoL's pre-prototype DLP linear ion trap mass spectrometer (LIT-MS) for security and forensic applications.

6.3.4. Experimental setup

Experiments with DLP LIT were performed using a Pfeiffer miniature vacuum system consisting of diaphragm pump MVP 006-4 with 6 L/min pumping speed and turbomolecular pump HiPace 10 with 10 L/s pumping speed. The system provides base pressure of 5 x 10^{-6} Torr with a small spectrometer chamber connected to it. Test sample vapors were injected into the vacuum system using membrane inlet assembled in a 6.35 mm Swagelok fitting union with 0.12 mm SIL-TEC sheet membrane. DLP LIT was assembled with in-house made electron impact (EI) ion source with a three-lens system (as shown in chapter 5) and dual thoria filaments, and channeltron type electron multiplier detector (Photonis, US). The whole LIT spectrometer was assembled on a CF40 vacuum flange. Data acquisition was performed with in-house built PCB-based electronics closely coupled to the flange with operational power consumption of 34 W.

6.3.5. Experiments

After non-scanning DLP LIT mass spectrometer has been assembled, tuned and calibrated, it was tested with simulants for cocaine, TNT and sarin, which are respectively methyl benzoate (Fisher Scientific Ltd, UK), 2-nitrotoluene (Sigma Aldrich Co. LLC., UK) and dimethyl methylphosphonate (Sigma Aldrich Co. LLC., UK). Since all the samples were in a liquid form, they were prepared in 1 l flasks by injecting drops from the micropipetter (Brand GmbH, Germany). Concentrations of 5 ppm were made for each sample by injecting suitable drop size into a flask, covering flask top with several layers of parafilm and leaving the sample at room temperature for 3 hours to reach equilibrium. After preparation, sheet membrane inlet connected to the vacuum system was inserted into the flask through parafilm to perform sample analysis. In this way, volatile organic compounds (VOCs) from sample vapours would enter the vacuum system through the sheet membrane. The vacuum system pressure was initially at 1 x 10^{-5} Torr with the sample inlet valve fully open and it was increased to 8 x 10^{-5} Torr after adding helium buffer gas for ion cooling and sensitivity enhancement.

The mass analysis cycle for individual mass fragments included following steps: ionisation/ion injection (10 ms), ion trapping (1 ms), mass selection (1 ms) and ion ejection (10 ms). An EI ion source provided 100 μA electron emission current with 1.73

A filament current. The EI source electron repeller was held at -20 V, ion cage at 3 V, ion focusing lens at -100 V and ion deceleration lens at zero. LIT entrance endcap was held at 20 V and switched to zero during ion injection. Exit endap was at 20 V and switched to -100 V during ion ejection. The LIT was driven at 985 kHz RF frequency and RF voltage on *y*-rods was set for each ion mass and kept constant during the whole analysis cycle. Negative and positive DC pulses were applied to *x* and *y*-rods respectively only during mass selection to set mass window width. The electron multiplier was held at -1200 V for analysis of all samples. Figure 6.10 presents graphically the LIT-MS voltage control sequence.

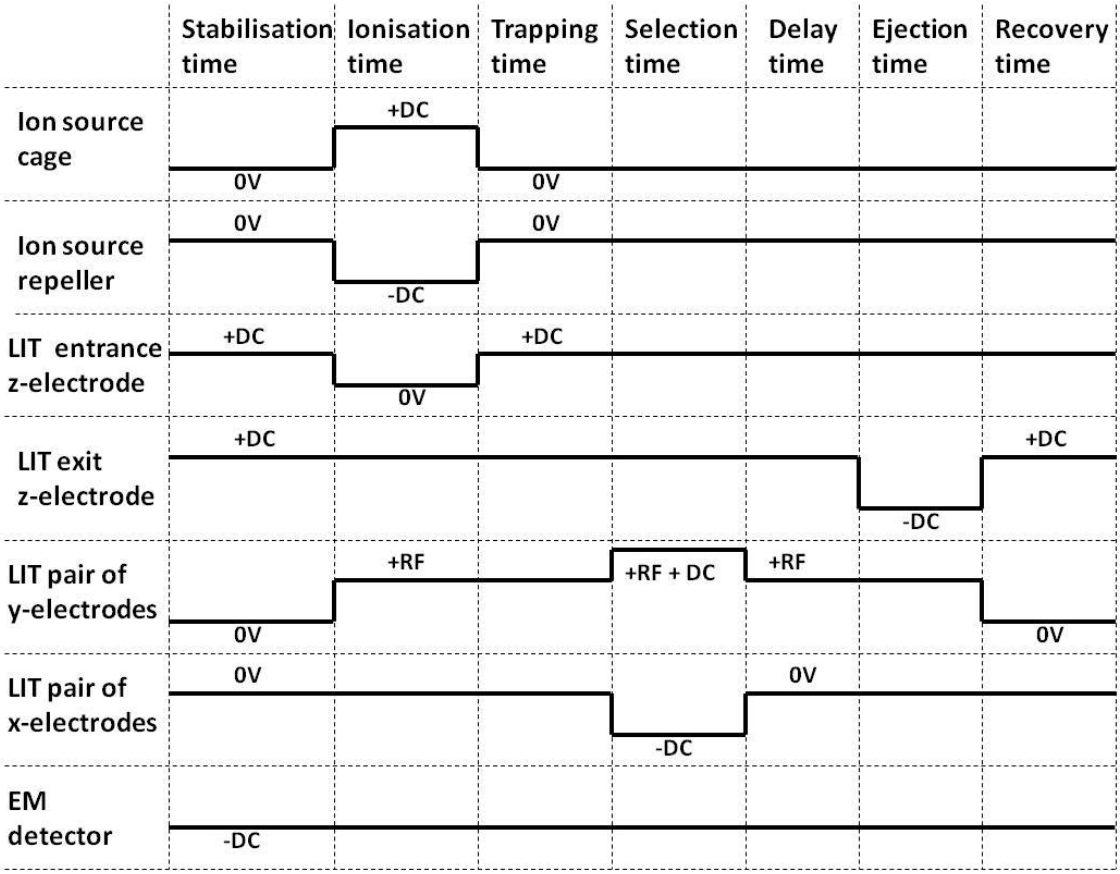

Figure 6.10: Pre-prototype LIT-MS system voltage control sequence.

Figures 6.11 to 6.13 show key experimental mass fragments for methyl benzoate, 2-nitrotoluene and dimethyl methylphosphonate obtained from the non-scanning DLP LIT. The chosen mass fragments represent most abundant mass peaks and molecular masses for each compound. The RF and DC voltages used for isolation of each mass fragment are the following:

- ❖ methyl benzoate: 188 Vp-p RF and ±7.9 V DC for *m/z* 105; 244 Vp-p RF and ±10.2 V DC for *m/z* 136,
- ❖ 2-nitrotoluene: 216 Vp-p RF and ±9 V DC for *m/z* 120; 246 Vp-p RF and ±10.3 V DC for *m/z* 137,
- ❖ dimethyl methylphosphonate: 170 Vp-p RF and ±7.1 V DC for *m/z* 94; 222 Vp-p RF and ±9.3 V DC for *m/z* 124.

The mass window width obtained for each fragment peak was 6 Th, keeping RF/DC ratio constant for each mass. Upper and lower limits of the mass window were determined by increasing RF/DC voltages at same ratio until the mass peak disappeared. With fine adjustments and small alteration of RF/DC ratio, 4 Th width could be achieved. Our simulation results have also shown that a swift DC ramp on the rods (in µs) within small DC range can filter out adjacent masses and possibly allow unit resolution for this type of non-scanning LIT [19]. This could significantly increase the number of applications for a simple and low cost mass spectrometer.

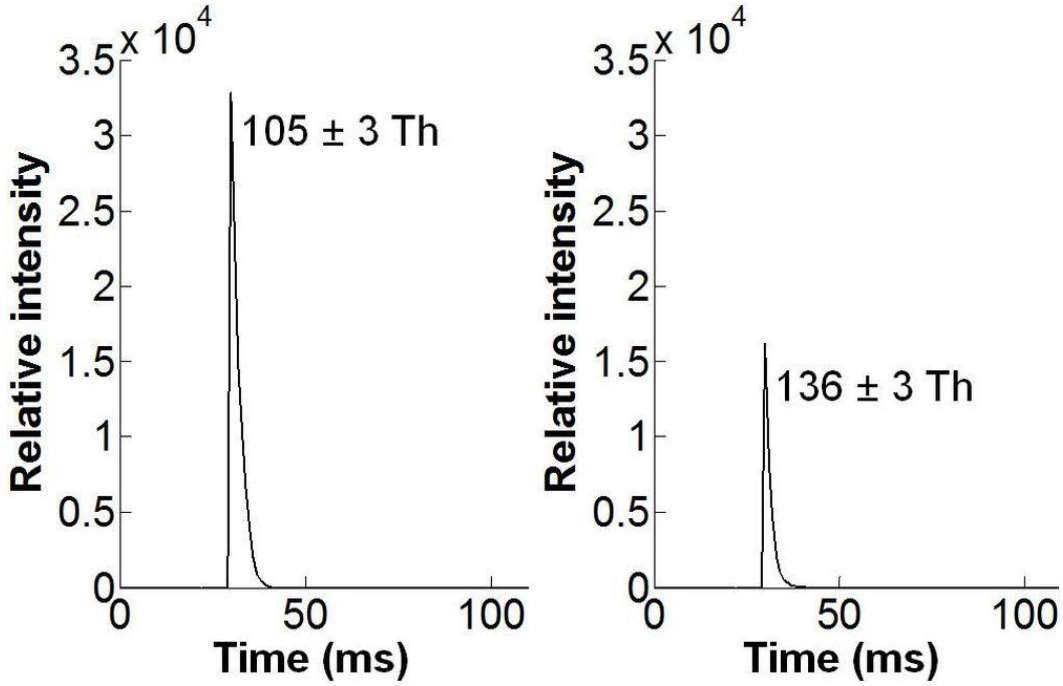

Figure 6.11: Key experimental mass fragments for methyl benzoate (cocaine stimulant) obtained from the non-scanning DLP LIT.

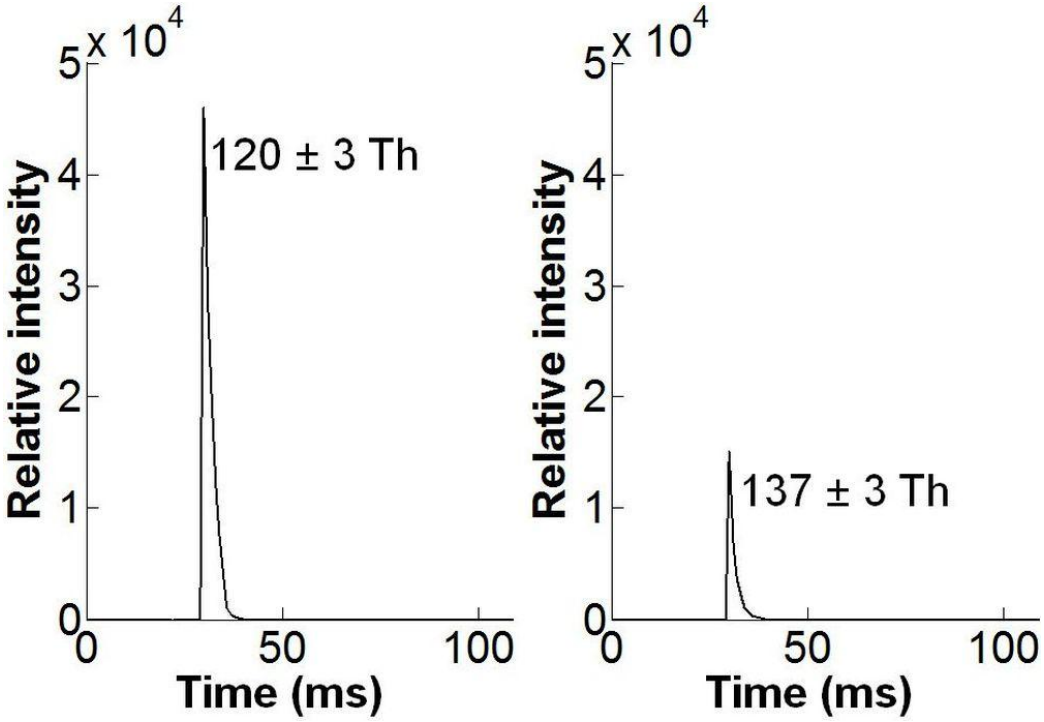

Figure 6.12: Key experimental mass fragments for 2-nitrotoluene (TNT stimulant) obtained from the non-scanning DLP LIT.

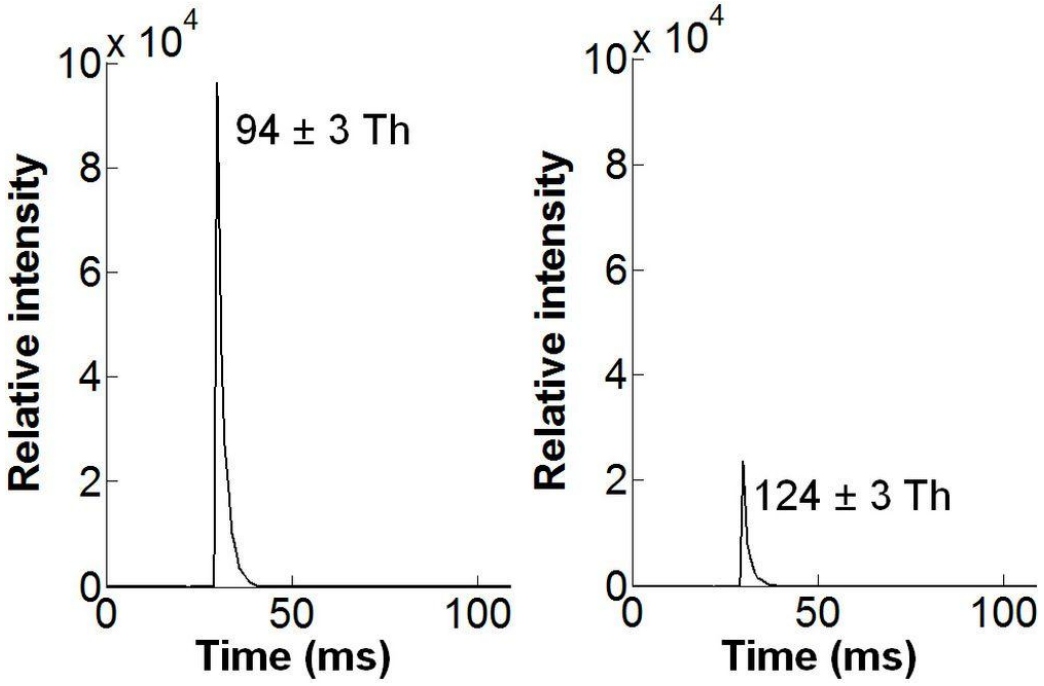

Figure 6.13: Key experimental mass fragments for dimethyl methylphosphonate (sarin stimulant) obtained from the non-scanning DLP LIT.

6.4. Target beta LIT-MS system

The LIT-MS system beta unit is under development and will be integrated by the end of this year. Compared to the pre-prototype LIT system version, it will be approximately half in size (H x W x D: 16 cm x 38 cm x 30 cm) and weight (7kg), keeping though the same technical characteristics as described above. It will consist of the main components (approximate weights are given in brackets):

a. Enclosure: custom built (2 kg),
b. LIT-MS: novel ion source, DLP LIT, EM detector, KF flange (0.5 kg),
c. Vacuum chamber: miniature tube and adaptor (0.5 kg),
d. Vacuum system: miniature getter pump (1.5 kg),
e. Electronics: fixed electronic control unit - ECU (0.5 kg),
f. Battery and power supply: vacuum system, ECU, pressure gauge, I/O controller, battery meter and DAPI inlet (0.5 kg),
g. Support components: inlet(s), pressure gauge, I/O controller, tablet PC, etc. (1 kg),
h. Buffer gas: He mini cylinder (0.5 kg) for ion cooling and sensitivity enhancement.

In the LIT system beta unit, the vacuum system has been replaced by a miniature and light getter pump. This was done for weight and space reduction. The portable sniffer will initially be vacuumed down to low ultimate pressure using in a docking station. When high vacuum is achieved, it will be removed and properly sealed. High vacuum will then be retained in the system for several hours or days by the getter pump which will be used to continually remove air, water and other degassed molecules from the LIT-MS system vacuum chamber. Docking station will also be used for storage purposes. Moreover, electronic control unit will be further reduced in both in size and weight (approximately two times smaller and lighter compared to the initial).

6.5. Conclusions

This chapter demonstrates optimization of a polymer-based non-scanning LIT fabricated using DLP rapid prototyping technique. Usage of ceramic resin material for making LIT rod electrodes and electrode housing has minimized outgassing, while specialized electroplating of the rods with copper, nickel and gold has provided very firm coating with longer electrode life. With such optimization, DLP LIT has been

made more suitable for a commercial system. Experimental results for cocaine, TNT and sarin simulants are shown for enhanced DLP LIT operating in a non-scanning mode with simplified control electronics. Such simplification and cost reduction of a mass analyzer and electronics provide a good basis for a portable application-specific mass spectrometer.

6.6. References

[1] B. Brkić, N. France, S. Taylor, *Oil-in-Water Monitoring Using Membrane Inlet Mass Spectrometry,* Anal. Chem. **83,** 6230-6236 (2011).

[2] P. T. Palmer, T. F. Limero, *Mass spectrometry in the U.S. space program: Past, present and future,* J. Am. Soc. Mass Spectrom. **12,** 656-675 (2001).

[3] P. Kusch, V. Obst, D. Schroeder-Obst, W. Fink, G. Knupp, J. Steinhaus, *Application of pyrolysis-gas chromatography/mass spectrometry for the identification of polymetric materials in failure analysis in the automotive industry,* Eng. Fail. Anal. **35,** 114-124 (2013).

[4] P. Nemes, A. Vertes, *Ambient mass spectrometry for in vivo local analysis and in situ molecular tissue imaging,* Trends Anal. Chem. **34,** 22-33 (2012).

[5] S. Soparawalla, F. K. Tadjimukhamedov, J. S. Wiley, Z. Ouyang, R. G Cooks, *In situ analysis of agrochemical residues on fruit using ambient ionization on a handheld mass spectrometer,* Analyst **136,** 4392-4396 (2011).

[6] P. I. Hendricks, J. K. Dalgleish, J. T. Shelley, M. A. Kirleis, M. T. McNicholas, L. Li, T. C. Chen, C. H. Chen, J. S. Duncan, F. Boudreau, R. J. Noll, J. P. Denton, T. A. Roach, Z. Ouyang, R. G. Cooks, *Autonomous in situ analysis and real-time chemical detection using a backpack miniature mass spectrometer: Concept, instrumentation development, and performance,* Anal. Chem. **86,** 2900-2908 (2014).

[7] C. Zhang, H. Chen, A. J. Guymon, G. Wu, R. G. Cooks, Z. Ouyang, *Instrumentation and Methods for Ion and Reaction Monitoring Using A Nonscanning Rectilinear Ion Trap,* Int. J. Mass Spectrom. **255-256,** 1-10 (2006).

[8] B. Brkić, S. Giannoukos, N. France, A. Janulyte, Y. Zerega, S. Taylor, *Modeling of an ion source lens system for sensitivity enhancement in a non-scanning linear ion trap,* Int. J. Mass Spectrom. **353,** 36-41 (2013).

[9] B. Brkić, N. France, A. T. Clare, C. J. Sutcliffe, P. R. Chalker, S. Taylor, *Development of Quadrupole Mass Spectrometers Using Rapid Prototyping Technology,* J. Am. Soc. Mass Spectrom. **20,** 1359-1365 (2009).

[10] A.T. Clare, L. Gao, B. Brkić, P.R. Chalker, S. Taylor, *Linear Ion Trap Fabricated Using Rapid Manufacturing Technology,* J. Am. Soc. Mass Spectrom. **21,** 317-322 (2010).

[11] M. Fico, M. Yu, Z. Ouyang, R. G. Cooks, W. J. Chappell, *Miniaturization and geometry optimization of a polymer-based rectilinear ion trap,* Anal. Chem. **79,** 8076-8082 (2007).

[12] M. Fico, J. D. Maas, S. A. Smith, A. B. Costa, Z. Ouyang, W. J. Chappell, R. G. Cooks, *Circular arrays of polymer-based miniature rectilinear ion traps,* Analyst **134,** 1338-1347 (2009).

[13] J. D. Maas, P. I. Hendricks, Z. Ouyang, R. G. Cooks, W. J. Chappell, *Miniature monolithic rectilinear ion trap arrays by stereolithography on printed circuit board,* IEEE J. Microelectromech. Syst. **19,** 951-960 (2010).

[14] W.M. Brubaker, W.S. Chamberlin, NASA Report (1970).

[15] J. R. Gibson, S. Taylor, *Prediction of quadrupole mass filter performance for hyperbolic and circular cross section electrodes,* Rapid Commun. Mass Spectrom. **14,** 1669-1673 (2000).

[16] Data obtained from Envisiontec GmbH, www.envisiontec.com.

[17] R.D. Brown, Vacuum 17 (1967) 505.

[18] SNIFFLES, http://www.sniffles.eu/.

[19] J.R. Gibson, University of Liverpool, private communication.

Chapter 7

Conclusions and future work

The main aim of this project was to develop, test and optimise portable mass spectrometry based systems for artificial sniffing, for in-field security and border control applications. Exploration of the existing technologies available in the market for threat scent sensing was first undertaken. More specifically, a comparison of electronic noses including their models and technical characteristics, from a wide range of international suppliers, was completed to provide an overview of the current instrumentation status for illicit and hazardous substance detection and monitoring. Brief descriptions on how each technology works were given. A database of volatile compounds identified in human body odour (e.g. axillary and non-axillary skin) was deployed. Human body VOCs were categorised according to their source origin and chemical class. An assortment of common threat substances (narcotics, explosives and chemical weapons) was also produced.

Onsite human scent detection is still limited with existing mainstream instrumentation. Proof of principle of human presence detection in a confined space using a portable MI-QMS system was demonstrated. The confined space used for the experiments was a small size shipping container simulator. The tests ran under reproducible conditions for over a month and were done for both genders as well as for multiple humans. Different types of membranes were tested to examine their selectivity. Various membrane heating temperatures and suction flow rates were examined. During tests, VOCs with masses in the range from 1 to 200 Da produced from human breath, sweat, skin and other body secretions were emitted into the simulator ambient air and constantly monitored. The observed mass fragments can potentially be used as characteristic markers of human presence. Components such as NH_3, CO_2, CO, water, acetone, isoprene, carboxylic acids and many hydrocarbons were detected and their relative abundances were recorded, resulting in characteristic human scent chemical profiles.

In order to examine MI-QMS performance with chemical threat compounds a series of detection and monitoring experiments was organized and performed. Gaseous standards of 12 threat stimulants were prepared from the low ppb to the low ppm concentration area. A membrane sampling probe was used for sniffing standard samples. Proof of concept for trace detection was demonstrated. Excellent analytical performance (repeatability, linearity, high ppt LODs, fast rise and fall response times) was presented. Preliminary field tests were completed to evaluate the technique with real illicit substances. Positive detection results were shown, allowing future further investigation.

Numerical investigation of ion injection and confinement in a non-scanning LIT-MS using CPO simulation software was done. By altering the geometrical parameters of the ion source lens system coupled to a non-scanning linear ion trap, improved sensitivity was achieved by a factor of 4 compared to commercial standard EI lens systems. Adoption of the optimized ion source lens distances, leads to lower focusing voltages, which subsequently results in low ion injection energies and finally enhanced sensitivity. Examined target mass fragments were m/z 182 and 304 for cocaine. During simulation stage, a novel built in-house software (LIT2) was used to numerically improve ion trapping in a non-scanning LIT mass analyser. The geometrical parameters (endcap hole radius, endcaps to rod electrodes distance and rod electrodes lengths) of the LIT were again varied to achieve optimised ion trapping. Tested mass fragments were the following: m/z 182 and 304 for cocaine molecule and m/z 210 and 227 for TNT.

Finally, an in-house portable (14 kg) artificial sniffer based on LIT mass spectrometry was designed, implemented and tested with threat simulant compounds. The LIT mass analyser was manufactured using a low cost DLP technique. DLP LIT electrodes presented minimized outgassing, while their coating synthesis showed stable results. DLP LIT-MS operates in a non-scanning mode making it ideal for enhanced chemical analysis in targeted field applications. The non-scanning mode implies simpler, light-weight and low-cost control electronics which is highly desirable for portable systems. Brief descriptions and explanations of the ultimate portable e-nose (7 kg) are also presented.

Future research plans for the following years include the following:

1. System integration, lab testing and validation of the final version of the target portable LIT-MS gas sensor for multi-mode analysis (direct leak, pre-concentrator and ambient *in-situ*).
2. Expanded investigation of human chemical signatures evolving a bigger number of participants from different ethnic backgrounds and according to various selection criteria (e.g. diet, lifestyle, smoking habits, age, etc.). An algorithm-code of the human scent chemical profile needs to be further developed and clarified. Field experiments in harsh environments under real weather conditions and other interferences would be beneficial for evaluating MI-QMS performance. Additional gas sensing instrumentation (e.g. other types of MS based systems such as mini PTR-MS, mini ToF-MS, mini GC-MS, etc.) could be used to enrich current knowledge on human chemical signatures as well as to investigate further human body VOC emissions in depth.
3. Field testing and validation of both MI-QMS and LIT-MS systems with real threat substances e.g. drugs and explosive materials. Development of signal processing algorithms to improve sensitivity by enhancing signal extraction from the background base level. It would be beneficial to replace the existing EI ion source with a chemical ionization ion source in order to produce clearer mass spectra. Further weight and size reduction is also planned.
4. Comparable field study and evaluation of the MS based artificial sniffers' performance (MI-QMS and LIT-MS) with sniffer dogs' performance, during hidden human or threat substances detection experiments. This includes the experimental determination of the canines' olfactory capabilities (odour threshold) during security operations.
5. Further LIT simulation work involving other rod geometries (circular and square) and electrode displacements.

Appendix

Journal Publications

1. B. Brkić, **S. Giannoukos**, N. France, A. Janulyte, Y. Zerega and S. Taylor, *Modeling of an ion source lens system for sensitivity enhancement in a non-scanning linear ion trap*, Int. J. Mass Spectrom. **353,** pp. 36-41 (2013).
2. **S. Giannoukos**, B. Brkić, S. Taylor and N. France, *Monitoring of human chemical signatures using membrane inlet mass spectrometry*, Anal. Chem. **86,** (2), pp. 1106-1114 (2014).
3. M. Statheropoulos, G. Pallis, K. Mikedi, **S. Giannoukos**, A. Agapiou, A. Pappa, A. Cole, W. Vautz, C. L. P. Thomas, *A dynamic vapor generator that simulates transient odor emissions of victims entrapped in the voids of collapsed buildings*, Anal. Chem., **86** (8), pp. 3887–3894 (2014). (work done before the start date of my PhD project.)
4. B. Brkić, **S. Giannoukos**, N. France, R. Murcott, F. Siviero, S. Taylor, *Optimized DLP linear ion trap for a portable non-scanning mass spectrometer*, Int. J. Mass Spectrom. **369,** pp. 30-35 (2014).
5. **S. Giannoukos**, B. Brkić, S. Taylor and N. France, *Membrane inlet mass spectrometry for homeland security and forensic applications*, J. Am. Soc. Mass Spectrom. **26,** pp. 231-239 (2015).
6. **S. Giannoukos**, B. Brkić, S. Taylor and N. France, *Monitoring of chemical odor signatures of drugs, explosives and chemical weapons using membrane inlet mass spectrometry*, (submitted to J. Mass Spectrom.).

Conference Publications

1. B. Brkić, **S. Giannoukos**, S. Taylor, *Artificial sniffer using linear ion trap technology*, IET / IOP Half Day Meeting on Mass Spectrometry, Surface Tomography and Sensing, University of Liverpool, Liverpool, UK (March 2012).

2. B. Brkić, **S. Giannoukos**, A. Janulyte, Y. Zerega and S. Taylor, *Numerical investigation of ion injection and confinement in linear ion traps,* The 60th ASMS Conference, Vancouver, Canada (May 2012).
3. B. Brkić, **S. Giannoukos**, N. France, A. Chalkha, A. Janulyte, Y. Zerega, F. Siviero, C. Dragoni, Robert Murcott and S. Taylor, *Development Trends in Portable Ion Trap Mass Spectrometry,* Innovations in Mass Spectrometry Instrumentation Conference, Saint-Petersburg, Russia (July 2013).
4. **S. Giannoukos**, B. Brkić, S. Taylor, *Detection of human chemical signatures in homeland security applications,* 44th IUPAC World Chemistry Congress, Istanbul, Turkey (August 2013).
5. **S. Giannoukos**, B. Brkić and S. Taylor, *Portable membrane inlet mass spectrometer for illegal human migration detection,* The 9th Harsh Environment Mass Spectrometry (HEMS) Workshop, St. Pete Beach, Florida, USA (September 2013).
6. B. Brkić, J. R. Gibson, **S. Giannoukos** and S. Taylor, *LIT2: A Novel Software Simulation Package for 3D Modeling of Linear Ion Traps,* Pittcon Conference & Expo 2014, Chicago, Illinois (March 2014).
7. S. A. de Koning, B. Brkić, **S. Giannoukos**, N. France, J. R. Gibson, A. Chalkha, A. Janulyte, Y. Zerega, F. Siviero, C. Dragoni, R. Murcott, S. Taylor, *Sniffles: Development of a Portable MS,* SNIFFER Public Workshop, Paris, France (April 2014).
8. S. A. de Koning, E. Beekwilder, B. Brkić, **S. Giannoukos**, S. Taylor, *SNIFFLES – A Portable MS-based Sniffer Instrument,* 38th International Symposium on Capillary Chromatography (ISCC) and 11th GCxGC Symposium, Riva del Garda, Italy (May 2014).
9. **S. Giannoukos**, B. Brkić, S. Taylor, *Portable membrane inlet mass spectrometer for rapid detection of drugs, explosives and chemical weapons,* The 62nd ASMS Conference on Mass Spectrometry and Allied Topics, Baltimore, USA (June 2014).
10. **S. Giannoukos**, B. Brkić, N. France, S. Taylor, *Membrane Inlet Mass Spectrometry for In-Field Security Applications,* The 20th International Mass Spectrometry Conference, Geneva, Switzerland (August 2014). Invited speaker at the JMS Award Symposium.
11. **S. Giannoukos**, B. Brkić, S. Taylor, *Portable mass spectrometry for threat detection,* 5th Vacuum Symposium, Coventry, UK (October 2014).

12. **S. Giannoukos**, B. Brkić, N. France, S. Taylor, *Artificial Sniffing for Border Security and Civil Defence Applications*, SET for Britain event, House of Commons, London, UK (March 2015).

Awards

1. British Mass Spectrometry Society, Student Travel Grant, GBP 300.00, July 2013.
2. Richard A. Schaeffer Memorial Fund Award 2014, USD 750.00, April 2014.
3. The 6th Journal of Mass Spectrometry Award, EUR 1200.00, August 2014.